PHYSICOCHEMICAL CHARACTERIZATION OF *PLECTRANTHUS EDULIS* (ETHIOPIAN POTATO) STARCH AND ITS EVALUATION AS A DISINTEGRANT IN PARACETAMOL TABLET FORMULATIONS

BY

ANTENEH ASSEFA (B.PHARM)

ADDIS ABABA UNIVERSITY

ADDIS ABABA, ETHIOPIA

JANUARY, 2015

PHYSICOCHEMICAL CHARACTERIZATION OF *PLECTRANTHUS EDULIS* (ETHIOPIAN POTATO) STARCH AND ITS EVALUATION AS A DISINTEGRANT IN PARACETAMOL TABLET FORMULATIONS

ANTENEH ASSEFA (B.PHARM)

A THESIS SUBMITTED TO THE SCHOOL OF PHARMACY, DEPARTMENT OF PHARMACEUTICS AND SOCIAL PHARMACY IN PARTIAL FULFILLMENT OF THE REQUIREMENTS FOR THE DEGREE OF MASTER OF SCIENCE IN PHARMACEUTICS

ADDIS ABABA UNIVERSITY

ADDIS ABABA, ETHIOPIA

JANUARY, 2015

Addis Ababa University School of Graduate Studies

This is to certify that the thesis undertaken by Anteneh Assefa, entitled "Physicochemical Characterization of *Plectranthus edulis* (Ethiopian potato) Starch and its Evaluation as a Disintegrant in Paracetamol Tablet Formulations" and submitted in partial fulfillment of the requirements for the Degree of Master of Science in Pharmaceutics complies with the regulations of the University and meets the accepted standards with respect to originality and quality.

Approved and signed by the Examining Committee:

Name	Signature	Date
1. Prof. Tsige Gebre-Mariam (Advisor)	_____	_____
2. Dr. Anteneh Belete (Advisor)	_____	_____
3. Dr. Kaleab Asres (Examiner)	_____	_____
4. Dr. Nisha Mary Joseph (Examiner)	_____	_____

Head, Department of Pharmaceutics and Social Pharmacy, School of Pharmacy, Addis Ababa University

ABSTRACT

Plectranthus edulis, Vatke (*P. edulis*) [fam., Lamiaceae], is an ancient Ethiopian tuber crop and one of the traditional root crops indigenous to Ethiopia. It is a large (~1m high) and an erect herbaceous plant with hirsute, decumbent and glandular stems, and leaves of lanceolate to elliptic and root of swollen nodes which produces edible underground potato-like tubers.

Starch from the tubers of *P. edulis* was isolated using 0.075% (w/v) sodium metabisulphite and it gave a yield of about 80.4% on dry weight basis. The starch was examined for the chemical composition, amylose content, physicochemical properties and evaluated for its applicability as a pharmaceutical disintegrant in tablet formulations.

The proximate composition of the starch on dry weight basis was found to be 0.14% ash, 0.21% lipid, 0.43% protein, and 99.22% starch. The amylose content was 30.6%. Its true density, moisture content and pH values were 1.47 g/ml, 11.2% and 6.6, respectively. Scanning electron microscopy (SEM) of the starch granules showed characteristic morphology that was oblong (elliptical) with some oval in shapes. The starch showed a monomodal normal granule size distribution with a mean particle size of 36.2 μm and specific surface area of 0.302 m^2/g. The DSC thermograms of *P. edulis* starch exhibited higher T_0 (69.2 ^oC), T_p (74.3 ^oC) and T_e (83.3 ^oC) values than potato starch. X-Ray Diffraction pattern of the starch was typical B-type with a distinctive maximum peak at 17.5^o 2θ. The FTIR spectral features of the starches show characteristic peaks at 3325, 2930, 1462, 1377, 1155, 860 cm^{-1} attributed to various stretching and bending vibrations of O–H, C–H, C–O, or C–O–C bonds for starches. It has typical swelling power, solubility and moisture sorption pattern at different conditions of temp and relative humidities. It possesses higher values relative to potato starch, but its solubility values are lower than potato starch at all temp studied.

The comparative disintegrant abilities of these starches in paracetamol tablet formulations prepared by wet granulation method were studied. The granules prepared with the starches (*P. edulis* starch and potato starch) at different disintegrant concentrations were characterized for particle size distribution and flow properties. The excellent flow property of the granules was manifested by the weight uniformity of tablets. The crushing strength, friability, disintegration time, and dissolution rate of the tablets were studied using standard methods. The results

indicated that the properties of paracetamol tablets formulated with both starches as disintegrants were affected by their concentration and the compression force (CF). Increasing the concentration of the starches reduced the crushing strength and disintegration time of the tablets and increased the percent friability of the tablets. Conversely, increasing the CF increased crushing strength and disintegration time of the tablets and reduced the percent friability of tablets. The results have shown that *P. edulis* starch has favorably competed with potato starch as a disintegrant in the paracetamol tablet formulations.

The optimization study of *P. edulis* starch as a disintegrant in paracetamol tablets was carried out by selecting the CF (X_1) and *P. edulis* starch concentration (X_2) as factors, and crushing strength, percent friability and disintegration time as response variables; and employing central composite statistical design (CCD). Design-Expert 8.0.7.1 software was utilized in the experimental design, statistical analysis and optimization process. Using the software several statistical parameters were compared, quadratic model for all the three responses were selected, and the adequacy of the models were checked by analysis of variance (ANOVA). The ANOVA results revealed that quadratic model is significant for the terms (factors) and responses studied. A quadratic mathematical model was developed; and the optimum formulation of paracetamol tablet containing *P. edulis* starch as a disintegrant was obtained by simultaneous optimization of the responses. From the optimum region, a CF (X_1) of 14.40 KN and a disintegrant concentration (X_2) of 5.96% was selected to check the validity and predictability of the design. The predicted values of crushing strength, friability and disintegration time of the formulation at the aforementioned levels of factors closely matched with the results of actual experimentation. Thus, the optimization technique provided the optimum formulation of paracetamol tablet containing *P. edulis* starch as a disintegrant.

The results of the physicochemical characterization of *P. edulis* starch, as well as the comparative and optimization study of the starch as a disintegrant in the tablet formulations indicate that *P. edulis* can be used as an alternative source of starch for applications in the pharmaceutical industry.

Keywords: *Plectranthus edulis*, Starch, Differential scanning calorimetry, Scanning electron microscopy, X-ray diffraction, Tablet disintegrant, Optimization, Central Composite Design

ACKNOWLEDGEMENTS

First and foremost, I exalt the Lord Jesus Christ, the Son of the Almighty God for his unconditional love and innumerable blessings in my life!

My deepest and sincere gratitude and appreciation goes to my advisors, Prof. Tsige Gebre−Mariam and Dr. Anteneh Belete for their encouragement, follow up, and support throughout the study. Their meticulous guidance, constant motivation and dynamic approach encouraged me to successfully accomplish this thesis work.

I would also like to acknowledge AAU, Department of Pharmaceutics and Social Pharmacy for allowing access to laboratory facility and its staff for cooperation and help; Department of Biology and Chemistry, for authentication of my plant material and providing chemicals for chemical tests, respectively; Martin Luther University, Germany for the Scanning Electron Microscopic study of *P. edulis* starch; The Ethiopian Geological Survey Laboratory for XRD study and the EHNRI for the determinations of protein content, ash value and lipid content of the starch; and Ethiopian Pharmaceutical Manufacturing Sh. Co. (EPHARM) for providing me access to their laboratory for the various studies.

My appreciation also goes to Addis Pharmaceutical Factory, PLC for providing me with paracetamol powder.

I extend my heartfelt gratitude to Ato Fekade Tefera for his technical support in the lab; Efrem Nigussu for his facilitating the DSC study of starch samples in Germany, Getahun Paulos, Zewdu Yilma, Yonas Brhane, Addise Bekele and all my classmates for their support during this work; and staff members of the Shashigale (Wolaita) primary and secondary school teachers for their help in collecting *P. edulis* tubers.

My deepest gratitude also goes to all my family, my mom, Tadelech H/Galale, and my dad Assefa K/Kidore− you have special place in my life. Hirut Assefa, Mulugeta Abebe, Belayneh Assefa, Mengistu Assefa, Amanuel Markos, Derese Assefa, Tiruneh Belete, your support and words of encouragement reside in me forever.

My last, but not least appreciation goes to Addis Ababa University for sponsoring my thesis work and Somali Regional State Health Bureau for offering me study leave.

TABLE OF CONTENTS

LIST OF FIGURES

LIST OF TABLES

ACRONYMS

ANOVA	Analysis of Variance
AOAC	Association of Official Analytical Chemists
APIs	Active pharmaceutical ingredients
BP	British Pharmacopoeia
CCD	Central Composite Design
CF	Compression Force
DoE	Design of Experiments
DSC	Differential Scanning Calorimetry
ENBSAP	Ethiopian National Biodiversity Strategy and Action Plan
EPHARM	Ethiopian Pharmaceutical Manufacturing Sh. Co.
FD	Factorial Design
FTIR	Fourier-Transform Infrared
GIT	Gastrointestinal Tract
ΔH_{gel}	Enthalpy of gelatinization
KN	Kilo Newton
LOF	Lack of Fit
PLC	Private Limited Company
RH	Relative humidity
RSM	Response Surface Methodology
SD	Standard deviation
SEM	Scanning Electron Microscope
SNNPR	Southern Nations, Nationalities and Peoples Region
USP/NF	United States Pharmacopoeia /National Formulary
UV/Vis	Ultra Violet/Visible
XRD	X-Ray diffraction/diffractometry

1. INTRODUCTION

1.1. Starch

Starch is by far the major storage compound accumulated by plants, making it one of the most abundant polysaccharides present on earth. It remains the most important source of calories in the human and animal diet (Buléon *et al.,* 1997). Starch occurs abundantly in most plants. It is formed in the leaves and other green parts of plants from water and carbon dioxide in presence of light and chlorophyll by a process known as photosynthesis, which is then stored in several organs such as tubers of cassava, potato and yam; caryopsis of maize, sorghum, fonio, millet and rice and as well as in leaves, stems and roots, but are largely stored in grains and tubers (Muazu *et al.,* 2012a).

Starch is one of the most widely used biomaterials in the food, textile, cosmetics, plastic, adhesives, paper and pharmaceutical industries (Buléon *et al.,* 1997). The diverse industrial usage of the materials is premised on its availability at low cost, high caloric value, inherent excellent physicochemical properties and the ease of its modification to other derivatives (Gebre–Mariam and Schmidt, 1996a).

Starch structural characteristics such as amylose content, branch chain length distribution of amylopectin, protein and lipid contents and granular size are related to their botanical sources and are affected by climatic conditions and soil type during growth. These features affect their functional roles for various industrial applications (Morrison and Azudin, 1987; Gebre-Mariam and Schmidt, 1996a; Charles *et al.,* 2004; Peroni *et al.,* 2006). Therefore, the search for potential sources of starch for its versatile industrial applications calls for a better understanding of its unique physicochemical, functional and structural properties.

1.2. Sources of starch

Starch granules are synthesized in a broad array of plant tissues and within many plant species. Cereals, roots and tubers strike top in the list of starch sources. Different sources of starch such as ginger, cassava, cocoyam, sorghum, plantain, rye, barley, yam, enset, and colocasia have been researched to cope up with accelerating global needs (Gebre–Mariam and Schmidt, 1996a; Gebre–Mariam and Schmidt, 1998; Tester *et al.,* 2004).

Most commercially available starches are isolated from cereals (corn, wheat and rice), tubers (potato) and roots (cassava, sweet potato, arrow root) (Hofvander, 2004). Corn is by far the biggest

crop corresponding to 80% of total starch production and most of this is produced in the USA. Europe is the major producer of wheat and potato starches. In Europe, about 7.7 $x10^6$ tons of starch is produced annually. It consists of corn starch (49%); wheat starch (29%); and potato starch (22%), where as cassava starch is produced in Asia (Jayakody *et al*., 2007; Salwa *et al.*, 2010) and Africa (Nang'ayo *et al.*, 2005).

Some of the Ethiopian plants which have been shown to possess starch of commercial value include Enset (Gebre-Mariam and Schmidt, 1996a); Ethiopian Yam (Gebre-Mariam and Schmidt, 1998); Godare (Adane *et al*., 2006); Anchote (Nigussie *et al*., 2006); Cassava (Paulos *et al*., 2009) and Kottee Harree (Mohammed *et al*., 2007).

Literature survey reveals no report on the physicochemical and structural properties of starch from the widely available *Plectranthus edulis,* Vatke (Ethiopian potato) and its evaluation as a pharmaceutical excipient.

1.3. *Plectranthus edulis* plant

Sheffield (1986) reported that the genetic diversity in crops is concentrated in certain areas of the world. Ethiopia is among such areas in the world where crop domestication started.

There are about 7000 vascular plant species that occur in Ethiopia, of which 12% are believed to be endemic. It is also stated in the Ethiopian National Biodiversity Strategy and Action Plan (ENBSA) (2005) that crops such as tef (*Eragrostis tef* (Zucc.) Trotter), noog (*Guizotia abyssinica* (L.F.) Cass.), gesho (*Rhamnus prinoides* (L'Hér.), kosso (*Hagenia abyssinica* (Bruce) J. F. Gmel), Ethiopian mustard (*Brassica carinata* (A.Br.), enset (*Ensete ventricosum* (Welw.) Cheesman), khat (*Catha edulis* (Vahl.) Endl.), Oromo dinch (*P. edulis* (Vatke) Agnew), anchote (*Coccinia abyssinica* (Lam.) Cogn.) and buna (*Coffea arabica* L.) are believed to originate in Ethiopia.

P. edulis (fam., Lamiaceae), syn. *Coleus edulis* Vatke, is one of the four economically important tuber crops of the genus *Plectranthus*, together with *Plectranthus esculentus* (Livingstone potato), *Plectranthus parviflorus* (Sudan potato) and *Plectranthus rotundifolius* (Madagaskar potato) (Mulugeta, 2008; Rice *et al.*, 2011).

P. edulis is locally known by various vernacular names such as *Wolaita donuwa, Dincha Oromo, Gurage dinch, Agew dinch* and generally, as Ethiopian potato (Mulugeta *et al*., 2007; Yeshitila and Weibull, 2007). The plant was one of the traditional root crops, especially to Wolaita and Hadiya

people, before the introduction of other tuberous plants like cassava and sweet potato to the region. It is cultivated in mid and high altitudes (1880 to 2200 meters above sea level) in the north, south and western Ethiopia primarily for its edible tubers (Asfaw and Woldu, 1997; Mulugeta *et al*., 2007).

Botanically, *P. edulis* is large, erect, coarse, and aromatic herb growing up to 1m high (Figure 1.1). Its stems are hirsute, glandular and decumbent. The plant produces edible underground potato-like tubers on slender rhizomes. Its leaves are lanceolate to elliptic-lanceolate, with acute, dentate and rounded sessile base (Hedberg *et al.*, 2006).

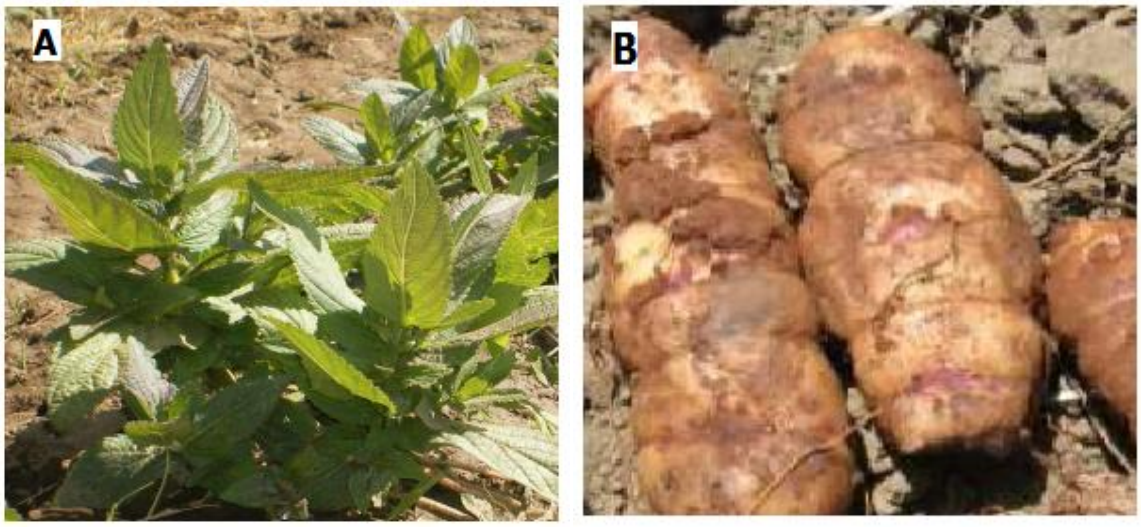

Figure 1.1: *P. edulis* plant (A) and its tuber (B) (Mekbib *et al.*, 2007).

Due to its high yielding potential (Mulugeta et *al*., 2007), excellent caloric and nutrient source, wide adaptability, drought and insect pests resistance, and multifunctional usage, farmers and governmental and non-governmental organizations have recently shown a renewed interest in *P. edulis* (Mulugeta, 2008).

1.4. Physicochemical characterization of starches

1.4.1. Chemical composition of starch

Starch consists of two types of molecules, amylose and amylopectin. Amylose is a linear polymer composed of glucopyranose units linked through α-D-(1→4) glycosidic linkage while amylopectin is a branched polymer with one of the highest molecular weights known among naturally occurring polymers (Karim *et al.*, 2000).

As compared to amylopectin, amylose is a smaller molecule with longer chains and a limited number of branch linkages. The long chains of amylose have a high capacity to bind iodine in solution and this imparts a blue color to amylose containing starches when these are stained with iodine. Amylopectin has a much lower iodine-binding capacity and stains violet with iodine solution (Dayner *et al.*, 2001).

Amylose in solution very readily crystallizes in the starch granule. It is supposed that amylose resides largely in the amorphous regions of the granule. Amylose molecules consist of single mostly-unbranched chains with 500-20,000 α-(1-4) -D-glucose units dependent on source (Figure 1.2A). In many instances, the amylose content of these starches have been determined by colorimetric procedures by not taking into account the iodine complexing ability of the long external amylopectin chains of tuber starches (Hoover, 2001).

Amylopectin is one of the largest natural polymers with an average molecular weight of the order 10^7–10^9. Each molecule of amylopectin is composed of many short chains of glucose molecules. These 1, 4-linked chains are joined together by 1, 6 branch points and the chains are arranged into clusters in which adjacent chains form double helices (Figure 1.2b). This branching is determined by branching enzymes that leave each chain with up to 30 glucose residues (Buleon *et al.*, 1998; Richardson and Gorton, 2003).

Amylopectin molecules are arranged radially within the starch granule with the ends of the chains pointing towards the surface. The clusters of double-helical chains in adjacent amylopectin molecules can align themselves to form semi-crystalline arrays within the granule. However, not the entire granule is crystalline. There are alternating concentric layers of amorphous and semi-crystalline amylopectin which are visible, in some circumstances, as growth rings within the granules (Dayner *et al.*, 2001).

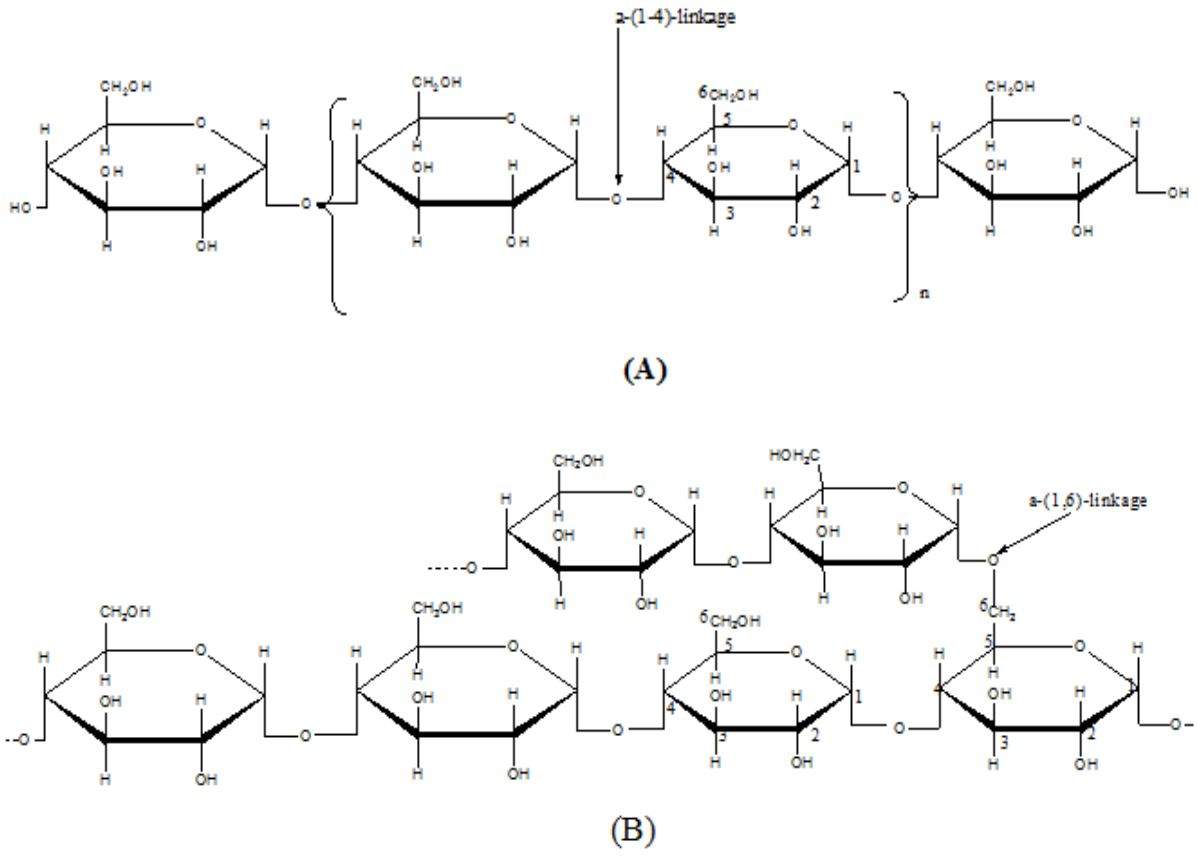

Figure 1.2: Chemical Structure of amylose (A) and amylopectin (B)

The relative proportion of amylose to amylopectin varies according to the botanical origin of the starch (Peroni *et al.,* 2006). Normal starches contain about 20-35% amylose, the difference being made up by amylopectin. Waxy and high amylose starches contain less than 15% and greater than 40% amylose, respectively (Tester *et al.,* 2004). Starch granules also contain other minor components: ash, lipids, proteins and moisture (Gebre-Mariam and Schmidt, 1996a).

1.4.2. Morphological characteristics of starch granules

Morphological characteristics of starch granules depend on the biochemistry of the chloroplast or amyloplast, as well as the physiology of the plant. Microscopic analysis, light or SEM has been used to study the morphological characteristics of starch granules. Light microscopy is used for identifying type of starch, and general size and shape of granules from different sources can be observed. SEM allows the shape and surface of starch granules to be viewed in three dimensions (Thomas and Atwell, 1999).

Starch granules from different botanical origins differ in size and morphology. Granules of tuber and root starches, for example, are oval, although round, spherical, polygonal, and irregular shaped granules also exist. Taro, dasheen and parsnip starches consist of very small granules compared to other root and tuber starches. The small granule size fractions of wheat, barley, rye and triticale have a different morphology than their larger counterparts. Granules of bean and pea starches are characterized as thick disks with a 'cut' around the middle or at the ends and an indentation at one end. Starch granules from fruits and nuts vary in shape. Some nut starches have unusual granule morphology of half-spheres, although most are round in shape (Lindeboom *et al.*, 2004). In general, granule size may vary from less than 1 μm to more than 110 μm (Hoover, 2001).

1.4.3. Crystalline structure

Starch has a definite crystalline nature which is attributed to the well-ordered structure of the amylopectin inside the granules. The branches of amylopectin form double helices which are arranged in crystalline domains. Contrarily, amylose largely makes up the amorphous regions which are randomly distributed between the amylopectin clusters (Tester *et al.*, 2004).

X-ray diffractometry is used to determine the crystalline nature of starches. X-ray diffraction pattern is the "fingerprint" of the crystal structure within starch grains (Zeng *et al.*, 2011). The two principal crystalline patterns of native starches based on the X-ray diffraction patterns have been classified as A or B. A-type starches contain shorter average branch-chain lengths than the B- and C-type starches; the C type is proposed to be a mixture of both A and B types (Hizukuri, 1985). The main difference between A and B types is that the former adopt a close-packed arrangement with water molecules between each double helical structure, while the B-type is more open, there being more water molecules, essentially all of which are located in a central cavity surrounded by six double helices (Cheetham and Tao, 1998).

Starches from different botanical sources exhibit different crystalline patterns (Stevenson *et al.*, 2006; Singh *et al.*, 2006). Most cereal starches (e.g. normal corn, rice, wheat and oats) display the A-type, while tuber starches (e.g. enset, dioscorea, potato) exhibit the B-type (Gebre-Mariam and Schmidt, 1998) and starch from the seeds of legumes (e.g., peas) demonstrate the C-type (Wang *et al.*, 1998). Nevertheless, starch from the tubers of cassava exhibited the A-type pattern (Paulos *et al.*, 2009).

A-type starches show peaks at 15^o, 17^o, 18^o and 22^o 2θ angles while B-type has four main reflection intensities at 5.5^o, 17^o, 22^o and 24^o 2θ angles. The B-type X-ray pattern of starch is usually characterized by the position and relative peak intensity in the range of $2\theta = 5\text{-}6^o$, while the absence of this peak is characteristic of A-type starch. The C type X-ray pattern reflects at 5.5^o, 17.0^o, 18.0^o, 20.0^o and 23.5^o 2θ, which is believed to be a superposition of the A-and B-type patterns (Zobel *et al.*, 1988; Buléon *et al*., 1998).

1.4.4. Differential scanning calorimetry (DSC) study of gelatinization

Although starch granules are insoluble in cold water, they can swell slightly and become hydrated, resulting in an increase in the diameter of the granules. This process is reversible. When heat is applied to such a system, however, irreversible changes occur. As the granules are heated, they reach a specific temp at which they swell more. With continued heating, the viscosity of the suspension increases dramatically. The starch then absorbs more water and the granules swell more or continue to expand above the melting temp. This sequence of change from dispersion to paste is known as starch gelatinization (Gebre-Mariam and Schmidt, 1996a).

Gelatinization generally refers to the disruption of molecular order within starch granules, when they are heated above the gelatinization temp in the presence of sufficient amount of water. Evidence for the loss of molecular order includes: irreversible granule swelling, loss of birefringence, loss of crystallinity, viscosity development and starch solubilization (Nelles *et al.*, 2000).

1.4.5. Swelling and solubility

Swelling and solubility provide evidence of non-covalent bonding between starch molecules and therefore allow comparison of relative bond strength at specific temp (Moorthy, 2002). Swelling and solubility of starch occurs when starch is heated in excess water resulting in a disruption of crystalline structure due to breaking of hydrogen bonds. The hydroxyl groups of amylose and amylopectin are then exposed and the water molecules become bonded to these hydroxyl groups through hydrogen bonding resulting in an increase in granule swelling and solubility (Hoover, 2001).

Thus, swelling and solubility of starch are temp dependent, increasing with increasing temp due to weakening of internal associative forces maintaining the granular structure (Peroni *et al.*, 2006). Swelling and solubility are influenced by chemical composition such as amylose/amylopectin ratio, phosphate and lipid contents, granular morphology, and the structural characteristics of amylose and amylopectin (Lu *et al.*, 2008). It has been suggested that the amorphous regions are responsible for

the reversible swelling of starch upon adsorption of water (Ofoefule *et al.*, 2004). High contents of phosphate monoesters result in increased swelling and solubility of starches due to increased repulsions between phosphate groups on the adjacent amylopectin molecules (Singh *et al.*, 2003).

1.4.6. Moisture sorption pattern

Starch has been classified as a moderately hygroscopic material. Moisture is known to modify the flow and mechanical properties of many powders including starch. Therefore, knowledge of moisture sorption properties of starch is necessary where controlled powder flow or compaction is critical (Gebre-Mariam and Schmidt, 1998). The moisture sorption isotherms show the equilibrium amount of water sorbed onto a solid as a function of steady state vapor pressure at a constant temp. In the natural state, starch granules are at moisture equilibrium with the surrounding atmosphere and under ordinary atmospheric conditions, contain 8-12% moisture. This value bears a definite relationship to the humidity of the air in which the granules are equilibrated and varies with the humidity in standard fashion. The moisture contents of cassava, potato and corn starch have been shown to increase with relative humidity (RH) during storage (Swaminathan and Kildsig, 2001).

Knowledge of water sorption properties is important in predicting the physical state of materials at various conditions, because most structural transformations and phase transitions are significantly affected by water. Prediction of water sorption is needed to establish water activity and water content relationship for materials (Airaksinen, 2005).

1.5. Starch applications

1.5.1. Pharmaceutical applications of starch

Starch is the most commonly used pharmaceutical excipient in the manufacture of tablets. Pharmaceutical excipients are defined as substances other than the active drug or prodrug which have been appropriately evaluated for safety and are included in a drug delivery system to either aid in the processing of system during its manufacture; or protect, support or enhance stability, bioavailability, or patient acceptability; assist in product identification; or enhance any other attribute of the overall safety and effectiveness of the drug during storage or use (Robertson, 1999). The role of excipients in determining the quality of a formulation and in many cases the bioavailability of a drug from tablets has received considerable attention in recent years (Enauyatifard *et al*., 2012).

Starch is an important pharmaceutical raw material, popularly used in solid pharmaceutical dosage forms as diluent, binder, glidant and disintegrant. The wide availability and relatively low cost are major factors governing the wide spread use of starch (Gebre-Mariam and Schmidt, 1996a; Madu *et al.*, 2011).

During recent years, starch has been taken as a new potential biomaterial for pharmaceutical applications because of the unique physicochemical and functional characteristics (Cristina Freire *et al*., 2009).

Starch based microparticles have been used for the nasal delivery of drugs and for the delivery of vaccines administered orally and intramuscularly. A major area of application of microparticles is as dry powder inhalation formulations for asthma and for deep-lung delivery of various agents (Sharma *et al.*, 2001). Starch can also be used in microencapsulation of drugs (Fontes *et al.*, 2012). The microcapsule provides a simple and cost-effective way to enclose bioactive materials within a semipermeable polymeric membrane. For instance starch nasal bioadhesive microspheres with significantly extended half-life have been reported for several therapeutic agents including insulin (Callens *et al.*, 2003). Improved bioavailability of gentamycin-encapsulated starch microspheres as well as magnetic starch microspheres for parenteral administration of magnetic iron oxides to enhance contrast in magnetic resonance imaging has been reported (Le Corre *et al.*, 2010).

1.5.2. Other applications

Starch has also versatile applications in food, textile, plastic and paper industries. Starch serves in food industries as thickener, gelling aid, texturizer, emulsifier, appearance modifier, bulking agent, coating, adhesive, and lipid substitute (Omojola *et al.*, 2010). It has also been used for centuries as a binder in making paper and this continues to be an important use.

1.6. Tablet disintegrants

Disintegrants are substances incorporated into tablets to facilitate break-up after administration. The active ingredients in a tablet must be released from the tablet matrix as efficiently as possible to allow its rapid dissolution (Musa *et al.*, 2011). The use of starch as a disintegrant in tablet formulation is as old as the history of tablet manufacture (Mustapha *et al.*, 2010). Before 1906 potato starch and corn starch were used as disintegrants in tablet formulation (Debjit *et al.*, 2010). The disintegrants have a major function to oppose the efficiency of the tablets binder and the physical

forces that act under compression to form tablet; the stronger the binder, the more effective must be the disintegrating agent in order for the tablet to release its medication (Bhowmik *et al.*, 2010) and consequently be available for absorption into the systemic circulation from the GIT.

Disintegrants effect break-up of tablet matrix into granules by accomplishing one or more of the following processes: Swelling of the tablet in an aqueous environment as a result of water intake with subsequent bursting resulting in tablet break-up; hydration leading to the weakening of bonds in the tablets and Capillary action: This is the absorption of water by wicking action creating an internal pressure which subsequently breaks the tablet (Musa *et al*., 2011). Starch has greater affinity for water and swells when moistened, thus facilitating the rupture of the tablet matrix; its disintegrating action in tablets is due to capillary action because of spherical shape of starch increases the porosity of tablet thus promoting wicking action. Other concept relates to swelling of starch grains on exposure to water, a phenomenon that physically ruptures the particle-particle bonding in tablet matrix (Gadalla *et al*., 1989; Chaudhary *et al.*, 1992).

The nature and concentration of disintegrants have been shown to affect the strength, disintegration time and dissolution rate of tablets (Gebre-Mariam and Schmidt, 1996b; Adane *et al.*, 2006; Adebayo *et al*., 2008). Therefore, the appropriate type and amount of disintegrant is in many cases the critical factor to determine the tablet quality, although particle size, particle shape and packing geometry of disintegrant in a tablet has to be taken into account.

The desired concentration of disintegrant normally varies from 5% to 20%. Incorporation of disintegrant in tableting is achieved by either addition of total amount of disintegrant to powder before granulation (intra granular disintegrants) or addition of total amount of disintegrant to granules just before compression (extra granular disintegrants). However, 50% disintegrant may be added before granulation and 50% after granulation (intra-extra granular disintegrants) (Muazu *et al.*, 2012b). The optimal selection of disintegrant is an important step, which needs a lot of laboratory experiments for the optimum tablet formulation.

1.7. The present study

Ethiopia is home to many plant species, which can be used as source of starch for pharmaceutical and other industrial applications. Starches from some species have already been investigated for various pharmaceutical applications including *Ensete ventricosum* (Gebre-Mariam and Schmidt,

1996a), *Dioscorea abyssinica* (Gebre-Mariam and Schmidt, 1998), *Colocasia esculenta* (Adane *et al*., 2006) and *Manihot esculenta* (Paulos *et al*., 2009). Another potential source is *Plectranthus edulis*, Lamiaceae, commonly called Ethiopian Potato.

As the functional properties and physicochemical characteristics of a given starch are typical of its biological origin, knowledge of physicochemical properties of starch is necessary for its industrial applications.

Literature survey has been carried out and reveals no studies concerning the composition and physicochemical properties of starch from *P. edulis*. The other members of the genus Plectranthus, namely, *P. esculentus (*Livingstone potato), which is widely cultivated in Western and Southern Africa (Rice *et al.*, 2011) has been studied and its physicochemical properties determined and its potential for pharmaceutical application evaluated. Its amylose content was reported to be 24%, mean particle size 20.16 μm, true density 1.45 g/ml, and swelling power 20.04%. *P. esculentus* starch was found to compare well with maize starch BP in physicochemical properties (Muazu *et al.*, 2011). Its binding and disintegrating ability in paracetamol tablets was also studied, and it had shown comparable binding and disintegration capacity to potato and maize starch BP (Muazu *et al*., 2012a; Muazu *et al*., 2012b).

This work, attempts to study starch granule compositions and some physicochemical properties of *P. edulis* starch and assess its potential as pharmaceutical excipient (specifically disintegrant property) in tablet formulations.

The role of excipients in determining the quality of a formulation and in many cases the bioavailability of drug from tablets has received considerable attention (Enauyatifard *et al*., 2012) and disintegrants play a significant role in this regard. Since a tablet is not useful until its active component is made available for absorption, the disintegrant is an important excipient in a tablet to facilitate the breakup in a liquid environment into fine particles prior to dissolution of the active drug and its absorption from the GIT.

For tablets containing sparingly water soluble drugs, the disintegration time and the start of dissolution is often delayed by the poor wettability of the tablet surface and/or slow penetration of water into the tablet matrix. This causes increased disintegration time and retards drug release, necessitating the need for incorporation/addition of a disintegrant (Gissinger and Stamm, 1980).

Paracetamol, which is both poorly compressible and sparingly soluble drug, requires an effective binder and disintegrant, which could effectively disrupt the effects of the binder and pressure of tableting when the tablet is in aqueous media of the GIT. Hence, it is selected as a model drug for this study.

Furthermore, a detailed knowledge of the characteristics of starches from this and other local plants would enable tailoring the properties by physical and/or chemical modification and help Ethiopia be self-sufficient and compete effectively on starch markets globally. In the long run, utilization of these starches will save foreign currency, create employment opportunities and bring economic benefits to the local producers.

1.8. Objectives of the Study

1.8.1. General objective

- To isolate and characterize native starch of *P. edulis* and evaluate it as a disintegrant in tablet formulations.

1.8.2. Specific objectives

- To isolate starch from *P. edulis* tubers;
- To determine the amylose content of *P. edulis* starch;
- To determine the chemical composition of *P. edulis* starch;
- To characterize some physicochemical properties of the starch granules;
- To formulate tablets using *P. edulis* starch as a tablet disintegrant;
- To evaluate the properties of the tablets formulated; and compare the result with tablets formulated with potato starch BP; and
- To optimize tablets formulated using *P. edulis* starch as a disintegrant.

2. EXPERIMENTAL

2.1. Materials

2.1.1. Plant materials

Fresh *P. edulis* tubers were collected at its maturity age (7 months after planting) (Mulugeta, 2008) from Shashigalle Kebele, Wolaita Zone, SNNPR and authenticated by the Department of Biological Sciences, College of Natural Sciences, Addis Ababa University.

2.1.2. Chemicals and solvents

Sodium hydroxide and ethanol (Loba Chemie Pvt. Ltd., Mumbai, India), sodium metabisulphite and hydrochloric acid (BDH Chemicals Ltd, Poole, England), Lugol's solution (SIGMA Chemicals Co., USA), amylose and amylopectin (Merck, Germany), magnesium stearate (Bulvinos Chemicals Ltd, England), potato starch BP (BDH LTD., Poole, UK), paracetamol powder (China Associate Co Ltd, China), potassium dihydrogen phosphate (Sörensen, Leuren, Denmark), povidone (China associate Co. Ltd, China), sodium chloride (Oxford Laboratory, Mumbai, India), were used as received. All other chemicals used were of analytical grade.

2.2. Methods

2.2.1. Extraction of *P. edulis* starch

Starch isolation was carried out by the method described by Gebre-Mariam and Schmidt (1996a) with slight modification. Tubers of *P. edulis* were thoroughly washed and all foreign materials removed. The washed tubers were peeled and pulverised using a blender and suspended in large quantities of distilled water containing 0.075 % (w/v) of sodium metabisulphite. The material was allowed to settle, and the sedimented starch was repeatedly treated with sodium metabisulphite solution until the supernatant was free of colouring materials and the suspension was translucent. The material was then passed through fine muslin cloth to remove cell debris and the translucent suspension collected; re-filtered through the muslin cloth and allowed to settle. The sedimented starch was washed several times with distilled water until the wash water was clear and free of suspended impurities. The resulting starch was air dried at room temp. Finally, the dried *P. edulis* starch was ground and sieved through a 224 µm mesh sieve. The starch was kept in a tight-light resistant container (Gebre-Mariam and Schmidt, 1996a).

2.2.2. Extraction of starch from dried *P. edulis*

The extraction of starch from dried tubers of *P. edulis* was undertaken for the determination of the percent yield of starch from the tubers. The method employed in the extraction of starch from fresh *P. edulis* tubers was used here with some modifications (Madu *et al.*, 2011). The modifications being that after the tubers were reduced to small sizes, they were air dried before grinding. The ground tuber flour was then weighed accurately and same procedure was followed for the extraction of starch. The resulting starch was weighed and the percent yield noted.

2.2.3. Determination of chemical composition

2.2.3.1. Estimation of amylose content

Amylose content of *P. edulis* starch was determined by a colorimetric assay method (Gebre-Mariam and Schmidt, 1996a). A stock solution of each of amylose and amylopectin was prepared by dissolving 50 mg of the respective substance in 10 ml of 1.8% HCl. Two ml of each of the stock solutions were taken and diluted to 10 ml using 1.8% HCl. From the resulting solutions appropriate aliquots were taken and diluted with 1.8% HCl. Mixtures of amylose and amylopectin solutions were prepared to provide a starch concentration of 50 µg in 10 ml in any mixture. Various mixtures were prepared to contain 100, 80, 60, 40, 20, or 0% amylose or amylopectin, respectively. The absorbance reading of the resulting solutions were taken at 600 nm (for amylose) and 540 nm (for amylopectin) using Perkin Elmer UV/VIS Lambda 16 spectrometer equipped with a program recording several wavelengths, immediately after staining with Lugol's solution (diluted 1:3). 100 µg of the diluted Lugol's solution were used for staining 2 ml of the mixture. Similarly, absorbance readings of each of the pure amylose and amylopectin solutions of the same concentrations and solutions of starch were taken at the same wavelength. Blanks were run with stained 1.8% HCl. The amylose content of starch was estimated from the relationship between concentrations and absorbance of known mixtures of amylose and amylopectin at 600 nm as the interference from amylopectin at the concentration used was negligible. The results are the average of 5 determinations.

2.2.3.2. Ash value

Ash value of the starch was obtained by using the method described by Puwastien *et al.* (2011). A 2 g weight of each starch powder sample was poured into a nickel crucible which was initially heated at 105 ^{o}C to a constant weight and allowed to cool. The crucible with its content was then gently heated until it was completely charred. Subsequently, the heat was increased gradually until most of

the carbon vapourised. The sample was finally heated strongly until the residue is free from carbon (i.e. almost white). The crucible with its content was allowed to cool and weighed. The heating and cooling step was then repeated until the weight of the residue (ash) was constant. The weight of the ash was then determined and the percentage ash value calculated using the relation below:

$$Percentage\ ash\ value = \frac{WA}{WS} X 100 \quad \text{..... (2.1)}$$

Where, WA and WS are weight of ash formed and initial weight of starch powder, respectively.

2.2.3.3. Protein content

Protein content was analyzed by Kjeldahl method -destruction of starch sample by sulphuric acid. Nitrogen was liberated as ammonia, distilled, collected and titrated according to Association of Official Analytical Chemists (2000). Weighed starch sample (0.5 g) was placed in 500 ml digestion flask. 6 ml acid mixture (2 parts of conc. sulphuric acid and 1 part of conc. ortophosphoric acid) was added. The flask was placed on heater and allowed to react. As soon as the violent reaction was ceased, heat was increased and the destruction was continued until the content appeared light green (~1 h). It was then cooled and diluted with distilled water. The digested and diluted solution was transferred into sample compartment of the distiller. It was then distilled until a total volume of 150 ml was collected (NH_3 as distillate). Finally, the excess standard acid in the distillate was titrated with standard NaOH solution. The protein content was determined as a mean of three measurements, and reported by multiplying percent nitrogen by 6.25.

2.2.3.4. Lipid content

The total starch lipid content was determined by acid hydrolysis method (Association of Official Analytical Chemists, 2000). Into a 2 g sample, 2 ml alcohol was added and stirred to prevent lumping on addition of acid. 10 ml 24% HCl was added for hydrolysis and the beaker was put on a water bath held at 70-80 ^{o}C with frequent stirring. 10 ml alcohol was added and cooled and the mixture was then transferred to an extraction apparatus. 25 ml of petroleum ether was added and shaken thoroughly for 1 min. It was then allowed to stand until the upper liquid was practically clear. Petroleum ether lipid solution was drawn off through a filter. The liquid remaining was re-extracted twice, each time with only 15 ml of petroleum ether. Clear petroleum ether solution was drawn off through a filter. The petroleum ether layer was evaporated slowly on steam bath; the remaining was

dried on oven at 100 ^{o}C to constant weight. It was left to stand in air to constant weight and weighed. The result is reported as percent lipid by acid. It was determined in triplicates.

2.2.3.5. Moisture content

The moisture content was determined as per the method described by Olayemi *et al.* (2008). 2 g of starch was weighed into weighed, dried Petri-dish and heated at 130 ^{o}C in a hot air oven (Kottermann® 2711, Germany) to a constant weight, and the final weight noted. The moisture content was calculated using the following relationship and the results are the mean of triplicate determinations.

$$Moisture\ content = \frac{W_i - W_f}{W_i} \text{ x } 100 \quad \text{..... (2.2)}$$

Where W_i and W_f are starch weights before and after drying, respectively.

2.2.4. Physicochemical characterization of starch

2.2.4.1. Densities and related properties

Bulk density

Bulk density of *P. edulis* and potato starches were determined by carefully pouring 30 g powder into a graduated glass measuring cylinder. The cylinder was then lightly tapped twice to collect all the powder sticking on the wall of the cylinder. The volume was then read directly from the cylinder and used to calculate the bulk density. The bulk density (g/ml) was calculated by using Eq. 2.3. Bulk density was determined as a mean of three measurements.

$$Bulk\ density\ (\rho b) = \frac{m}{Vb} \quad \text{..... (2.3)}$$

Where m is the weight of the powder and V_b is bulk volume

Tapped density

For tapped density, 30 g of powder was tapped in graduated measuring cylinder 500 times using tapped densitometer (ERWEKA, Germany) to attain a constant volume reading from the cylinder and the tapped density was calculated from the weight and tapped volume of the powder by using Eq. 2.4. Tapped density (g/ml) was determined as a mean of three measurements.

$$Tapped\ density\ (\rho t) = m/Vt \quad \text{..... (2.4)}$$

Where m is the weight of the powder and V_t is the tapped volume

Carr's Index

Carr's Index (% compressibility) was calculated from the difference between the tapped and bulk density and divided by the tapped density.

$$Carr's\ Index\ (CI) = ([\rho t - \rho b]/\rho t)x100 \quad \text{(2.5)}$$

Hausner ratio

Hausner ratio was obtained from the ratio of tapped density to bulk density of the starches.

$$Hausner\ ratio\ (HR) = \rho t\ /\ \rho b \quad \text{(2.6)}$$

True density

True density was determined by liquid displacement method using xylene as immersion fluid (Odeku *et al.,* 2008). Two grams of starch sample of *P. edulis* or potato were placed in a pre-weighed empty pycnometer, closed after xylene was added and weighed. Sufficient xylene was added to wash down and overlay the sample; all spilled over liquid (xylene) was wiped off with an absorbent cloth. After 10 min, the sedimented starch was stirred with a glass-stirring rod to release entrapped air, the sample equilibrated for a few min and stirred again. When evolution of minute air bubbles through the supernatant xylene layer had stopped, the stirrer was removed and rinsed into the pycnometer with several milliliters of xylene. The sample was allowed to settle, the pycnometer filled with xylene and the meniscus was adjusted. True density (g/ml) was calculated with Eq. 2.7.

$$\rho = \frac{(\text{W1 x SG})}{[(\text{W1} + \text{W2}) - \text{W3}]} \quad \text{(2.7)}$$

Where, ρ = true density of starch; W1= weight (g) of starch, W2= weight (g) of the pycnometer filled with xylene, W3= weight (g) of pycnometer plus sample plus xylene, and SG = specific gravity of xylene (g/ml) (~0.855).

2.2.4.2. pH determination

Two grams of the powdered starch was shaken with 100 ml of distilled water for 5 min. The pH of the dispersion was immediately determined using pH meter.

All results are the mean of three parallel determinations.

2.2.4.3. Measurement of starch crystallinity

The starch samples were oven dried at 50 ^{o}C overnight and sieved with 224 μm mesh size sieve (Louis and Peter, 2011). The samples were then placed in the cavity of a disc sample holder of the diffractometer. The measurements were done using a Bruker AXS diffractometer (Bruker- AXS, Advanced D8, Germany) operating in the 2θ mode using computer software (Operational Soft Diffract^{+} 2000). A Cu target tube operated at a power setting of 40 kV (30 mA) with single crystal graphite monochromator equipped with a microprocessor to analyze peak position was utilized. The samples were exposed to the X-ray beam from an X-ray generator running at 40 kV and 30 mA. The scanning regions of the diffraction angle, 2θ were 4-35^{o}, which covers most of the significant diffraction peaks of the starch crystallites (Zobel *et al.,* 1988; Buléon *et al*., 1998).

2.2.4.4. Morphological characterization

The starch granule morphology was studied as described by Gebre-Mariam and Schmidt (1996a). The starch sample was mounted and sputter coated with gold to a thickness of about 30 nm (Sputter Coater Type E 5100, Biorad GmbH, Munich Germany) to increase their conductance. Scanning electron micrographs were taken with a DSM 940 SEM (Carl Zeiss, Oberkochen, Germany) at an accelerating voltage of 5 KV. The samples were then viewed and photographed.

2.2.4.5. Gelatinization property of starch

Differential scanning calorimetry (DSC) measurements of the starch-water mixture (starch/water ratio of 1:1 (w/w), on dry basis) was carried out using DSC 200 thermal analyzer (Netzsch, Selb, Germany) from which gelatinization temps were obtained. Starch sample of known moisture content was thoroughly mixed with distilled water and allowed to equilibrate in closed glass jars for 24 h at room temp. Portion of well mixed starch slurry was transferred into aluminum DSC sample pans and sealed hermatically. The sealed pan was placed in the DSC cell and heated from 20 ^{o}C to 110 ^{o}C at a rate of 10 ^{o}C/min. An empty sealed pan was used as a reference and a nitrogen environment. From the DSC trace: onset (T_o), peak (T_p) and endset (T_e) temp of the gelatinization (^{o}C), and enthalpy of gelatinization (ΔH_{gel}, J/g) were obtained.

2.2.4.6. Analysis of Fourier transform infrared (FTIR) spectra

FTIR spectra of *P. edulis* and potato starches were acquired at room temp using FTIR spectrophotometer (FTIR-8400S, SHIMADZU, Japan) in transmittance mode. The samples were first ground in a mortar to reduce the average particle size. About 5 mg of finely ground samples

were mixed with an oily mulling agent (Nujol) in a mortar and pestle. The sample mixture was then placed onto the face of a potassium bromide (KBr) plate and the second window was placed on top of the first salt plate to form a thin film of the mull by compression between the two plates. The sandwiched plates were placed in the infrared spectrometer and the spectra were obtained. Each IR spectrum was collected with 20 scans and spectral resolution of 2 cm^{-1}. Scanning was performed between wave numbers 4000 and 500 cm^{-1}. Background spectrum was collected before running each sample. IR solution software was used for data treatment.

2.2.4.7. Determination of starch hydration capacity

Hydration capacity of the starch was determined by using the method of Jubril *et al.* (2012). A 1g weight of starch was placed in a plastic centrifuge tube, 10 ml distilled water was added and then closed. The contents were shaken for 2 min then allowed to stand for 10 min and immediately centrifuged at 1000 rpm for 10 min in a bench centrifuge. The supernatant decanted and the weight of the wet starch was recorded. The hydration capacity was determined using the equation below:

$$Hydration\ capacity = Ws/Wd \quad \text{(2.8)}$$

Where W_s and W_d are the weights of the sediment and dry sample, respectively.

2.2.4.8. Particle size analysis

Particle size distribution analysis was performed using a Malvern Mastersizer 2000 laser diffraction particle-size analyzer (Malvern Instruments Ltd, Worcestershire, WR14 1XZ, UK). A small amount of *P. edulis* or potato starch was dispersed in 4 ml of distilled water (was already soaking into the sample port of the instrument) until an obscuration of 15-20% was recorded. The active beam length was set at 2.4 mm and the measuring time was 30 s. The mean volume particle size distribution, mean particle size and specific surface area were obtained with Mastersizer S, PSS0003-01 software (2002). Determinations were done in triplicates. The analysis was done under these conditions: Range (0.05–900 µm, 300RF); active beam length (2.4 mm); sample unit (MS_1: Small Volume Sample Dispersion Unit); Polydisperse; standard-wet, Presentation (3OHD).

2.2.4.9. Determination of swelling power and solubility

Solubility and swelling power (SP) of *P. edulis* and potato starches were determined using the method described elsewhere (Bello-Pérez *et al.,* 2000) with slight modification. Starch samples (0.5 g each) were dispersed in distilled water (10 ml) in pre-weighed centrifuge tubes. The tubes were

then kept in a thermostatically controlled water bath at 20, 37, 65, 75, 85 ^{o}C for 30 min, with shaking every 5 min and then left to cool to room temp. The suspensions were centrifuged for 15 min at 2000 rpm. The supernatants were decanted to pre-weighed Petridishes and dried in an oven for 2 h at 120^{o}C. The residues obtained after drying the supernatant represent the amount of starch solubilized in water. The solubility was calculated as gram per 100 g of sample on dry weight basis. The sediments obtained were weighed to obtain the swelling of the starches. All determinations were done in triplicate. The percent solubility (%S) and SP were determined according to Eq. 2.9 and 2.10, respectively.

$$S(\%) = \frac{W1}{W3} \times 100 \quad \text{(2.9)}$$

$$SP = \frac{W2 \times 100}{W3 \times (100 - S)} \quad \text{(2.10)}$$

Where W_1 is the weight (g) of soluble material in the supernatant, W_2 is the weight (g) of precipitate and W_3 is the weight (g) of starch sample.

2.2.4.10. Determination of moisture sorption pattern

The method described by Olayemi *et al.* (2008) was used. Pyrex desiccators containing distilled water, saturated solution of NaCl or appropriate concentrations (40, 31.58 and 24.66%) of NaOH were prepared to provide different (100, 75.6, 60, 40 and 20%, respectively) relative humidity (RH) chambers and stored at room temp. *P. edulis* or potato starch samples were pre-dried in an oven (Kottermann® 2711, Germany) for 4 h at 120 ^{o}C. Two grams of each starch sample was placed in Petri dish (dried and weighed) and transferred to particular (20, 40, 60, 75.6 and 100%) RH chamber. Samples were equilibrated for four weeks at room temp. The weights after four weeks were recorded and the moisture uptake of each sample was calculated as the weight difference of the starches before and after equilibration in a given RH chamber. Water sorption capacities of the starches were expressed as percent moisture uptake. Results were expressed as a mean of three parallel determinations.

2.2.5. UV calibration curve of paracetamol

A stock solution containing 200 µg/ml of paracetamol in phosphate buffer of pH 5.8 was prepared. From this stock solution, six different concentrations (2, 4, 6, 8, 10 and 12 µg/ml) were prepared. The UV absorbance readings of these solutions were measured at 243 nm using UV/Visible spectrophotometer (SOLAR Spectroflourimeter, CM2203, Belarus). Phosphate buffer (pH 5.8) was

used as a blank. The absorbance versus concentration of the solutions was plotted, and a linear regression equation and correlation coefficient were obtained.

2.2.6. Drug-excipient interaction study

2.2.6.1. Fourier transform infrared (FTIR) study

Possible drug-excipient interaction was investigated by FTIR spectroscopy as method described in section 2.2.4.6. The FTIR spectra of paracetamol powder alone and its physical mixture with *P. edulis* starch (1:1) at 500-4000 cm^{-1} were recorded using FTIR-8400S, Shimadzu, Japan.

2.2.7. Granulation

The compositions of tablet formulations are given in Table 2.1. The wet granulation method of massing and screening was used in preparing all the batches of paracetamol granules. In the present study, the disintegrant was incorporated in both the intra- (50%) and extra-granular (50%) phases. The paracetamol powder and the intra-granular disintegrant, *P. edulis* or potato starch of concentration between 5 to 15% w/w depending on the batch were dry-mixed for 5 min. An appropriate quantity of freshly prepared povidone solution was added in the above blend as a granulating agent and mixed for 20 min in a mortar. The wet mass was then passed through wet granulator with 1.6 mm sieve and dried in an oven (Kottermann® 2711, Germany) at 40 ^{o}C to a constant weight. Then, the dried granules were dry screened by passing them through a 1 mm sieve. The dried granules were stored in glass container until they were compressed into tablets.

Table 2.1: Paracetamol tablet formulations containing *P. edulis* or potato starch as a disintegrant.

Formulation ingredients	Amount of ingredients (% w/w)
Paracetamol	91.0-81.0
Disintegrant*	5.0, 7.5, 10.0, 12.5 and 15.0
PVP	3.5
Magnesium stearate	0.5

**(P. edulis or* potato starch)

2.2.7.1. Characterization of granules

2.2.7.1.1. Size distribution of granules

Thirty grams of granules from each batch were put in a set of sieves (ISO 3310-1) fixed on the universal drive unit (ERWEKA, Type AR 401, Germany) arranged in mesh size from top to bottom

with the coarsest sieve on the top. Then the sieves were shaken for 4 min. The granules remaining on each sieve were weighed and percent granules retained on each sieve recorded and mean granule size was calculated for each batch. The average granule size on any sieve was determined in microns by averaging the size of the openings of the sieve through which the granules passed and the size of the openings of the sieve upon which the granules were retained. The weight retained on each sieve was converted to percentage retention and multiplied by the average of two successive sieves. The sum of these products divided by 100 yielded an average granule size.

2.2.7.1.2. Determination of density and density related properties

Thirty grams of each batch of granules, ranging from 224-1000 μm in size, were put in 250 ml measuring cylinder. The bulk density, tapped density, Carr's index and Hausner ratio of the granules were calculated in the same way as described for starch powders above (Section 2.2.3.1).

2.2.7.1.3. Determination of granule flow rate and angle of repose

Thirty grams of granules were allowed to flow through a funnel having a 15 mm aperture from a 10 cm height. Time in second for the duration of flow was recorded. The average diameter and height of the powder piles formed were recorded. Angle of repose was calculated according to Equation 2.11

$$tan\,\theta = h/r \quad \text{..... (2.11)}$$

Where h is height of conical granule heap and r is the radius of the circular base

The flow rate (g/sec) was calculated according to Eq. 2.12

$$Flow\,rate = m/t \text{..... (2.12)}$$

Where m is the weight in grams and t is flowing time in seconds.

2.2.8. Tablet compression

2.2.8.1. Compression of granules into tablet

For evaluation of *P. edulis* against potato starch as disintegrant, granules ranging from 224-1000 μm in size with 10% fines were collected and thoroughly mixed for 10 min with the specified amounts of starch (incorporated as external disintegrant) in a Turbula® mixer (Willy A. Bachofen AG, Turbula® 2TF, Basel, Switzerland) at 49 rpm. Finely sifted magnesium stearate was then added and the mixture mixed for further 5 min. The mixture were then transferred into a hopper and

compressed into tablets at 10 and 18 KN compression forces on an automated tablet press (KORSCH XP1, 13509, Berlin, Germany) with a 10 mm die and concave-faced punch assembly. A set of tablets of target weight of 300 mg were produced at each pressure. After ejection, the tablets were stored for 24 h in airtight containers before they were subjected to analysis to allow for elastic recovery and hardening.

2.2.8.2. Evaluation of tablets

2.2.8.2.1. Weight, Thickness and Diameter

From each batch, 20 tablets were randomly selected and weighed individually on an analytical balance (Mettler Toledo, PR 203, Switzerland) and then the average weight and standard deviation were calculated. Tablet thickness and diameter (fixed 10 mm) were measured using sliding caliper scale (Nippon Sokutei, Japan).

2.2.8.2.2. Crushing strength

After 24 h of production, ten tablets were taken from each batch and the crushing strengths of the tablets were determined using hardness tester (Schleuniger, 2E/205, Switzerland).

2.2.8.2.3. Friability

Ten tablets of known weights from each batch were placed in a friability tester (ERWEKA, TAR 20, Germany) and were subjected to a combined effect of abrasion and shock by placing them in the plastic chamber that revolves at 25 rpm for 4 min. The tablets were then dedusted and weighed, and the percent loss in weight was calculated as friability.

2.2.8.2.4. Disintegration test

Disintegration test was carried out according to USP 30/NF 25 specification (2007). Six tablets from each batch were placed in a disintegration tester (CALEVA, G.B. Caleva Ltd., UK) filled with distilled water at 37 ± 2 ^{o}C. The tablets were considered completely disintegrated when all the particles passed through the wire mesh. The results are mean of three parallel determinations.

2.2.8.2.5. *In vitro* drug release study

The dissolution test was done according to the USP/NF specification using dissolution apparatus Type II (ERWEKA, DT600, Germany), with 900 ml phosphate buffer (pH 5.8) as the dissolution medium at 37 ± 0.5 ^{o}C which was stirred at a rate of 50 rpm. Five ml of aliquots of the dissolution

medium were removed at 5, 10, 15, 20, 30, 45 and 60 min and filtered using Whatman No.1 filter paper. Equal amount of fresh medium kept at the same temp was transferred into the dissolution vessel to keep the sink condition. One ml of the filtered samples was diluted to 25 ml and absorbance readings were taken with UV/Visible spectrophotometer (SOLAR Spectroflourimeter, CM2203, Belarus) at 243 nm. Phosphate buffer (pH 5.8) was used as a blank. All the necessary corrections for dilution were made when calculating the drug content.

2.2.9. Experimental design

Experimental designs have long been employed to optimize various industrial products and/or processes (Singh *et al.,* 2005). Optimization is a process of finding the best possible composition or operating conditions for the best possible effect (Singh *et al.*, 2004). The classical approach of changing one variable at a time and studying the effect of the variable on the response is inefficient technique especially in a multi-factor system (Ozdemir *et al.*, 2011). As the number of factors increases, this approach becomes highly inefficient to identify an acceptable solution.

Therefore, it has been merely superseded by statistical experimental design methodology known as Design of Experiments (DoE) (Barmpalexis *et al*., 2010). DoE is a general approach that can be used effectively for optimizing such systems. The primary goal of DoE is to determine the maximum information regarding the response variables affected by input parameters by using as few experimentations as possible (Lundstedt *et al.*, 1998; Ozdemir *et al.*, 2011).

Among the various DoE techniques, Response Surface Methodology (RSM) is the most frequently used optimization technique (Mandal *et al*., 2007). It is a widely practiced approach in the development and optimization of pharmaceutical dosage forms. RSM design is usually used to study the quadratic effects of factors. Central Composite Design (CCD) is the most commonly used RSM design as it saves time of experimentation and resources available (Roosta *et al*., 2014).

Central Composite Design contains an imbedded (2^k) factorial design augmented with a group of star points (2k) and a "central" point. The star (axial) points allow estimation of curvature and establish new extremes for the low and high settings for all the factors **(**Singh *et al.*, 2004; Techapun *et al*., 2002). It effectively combines the features of both factorial designs and the star design (Hamed and Sakr, 2001).

The total number of factor combinations in a CCD is given by $2^k + 2k + c_p$, where k is the number of independent variables, and c_p is the number of repetitions of the experiments at the center point **(**Celebi *et al*., 2008**).** The replicates at the center provide an independent estimate of the experimental error. All factors were studied at five levels: α, -α (axial points), +1, -1 (factorial points) and 0 (central point) and α-values depending on the number of variables and can be calculated by $\alpha=2^{k/4}$.

Hence for two factors, viz., disintegrant concentration: X_1 and CF: X_2, α=1.4142 was used (Singh *et al*., 2011; Savic *et al*., 2014) to optimize the varied response variables. Therefore, 13 formulations of CF to disintegrant concentration combinations were obtained from the CCD. All the 13 experiments were performed in a randomized order. Tablet hardness, friability and disintegration time were included as response variables. The optimization study was carried out using Design-Expert software (Version 8.0.7.1, Stat−Ease Inc, Minneapolis, MN).

2.2.10. Statistical analysis

Statistical analysis was performed using Analysis of Variance (ANOVA) with statistical software Origin 8 (Origin Lab™ Corporation, USA). Tukey multiple comparison test was used to compare the individual difference in the physicochemical properties of the starches and tablet properties. At 95% confidence interval, p values less than or equal to 0.05 were considered statistically significant. The optimization results were analyzed using Design-Expert software (Version 8.0.7.1, Stat- Ease Inc, Minneapolis, MN). The results are reported as mean and standard deviation (SD).

3. RESULTS AND DISCUSSION

3.1. Chemical composition of starch

Starch yield on dry weight basis was found to be 80.4% ± 0.45. Thus, starch is the major constituent of *P. edulis* tuber. The proximate composition and selected properties of *P. edulis* and potato starch granules are shown in Table 3.1. The quantity of protein and lipid associated with the starch depends on botanical origin of the starch and its processing during extraction. The lipid and protein content of *P. edulis* starch was significantly higher than potato starch ($p \leq 0.05$). The low amounts of proteins and lipids are typical of tuber and root starches (Charles *et al.*, 2004). However, its ash content was significantly lower than potato starch ($p \leq 0.05$), showing that the mineral content of *P. edulis* starch is lower than potato starch.

Moisture is known to affect a wide range of physico-mechanical properties of pharmaceutical formulations including powder flow, compressibility/compactibility, hardness of granules and tablets, die-wall friction and stability (physical, chemical and microbiological) (Hoag *et al*., 2008). Their moisture contents were comparable (i.e., 11.2% and 12.3% for *P. edulis* and potato starch, respectively).

Table 3.1: Proximate composition and some physicochemical properties of *P. edulis* and potato starch granules

Content (%)	*P. edulis* starch	Potato starch
Amylose	30.6 ± 0.62	28.8 ± 0.04
Ash	0.14 ± 0.01	0.30 ± 0.03
Protein	0.43 ± 0.03	0.15 ± 0.05
Lipid	0.21 ± 0.03	0.10 ± 0.02
Starch	99.2 ± 0.02	99.45 ± 0.02
Moisture	11.2 ± 0.17	12.3 ± 0.21
pH (in 2% dispersion)	6.6 ± 0.30	6.9 ± 0.01
Hydration capacity (g/g)	1.9 ± 0.14	1.73 ± 0.05

The relative amounts of the two homopolymers (D-glucose) of starch, amylose (linear) and amylopectin (branched), varies depending on its botanical source. Amylose, in aqueous solution, strongly interacts with iodine (I^{-3}) to form a blue coloured helical complex (λ_{max} 600–610 ηm). Amylopectin, on the other hand, weakly interacts with iodine (I^{-3}) to form a violet coloured complex (λ_{max} 530–540 ηm). Hence, this difference in the "iodine binding capacity" was used for the estimation of amylose content of the starch samples (Gebre-Mariam and Schmidt, 1996a). In this

work, amylose and amylopectin solutions as well as their mixtures stained with Lugol's solution showed linear relationship between absorption and concentration at 600 ηm and 540 ηm, respectively. The absorption coefficients of amylose and amylopectin ($\mu g.ml^{-1}.cm^{-1}$) were $20.4x10^{-2}$ and $1.8x10^{-3}$, respectively. The absorption coefficient of the various mixtures of amylose and amylopectin at 600 ηm was 17.7×10^{-2}. Thus, the amylose content of the starch was determined at 600 ηm without significant interference from the amylopectin.

Accordingly, the amylose content of *P. edulis* starch was found to be 30.6%. The corresponding value of potato starch was 28.8% (Table 3.1), which is in agreement with 29.3% (Gebre–Mariam and Schmidt, 1996a). However, there was no significant difference between the starches ($P>0.05$). Figure 3.1 shows the standard linear curve for amylose content determination ($A = 0.06897 + 0.01634C$; $R^2= 0.9994$; where A is absorbance (dimensionless), C is concentration of amylose (µg/ml)).

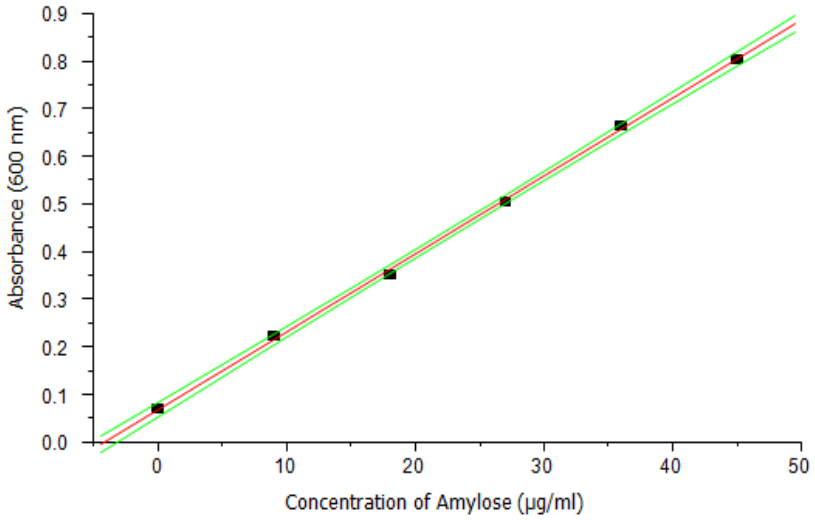

Figure 3.1: Standard linear curve for amylose content determination (600 ηm).

Hence, the result shows almost comparable chemical composition between *P. edulis* and potato starches, indicating that the effects of these components is low on swelling, crystallinity and on other related physicochemical properties of *P. edulis* starch.

3.2. Physicochemical characterization of the starch

3.2.1. Morphological characterization

Particle morphology is an important property in the characterization and identification of, especially powdered pharmaceutical excipients. It can also be used to predict certain functional properties that

relate particularly to flowability and compactibility of the powder and disintegrating characteristics of tablets (Builders *et al.*, 2013).

As can be seen from Figure 3.2., the granules of *P. edulis* have characteristic morphology- oblong (elliptical) and with some oval in shape, and existing as a single entity. The surface of the granules is smooth, but some exhibit fissure (cracks) when viewed at larger magnifications. These cracks or damage could be due to aging of the plant during starch isolation, as it has been previously reported (Vasanthan *et al*., 1999). The scanning electron micrographs of *P. edulis* starch is depicted on Figure 3.2.

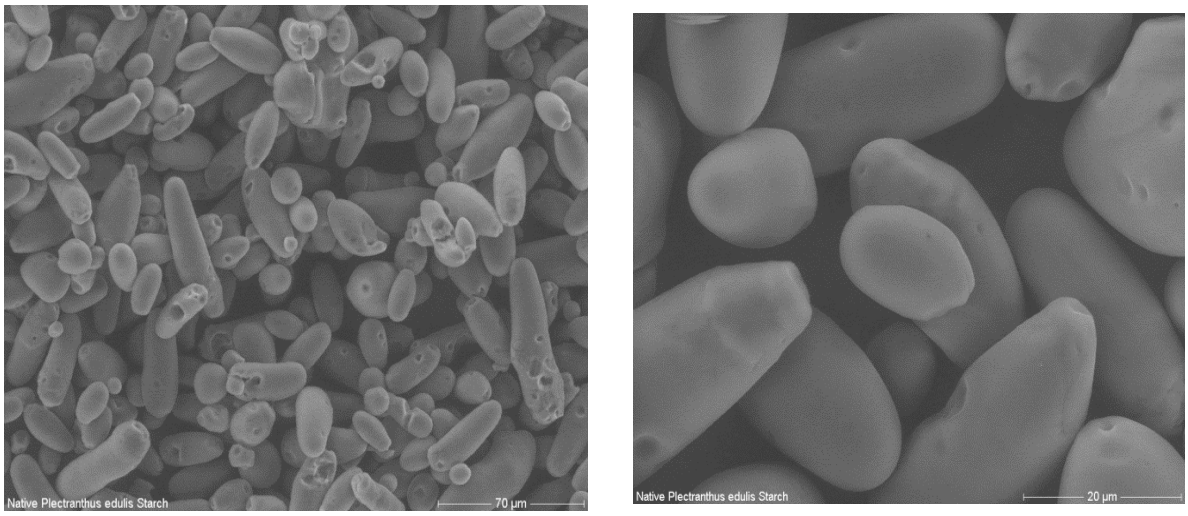

(A) (B)

Figure 3.2: Scanning electron micrographs of *P. edulis* starch granules; (A) lower magnification (70 µm scale bar); and (B) higher magnification (20 µm scale bar).

3.2.2. Granule size and specific surface area

The particle size and surface area of starch can affect the flow and tableting properties (Singh *et al.*, 2006). The volumetric particle size distribution of *P. edulis* and potato starch is depicted in Figure 3.3 and Table 3.2. The mean volumetric particle sizes of *P. edulis* and potato starches were found to be 36.20 µm and 41.51 µm, respectively. The volumetric particle size of *P. edulis* starch is slightly smaller than the potato starch. Due to this relatively smaller particle size, *P. edulis* starch has a higher specific surface area than potato starch. Hence, *P. edulis* starch is expected to have poor flowability as compared to potato starch. The exposure of larger surface of a granule to more number of particles results in resistance to flow of the individual particles (Muazu *et al*., 2011). This relatively lower flow property of *P. edulis* starch was characterized by its lower bulk densities as can be seen from Table 3.4 (section 3.2.5). It is however pertinent to note that particle size is not the only

factor affecting the flow of powders; moisture content, shape and surface charge of particles are known to retard flow properties of powders.

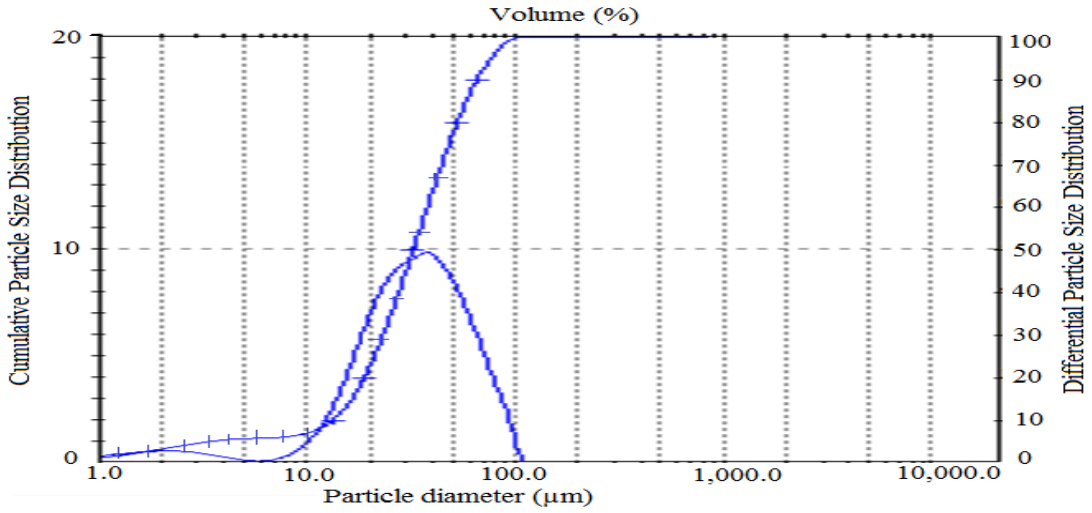

(A)

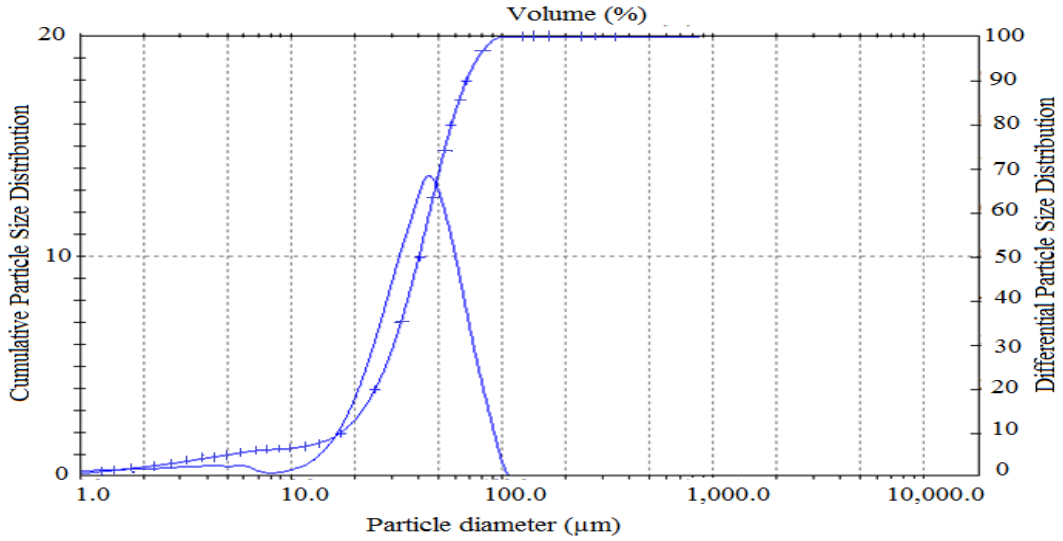

(B)

Figure 3.3. Volumeteric granule size distribution of *P. edulis* starch (A) and Potato starch (B).

Table 3.2. Granule size and size distribution of *P. edulis* starch and potato starch

Parameters	***P. edulis***	**Potato**
Average particle size (µm)	36.20 ± 20.9	41.51 ± 20.1
50% of the particles	<32.60 µm	<40.54 µm
10% of particles	<13.30 µm	<17.14 µm
90% of particles	<65.90 µm	<68.22 µm
Specific surface area (m^2/g)	0.30	0.24

3.2.3. Crystallinity of the starch

Starch has a definite crystalline nature and the crystallinity has been attributed to the well ordered structure of the amylopectin molecules inside the granules (Buléon *et al*., 1998).

The X-ray powder diffractograms of *P. edulis* and potato starch are presented in Figure 3.4, which show similar peaks for both starches (B-pattern). The starches exhibited maximum peaks at 17.5° *2θ.* The other significant peaks were at 4.5°, 14.5°, 19.5°, 22.2°, and 24.6° 2θ confirming typical B-type patterns. Thus, *P. edulis* starch has B-type X-ray diffractograms like other tuber starches.

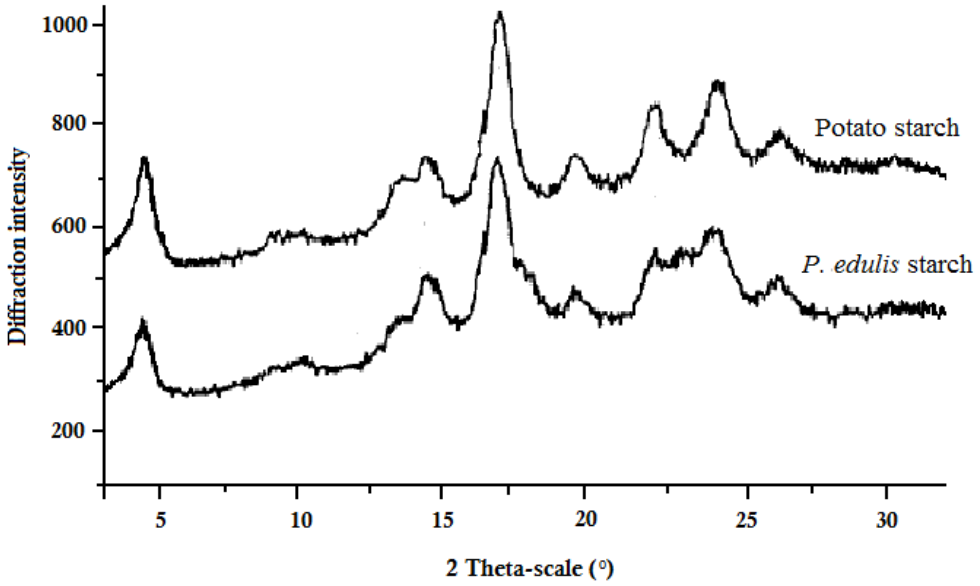

Figure 3.4: X-ray powder diffractograms of *P. edulis* and potato starches.

3.2.4. Differential scanning calorimeter (DSC) study of gelatinization

DSC provides an accurate, easy and reproducible method for the determination of the onset temp (T_o), peak temp (T_p), endset temp (T_e) and the enthalpy (ΔH_{gel}) of gelatinization. DSC gelatinization endotherms (T_o, T_p, T_e and ΔH_{gel}), however, are dependent on experimental conditions like availability of water for hydrating the starch granules and rate of heating (Moorthy, 2002). The starch samples were therefore, equilibrated with the specific amount of water for 24 h before DSC thermograms were conducted. The temp range of 20-110 °C at a heating rate of 10 °C/min was employed.

Figure 3.5 shows the DSC thermograms of *P. edulis* and potato starches analysed at a starch-water ratio of 1:1. As shown in Figure 3.5 and Table 3.3, the DSC thermograms (T_o, T_p and T_e) of *P. edulis* starch are higher than potato starch. As the gelatinization temp reflects the degree of orderly

arrangement of the molecules in the starch granules (Gebre–Mariam and Schmidt, 1996a), it may be assumed that *P. edulis* starch is less fragile than potato starch. Starch composition (amylose/amylopectin ratio, lipid complexed amylose chain, and phosphorus) and granule architecture (crystalline/amorphous ratio) have been known to influence the degree of gelatinization (Ratnayake *et al.*, 2002).

Gelatinisation enthalpy (ΔH_{gel}) depends on a number of factors such as crystallinity, intermolecular bonding, amylose/amylopectin ratio, amylopectin chain length, size and shape of the starch granules, genetic and environmental factors, etc (Singh *et al.*, 2006). For *P. edulis* starch, gelatinization enthalpy was about 3.809 J/g, whereas that of potato starch was 4.999 J/g. Since amylopectin has more crystalline nature, slightly higher amylopectin content of potato starch (Table 3.1) has been considered to be contributing to its higher enthalpy of gelatinization (Table 3.3).

Table 3.3: Gelatinization parameters of *P. edulis* and potato starches

Starch	Parameters				
	T_0 (^oC)	T_p (^oC)	T_e (^oC)	ΔH_{gel} (J/g)	ΔT (T_e-T_o)
P. edulis	69.2	74.3	83.3	3.81	14.1
Potato	62.5	68.3	79.4	5.00	16.9

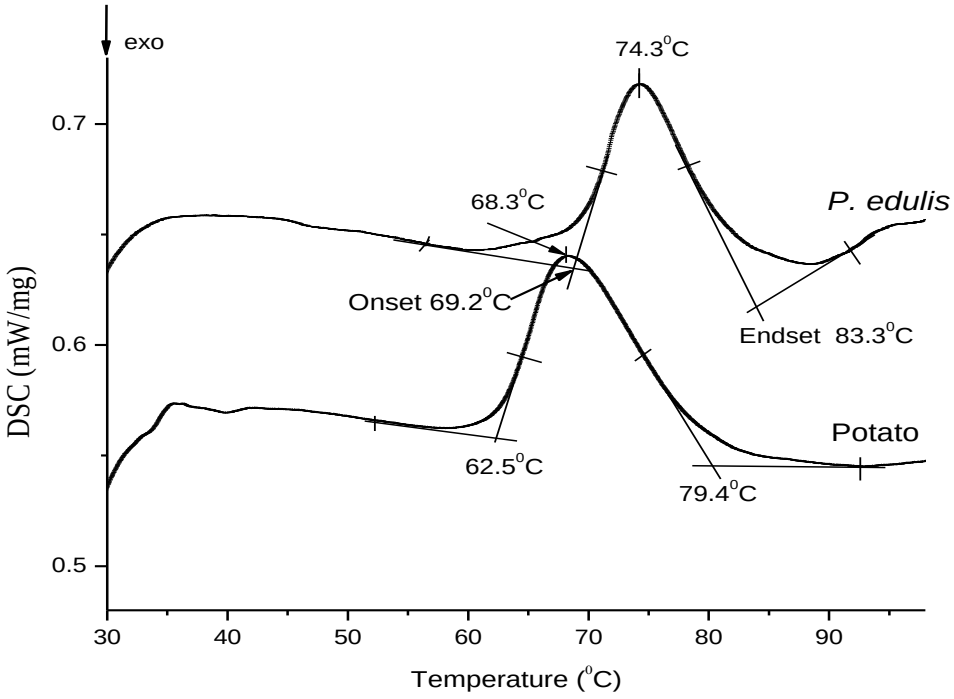

Figure 3.5: DSC thermograms of *P. edulis* and potato starches.

The narrow ΔT value for *P. edulis* starch as compared to potato starch could be due to its more uniform particle size distributions. Higher range has been attributed to a higher level of crystallinity (the proportion of long chain length amylopectin structures), which imparts higher structural stability so that the water molecules need longer time to penetrate the crystalline area (Moorthy, 2002).

3.2.5. Density and related properties

Powder properties are important parameters in manufacturing of solid dosage forms. The properties are determined by a combination of powder characteristics (i.e., particle size, size distribution, density, and surface properties) and operating conditions (moisture) (Sinka *et al*., 2004). For good tablets to be manufactured, the powder blend has to flow uniformly and form firm compaction. Good flowability ensures uniformity in die fill and thus uniformity in tablet weight. It also facilitates blending of fine powders encountered in direct compression blends (Atichokudomchai and Varavinit, 2003).

The absolute and relative densities of pharmaceutical solids play an important role in determining their performance (e.g. flow and compaction properties) in tablet dosage forms. The angle of repose could be used as a quantitative measure of the cohesiveness or the tendency of powder to flow. Angles of 30^{o} or below are usually indicative of free flowing materials while an angle of 40^{o} or above indicates a poor flow. Angle of repose is affected by the particle size distribution and it usually increases with a decrease in particle size. Bulk and tapped densities give an insight on the packing arrangement of the particles and the compaction profile of a material (Sarangapani and Rajappan, 2012). So, they can provide information on the flowability of powders and are used to calculate the Carr's index and Hausner ratio, which are a measure of the compressibility and flowability of a powder (Odeku and Picker-Freyer, 2009). Powders with high values of compressibility index are considered as materials with poor compressibility, indicating also relatively high inter-particle interactions. Concerning the Hausner ratio, the higher the ratio, the greater will be the tendency of the powder to densify during tableting (Jubril *et al*., 2012).

The density and its derived properties such as percent compressibility and Hausner ratio of *P. edulis* and potato starches are shown in Tables 3.4. The two starches have comparable true densities. The bulk and tapped density of *P. edulis* starch is lower than potato starch ($p<0.05$). This difference observed in the bulk and tapped density values could be due to the different particle size and shape which affect the packing arrangement of the powder particles (Schüssele and Bauer-Brandl, 2003).

The Carr's index of *P. edulis* is significantly higher than that of potato starch ($p<0.05$), but their Hausner ratio values are almost comparable ($p>0.05$). Therefore, *P. edulis* starch has comparable flowability, but lower compressibility to the potato starch.

Generally, *P. edulis* and potato starch possess Carr's compressibility index less than 15 and Hausner ratio of less than 1.25, implying that both starch granules have acceptable flow property (Schüssele and Bauer-Brandl, 2003).

Table 3.4: Density and related properties of *P. edulis* and potato starches

Parameters	*P. edulis* starch	Potato starch
True density (g/ml)	1.47 ± 0.02	1.48 ± 0.01
Bulk density (g/ml)	0.66 ± 0.017	0.73 ± 0.021
Tapped density (g/ml)	0.73 ± 0.021	0.76 ± 0.023
Carr's index (%)	9.84 ± 0.54	5.08 ± 0.160
Hausner ratio	1.10 ± 0.003	1.05 ± 0.002

3.2.6. Fourier transform infrared (FTIR)-spectral feature

The FTIR spectra of *P. edulis* and potato starch are shown in the Figure 3.6. The band absorbances in starch have been assigned and matched with the vibrational modes of the chemical bonds and the structures of starch molecules by many researchers.

The FTIR spectrum of starch samples was described by seven main modes, with maximum absorbance peaks near 3,500, 3,000, 1,600, 1,400, 1,000, 700 and 500 cm^{-1} (Sitohy *et al.*, 2000; Koksel *et al.*, 2008), and all these peaks were observed in the *P. edulis* and potato starches.

Extremely broad band appeared around 3,000–3,600 cm^{-1} in both *P. edulis* starch and potato starch, which is attributed to the complex vibrational stretches associated with free, inter and intra-molecular bound OH groups which make up the gross structure of starch. Both starches have shown peaks at about 3325, 3161 and 3110 cm^{-1} which is attributed to O–H stretching, but the broad band vibration of O–H group of the starches at 2930 cm^{-1} is merged with the extremely intense C–H stretching band of the mulling agent, Nujol. The peaks at 1462 cm^{-1} and 1377 cm^{-1} were attributable to the bending modes of H–C–H, C–H and O–H. The two peaks of 1155 and 1078 cm^{-1} were associated to represent the C–O stretching (Zeng *et al.*, 2011), whereas, bands at 983, 933 and 860

cm^{-1} represent (C-O-C) skeletal mode vibration of glycosidic linkage. The bands between 765 and 520 cm^{-1} represent skeletal mode of pyranose ring (Sekkal *et al*., 1995; Kemas *et al.*, 2012).

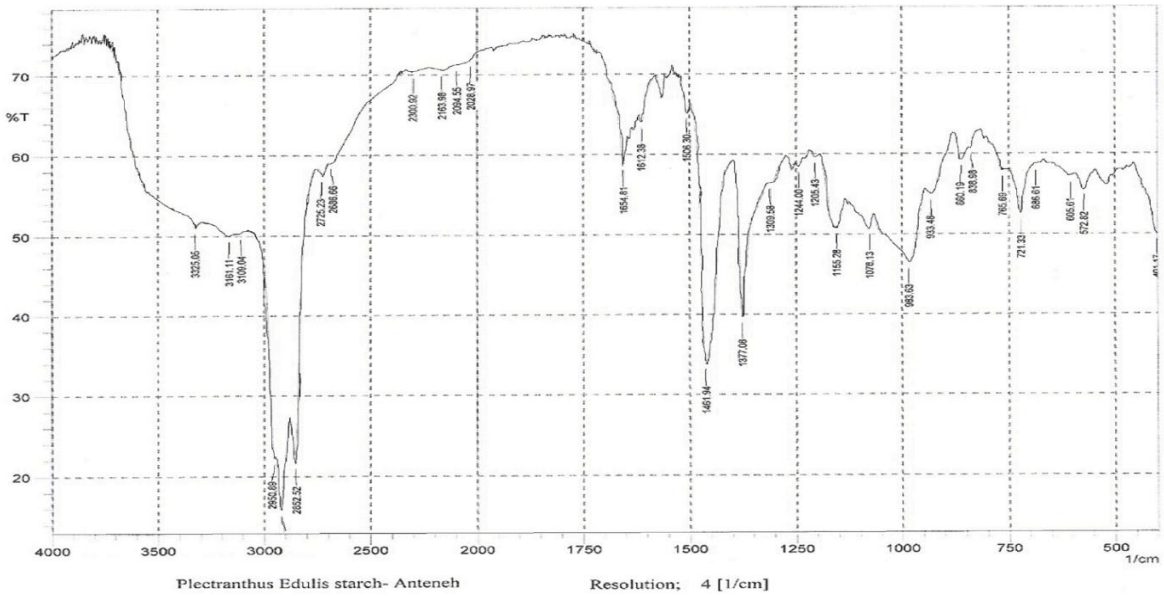

(A)

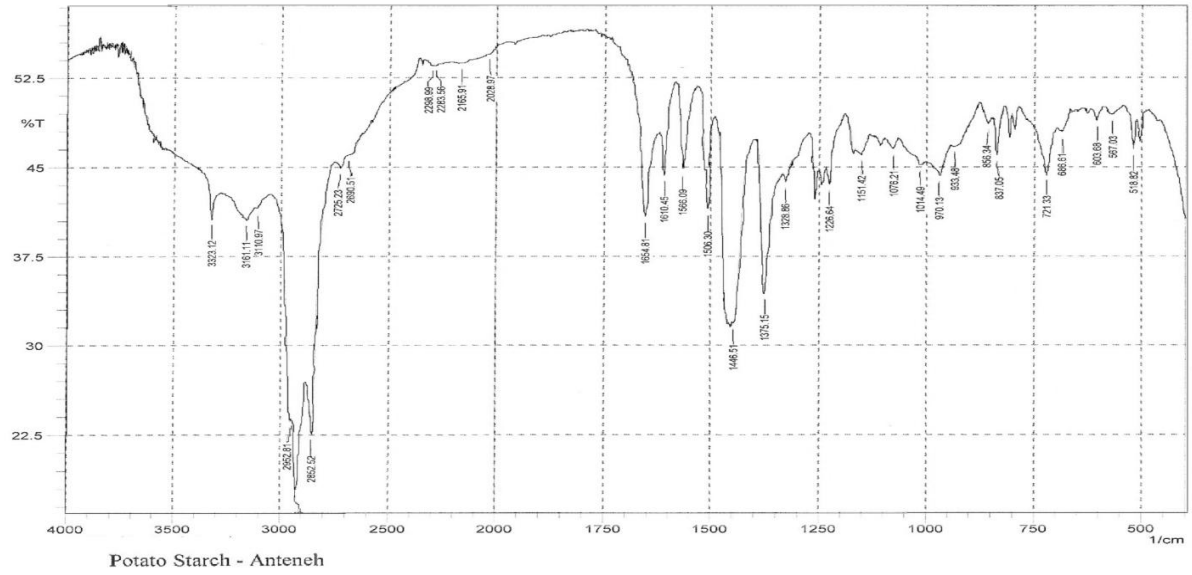

(B)

Figure 3.6: FTIR Spectra of (A) *P. edulis* starch and (B) potato starch

3.2.7. Hydration capacity

The hydration of starch represents the water absorbed by the particle or the particle surface (Ohwoavworhua *et al.*, 2007). Hydration capacity of *P. edulis* starch (1.9) was higher than that of the potato starch (1.73) as depicted in Table 3.1, which followed the particle size of the starches. Due to

its smaller particle size (Table 3.2), *P. edulis* starch has larger surface area for absorption of water. Statistically, the hydration capacity of *P. edulis* starch was significantly higher than that of potato starch ($p< 0.05$).

3.2.8. Swelling power and solubility of starch

When aqueous dispersions of starch granules are heated, the starch molecules hydrate and swell with a consequent leaching of some soluble starch into the liquid. Swelling power indicates the water holding capacity of starch and has generally been used to demonstrate various types of starches. It provides evidence of non-covalent bonding between starch molecules. Bonding forces within the granules of a starch affect the degree of swelling and the amount of leaching. Thus, highly associated starch granules with an extensive and strongly bonded micellar structure should display relatively greater resistance towards swelling. Factors like amylose-amylopectin ratio, chain length and molecular weight distribution, degree/length of branching and conformation (Chen, 2003), and their non-carbohydrate (i.e., lipid and protein) contents determine the degree of swelling and solubility (Schoch, 1994).

The swelling power and solubility profiles of *P. edulis* and potato starch are shown in Figure 3.7 and Table 3.5, respectively. Comparative studies have shown strong positive correlations between starch swelling and amylose content as well as amylose leaching (Zuluaga *et al.*, 2007). The higher swelling power of *P. edulis* starch has positively correlated with its slightly higher amylose content (Table 3.1).

Granule size and specific surface area have been found to affect the swelling pattern of starches. Small granules are associated with a higher rate of water absorption, earlier hydration and more swelling than are larger granules (Chiotelli and Meste, 2002). Greater specific surface area may also contribute to the higher water absorption of small starch granules (Chiotelli and Meste, 2002). The higher swelling power of *P. edulis* starch is therefore associated with its smaller granule size (36.2 *versus* 41.5 µm) and higher specific surface area (0.302 *versus* 0.24 m^2/g) than potato starch (section 3.3.2).

The swelling power and solubility of the starches was found to be affected by an increase in temp (Loss *et al.*, 1981). As expected, the swelling power and solubility of the *P. edulis* and potato starches increased with an increase in temp (20-85 ^oC). The swelling power of *P. edulis* starch was found to be significantly ($p<0.05$) higher than that of potato starch at lower temp (20-50 ^oC). For instance, the swelling power of *P. edulis* starch was 2.3 g/g as compared to 1.7 g/g for potato starch,

at 37.5 ^{o}C. At higher temp, there is a large increase in the extent of swelling and solubility, due to disruption of intermolecular hydrogen bonds which maintain the structural integrity of the granules leading to more substantial loss of amylose and amylopectin from the granules. Water molecules solvate the librates hydroxyl groups and the granules continue to swell. As a consequence of severe disruption of hydrogen bonds, the granule will be fully hydrated and finally the micellar network separates and diffuses into the aqueous medium (Hashim *et al.*, 1992).

The profiles have shown a three stage swelling pattern with an increase in temp. This is an indication of the water absorption characteristic of the granules during heating. There is first, a slight increase from 20-50 ^{o}C, and then strong increase from 50-65 ^{o}C followed by a slight level off till 75 ^{o}C and then another rapid increase from 75-85 ^{o}C. This pattern has been attributed to the various internal bonding forces that relax at different temp (Loss *et al.*, 1981). *P. edulis* and potato starches show almost comparable swelling powers at the elevated temp ($p>0.05$).

The increase in swelling power is indicative of suitability of a starch being used as a disintegrant in the pharmaceutical industry (Chowdary *et al.*, 2011). There is a comparable swelling property between *P. edulis* and potato starches; and thus *P. edulis* starch is expected to show comparable disintegration profile to potato starch in tablet formulation. In addition, high swelling power also results in high digestibility and ability to use starch in solution suggesting improved dietary properties and the use of starch in a range of dietary applications (Nuwamanya *et al.*, 2010); this confirms the applicability of *P. edulis* starch in other industries.

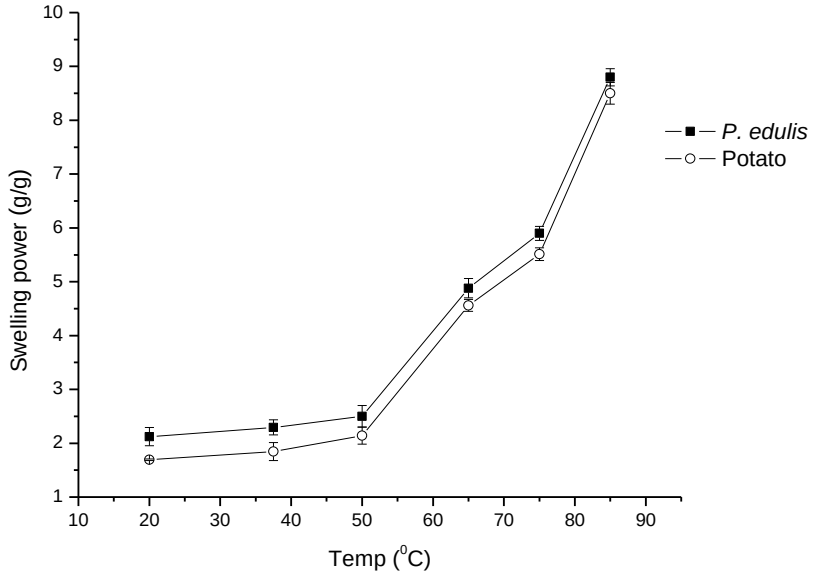

Figure 3.7: Swelling power of *P. edulis* and potato starches at different temps

The solubility of *P. edulis* and potato starch increased with temp. Potato starch have shown higher solubility than *P. edulis* at all temps studied. A complex set of factors contribute to this difference in solubility of the starches: the source, inter-associative forces within starch granules, the difference in swelling power and chemical composition (lipid and protein), etc. of the starches.

Table 3.5: Solubility of *P. edulis* and potato starches at various temps

Temp (^{o}C)		20	37.5	50	65	75	85
Solubility (g/g)	*P. edulis*	1.10± 0.25	3.80±0.20	4.80±0.45	10.5±0.95	13.2±0.81	19.7±1.82
	Potato	1.13 ±0.51	4.23±0.23	5.30± 0.44	12.5±0.50	16.3±0.70	22.5±1.52

3.2.9. Moisture sorption properties

An understanding of the moisture sorption characteristics of pharmaceutical excipients is imperative since most of physicochemical and functional properties of these materials either depend or are affected by it. Moisture may also induce unpredicted phase transitions in excipients which may also be imparted to the APIs when used in formulation. Generally, when starch is exposed to a moisture rich environment, the water molecules interact strongly with the polar groups of the amylose and amylopectin units, forming a monomolecular layer (Builders *et al.*, 2013).

Hygroscopic materials can experience significant increase in moisture content when exposed to humid air (Hoag *et al.,* 2008). Starch has been classified as a moderately hygroscopic material. The moisture sorbed has been attributed to intra- and intermolecular hydrogen bonding of water with the hydroxyl groups of the starch molecule. Moisture is known to modify the flow and mechanical properties of many powders including starches (Hancock and Shamblin, 1998). Therefore, knowledge of moisture sorption profiles of starches is necessary where controlled powder flow or compaction and disintegration of tablet are critical. Figure 3.8 shows the moisture sorption profiles of *P. edulis* and potato starches equilibrated at different relative humidity (RH) for four weeks.

As can be seen from Figure 3.8., *P. edulis* starch shows slightly higher moisture sorption profile than potato starch at all RH values studied. However, this difference is not statistically significant ($p>0.05$).

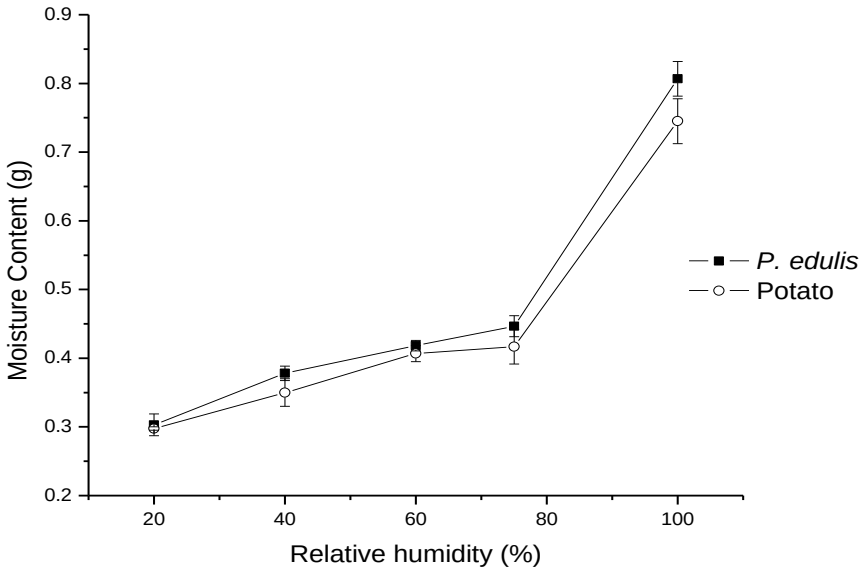

Figure 3.8: Moisture sorption pattern of *P. edulis* and potato starches

Higher moisture sorption of starch may indicate a possible higher susceptibility to moisture induced changes in quality (Adikwu, 1998). Therefore, *P. edulis* starch needs good control of moisture as compared to potato starch for its functional and mechanical properties to be maintained.

The higher capacity of starch to absorb water was indicated to facilitate disintegration (Jubril *et al.*, 2012). The result of moisture sorption profile together with swelling power reveals that *P. edulis* starch might have a favorable (or comparable) disintegrant property to potato starch in tablet formulation.

3.3. UV calibration curve of paracetamol

From stock solution of 200 µg/ml of paracetamol in phosphate buffer (pH 5.8), standard calibration curve was plotted at six different concentrations (2, 4, 6, 8, 10 and 12 µg/ml). The absorbance (at 243 nm) versus concentration of the solutions was plotted and a calibration curve with a linear regression equation of: $Y = 0.0678X + 0.0264$ (where Y is the absorbance and X is the concentration in µg/ml) and correlation coefficient of 0.9993 was obtained (Figure 3.9).

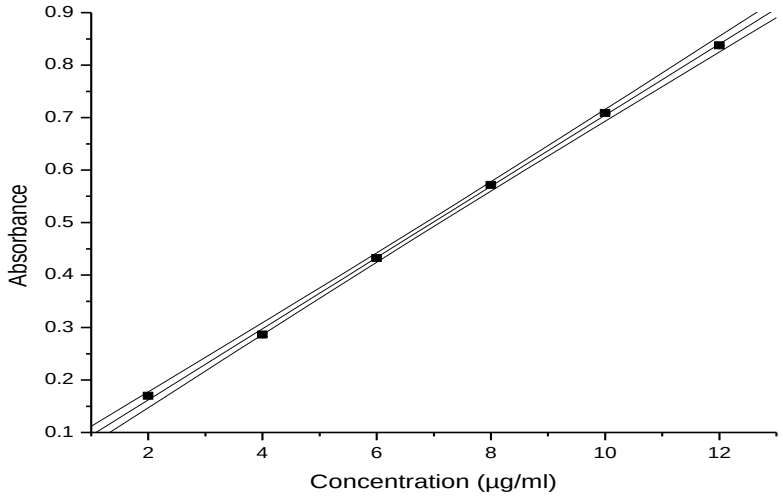

Figure 3.9: Standard calibration curve of paracetamol in phosphate buffer (pH 5.8) at 243 nm with 95% confidence bands for the mean; (R^2 = 0.9993).

3.4. Drug-excipient compatibility study

3.4.1. Fourier transform infrared (FTIR) study

FTIR Spectroscopy is an extremely effective method for identifying compounds. Its spectrum for a given compound is unique and characteristic (Philip *et al*., 2010). The FTIR spectra paracetamol pure drug and physical mixture (1:1) of paracetamol and *P. edulis* starch are shown in Figure 3.10 A and B, respectively.

Characteristic peaks of paracetamol are at 3400−3200 cm^{-1} (O−H stretching), 3500-3100 cm^{-1} (N−H stretching) and 1680−1630 cm^{-1} (C=O stretching); whereas amide II band at (1750−1515 cm^{-1}), C−N−H group (1350–1000 cm^{-1}) and the aromatic ring (C=C stretching bands from 1600–1450 cm^{-1}) and para-disubstituted aromatic ring (850−75oCm^{-1}) (Talegaonkar *et al.,* 2007; Bashar, 2010).

The observed characteristic peaks of paracetamol are at 3323.12 cm^{-1} (O-H stretching), 3159.18 cm^{-1} (N−H stretching) and 1654.81 cm^{-1} (C=O stretching of the carboxyl ion). Whereas, amide II band stretching at 1564.16 cm^{-1}, C−N−H group at 1259.43 cm^{-1} and para-disubstituted aromatic ring at 796.55 cm^{-1} were observed confirming the purity of the drug as per established standards.

The O−H stretching peak of paracetamol from 3400-3000 cm^{-1} was merged with broad band absorption of free, inter and intra-molecular OH groups of the starch. The OH stretching band at 3323 cm^{-1} in the spectrum paracetamol was also observed in the spectrum of its mixture with the starch. But it is difficult to differentiate whether the band is from the phenolic OH group of

paracetamol or of OH the starch. The absorption band at 3159.18 cm^{-1} (N–H stretching) and 1654.81 cm^{-1} (C=O stretching) appeared in the spectrum of the physical mixture of paracetamol and *P. edulis* starch. The C-H stretching band of paracetamol at about 2900-3000 cm^{-1} was merged with very intense absorption band of C-H of the mulling agent (nujol) in both the spectra of the pure drug and the physical mixture of paracetamol with *P. edulis* starch.

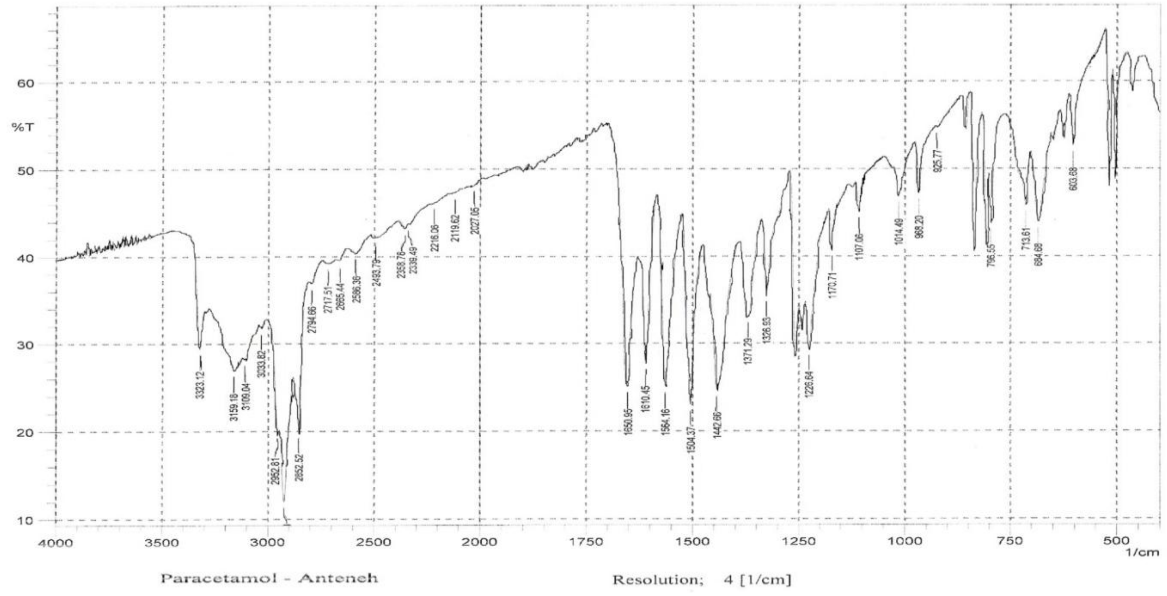

(A)

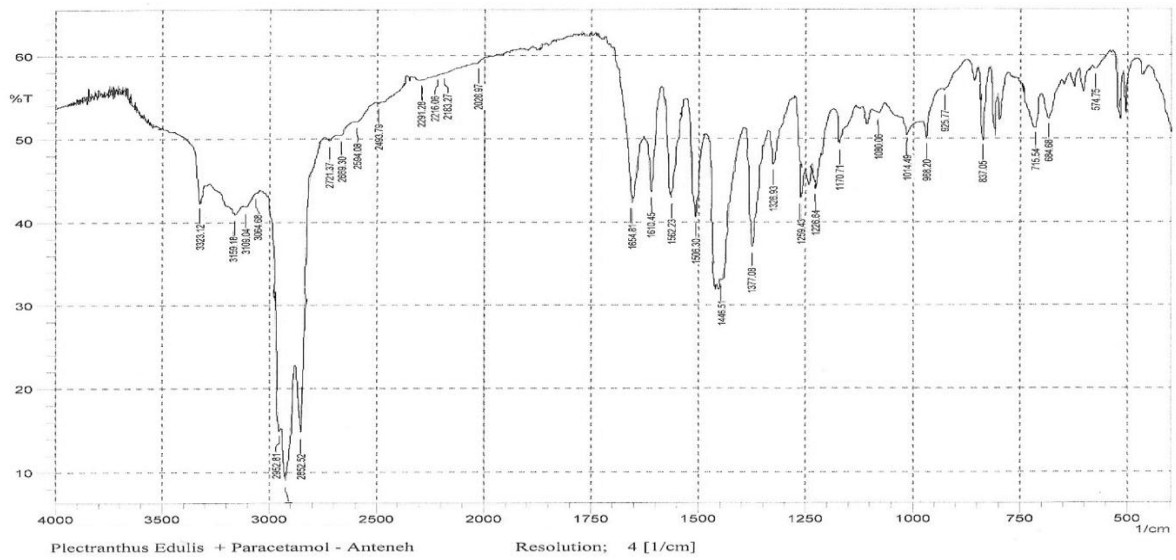

(B)

Figure 3.10: The FTIR spectrum of paracetamol alone (A) and physical mixture of paracetamol and *P. edulis* starch (B).

Therefore, the FTIR study of paracetamol and physical mixture of paracetamol and *P. edulis* starch could be possible indicator of absence of incompatibility between the two substances. Therefore, other methods of the drug-starch compatibility study such as, DSC study should be undertaken to further confirm the absence or extent of interaction between the two substances.

3.5. Characterization of granules and tablets

3.5.1. Granule particle size distribution

Despite the technical progress in tableting technology, the pharmaceutical properties of tablets are still controlled by the granules used in the formulation (Miyamoto *et al.*, 1998). Granule size distribution of paracetamol prepared with *P. edulis* starch and potato starch at different disintegrant concentrations are shown in the Figure 3.11.

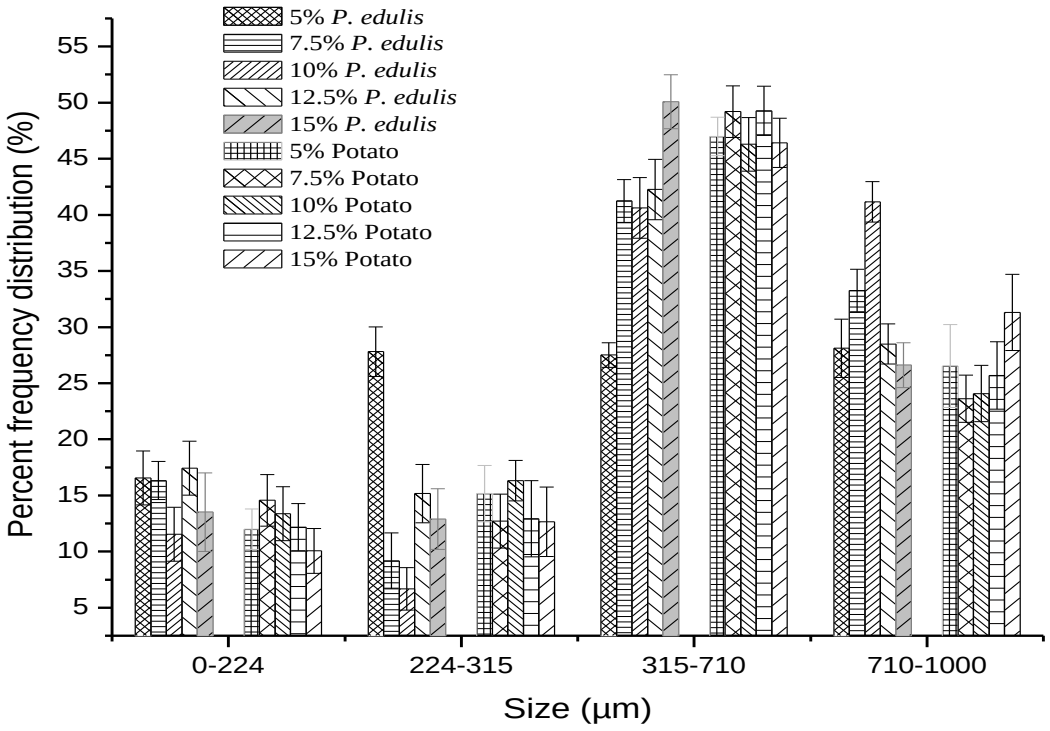

Figure 3.11: Percent frequency distribution by weight of paracetamol granules at different disintegrant concentrations (50% intragranular starch).

As can be seen from Figure 3.11, there is no major difference in size distribution of paracetamol granules prepared from *P. edulis* and potato starches as disintegrants.

3.5.2. Density and related properties

The absolute and relative densities of pharmaceutical solids play an important role in determining their performance (e.g., flow and compaction properties) in tablet dosage forms. Bulk density of granulation is an indirect measure of granule flow and determines the die fill volume. Granules having high bulk density tend to densify more than those having lower bulk density and hence have lower die fill volume, which may result in tablet weight variation. Density and related properties of the paracetamol granules are presented in Table 3.6.

The Hausner ratio and Carr's index give a preview on the degree of densification, which could occur during tableting; the lower the Hausner ratio, the lesser the tendency for densification to occur. As the values of these indices increase, the flow of the powder decreases (Staniforth, 1996) and more likelihood of producing tablets with more weight variation (Olayemi *et al*, 2008).

Multiple comparison test (Tukey test) indicate that there is no significant difference between the bulk and tapped densities of granules prepared from the two starches ($p>0.05$). The table also shows that all the formulations have Carr's index below 15% implying the granules have excellent flow property. The Hausner ratios were also observed to be less than 1.25, which also confirmed good flow property of the granules (Wells, 2002). Good flow property of the granulation is necessary to ensure efficient mixing and acceptable weight uniformity in compressed tablets (Yüksel *et al*., 2003).

Table 3.6: Density and related properties and flow rate of paracetamol granules at different disintegrant concentrations (Mean ± SD, n = 3).

Property	Starch type	Disintegrant concentration (w/w)				
		5%	7.5%	10%	12.5%	15%
Bulk density (g/ml)	*P. edulis*	0.44±0.02	0.43±0.01	0.42±0.00	0.42±0.03	0.41±0.04
	Potato	0.42±0.01	0.41±0.00	0.41±0.02	0.40±0.03	0.40±0.01
Tapped density (g/ml)	*P. edulis*	0.48±0.00	0.48±0.01	0.45±0.03	0.45±0.01	0.43±0.02
	Potato	0.44 ± 0.02	0.45±0.02	0.43±0.02	0.44±0.01	0.43±0.02
Carr's index (%)	*P. edulis*	7.35±0.60	10.0±0.30	8.33±0.40	6.94±0.40	5.41±0.30
	Potato	5.56±0.50	7.04±0.30	7.90±0.50	9.33±0.80	5.40±0.20
Hausner ratio	*P. edulis*	1.08±0.02	1.11±0.04	1.10±0.04	1.07±0.03	1.06±0.02
	Potato	1.06 ± 0.01	1.08 ± 0.02	1.09 ±0.05	1.10 ±0.03	1.06 ±0.05

Flow rate (g/sec)	*P. edulis*	4.48±0.05	4.46±0.06	4.40±0.08	4.38±0.30	4.20±0.05
	Potato	4.45±0.00	4.44±0.02	3.85±0.04	3.95±0.02	3.62±0.00
Angle of repose (^{o})	*P. edulis*	29.0 ±0.04	28.0 ± 0.02	29.6 ±0.00	29.4 ± 0.10	29.2 ± 0.07
	Potato	28.5±0.02	30.0±0.01	29.2±0.00	30.1±0.00	30.4±0.01

3.5.3. Granule flow rate and angle of repose

Measurement of granule flow rate is a direct method of determining granule flowability. Both *P. edulis* and potato starches yielded granules with good flow properties (Table 3.6). The flow rate of the granules was found to decrease with an increase in disintegrant concentration. The values of angle of repose are all less than or equal to 30^o indicating free flowing properties of granules.

3.6. Tablet properties

3.6.1. Weight and thickness

The paracetamol tablets prepared with *P. edulis* and potato starch as disintegrant and compressed at different CFs were examined for their weight and thickness uniformity. The results are summarized in Table 3.7. The tablets were within acceptable range of weight variation (± 5%) as per the British Pharmacopoeia for tablets weighing 250 mg or more (BP, 2009). Since the weight of a tablet being compressed is determined by the amount of granulation in the die prior to compression, the weight uniformity could be attributed to the good flow property of the granules as indicated in Sections 3.5.1 and 3.5.2. No significant difference in weight between formulations was observed ($p>0.05$). Since the drug substance forms the greater part of the tablet mass, the weight uniformity can reflect the uniformity in the content of active ingredient. However, there was slight weight and tablet thickness variation between the various batches of formulations; this might be related to the variations in powder density as well as compression behavior of the compacted material.

Table 3.7 also shows the thickness (mm) of the tablets compressed at various CFs. For all disintegrant concentrations used, increasing CF decreased tablet thickness and formulations compressed at various CFs had significant variation in the thickness of the tablets ($p <0.05$). The difference in tablet thickness among different formulations in the present study can be attributed to the varying CF and disintegrant concentration used in tableting (Ahmed *et al*., 2001).

Table 3.7: Paracetamol tablet weight and thickness at different disintegrant concentration (DC) and compression force (CF).

DC (w/w)	CF (KN)	*P.edulis*		Potato	
		Weight (g)	Thickness (mm)	Weight (g)	Thickness (mm)
5%	10	0.305 ± 0.14	3.40 ± 0.01	0.304 ± 0.01	3.49 ± 0.04
	18	0.304 ± 0.08	3.20 ± 0.03	0.306 ± 0.00	3.29 ± 0.09
7.5%	10	0.300 ± 0.05	3.51 ± 0.02	0.303 ± 0.02	3.47 ± 0.02
	18	0.299 ± 0.07	3.42 ± 0.02	0.300 ± 0.05	3.27 ± 0.03
10%	10	0.305 ± 0.06	3.60 ± 0.08	0.302 ± 0.07	3.45 ± 0.02
	18	0.305 ±0.05	3.42 ± 0.02	0.301 ± 0.03	3.27 ± 0.01
12.5%	10	0.297 ± 0.14	3.52 ± 0.02	0.304 ± 0.00	3.52 ± 0.04
	18	0.299 ± 0.12	3.37 ± 0.06	0.303 ± 0.02	3.31 ± 0.09
15%	10	0.302 ± 0.05	3.48 ± 0.01	0.299 ± 0.12	3.47 ± 0.02
	18	0.299 ± 0.07	3.37 ± 0.06	0.301 ± 0.04	3.34 ± 0.03

3.6.2. Crushing strength and friability

The effects of the starches as disintegrating agents on the crushing strength and percent friability of paracetamol tablets at a constant binder concentration (3.5% (w/w) povidone) are shown in Figure 3.12 and Figure 3.13, respectively.

As can be seen from Figure 3.12, an increase in disintegrant concentration shows a gradual reduction in the crushing strength of the tablets. Increasing the potato starch concentration reduces progressively the tablet crushing strength. The decrease in crushing strength of the tablets at higher concentrations of disintegrants may be attributed to the poor compressibility and softening effects of the starch at higher concentrations (Gebre–Mariam and Armstrong, 1995). For tablets prepared from *P. edulis* starch, first gradual decrease in crushing strength of the tablets was observed with increase in the disintegrant concentration. After certain concentration (10-12.5%); however, no further decrease in crushing strength was observed. This is partly due to the higher amount of lipid and protein associated with *P. edulis* starch as shown in Table 3.1. Tablets prepared with *P. edulis* starch were slightly stronger than those made with potato starch. As can be seen from Figure 3.13, an increase in disintegrant concentration resulted in corresponding increase in the percent friability of the tablets. At all concentrations of the disintegrant used, tablets formulated with *P. edulis* starch had lower friability than those prepared with potato starch.

Figures 3.12 and 3.13 also show the effect of CF on the crushing strength and friability of paracetamol tablets formulated using *P. edulis* and potato starch as disintegrants. Increasing the CF

increases tablet crushing strength and decreases friability of tablets prepared from both *P. edulis* and potato starches as disintegrants. This could be due to formation of more solid bonds and enhancement of area of contact between particles leading to an increase in tablet hardness and reduction in friability (Adane *et al.*, 2006). The effect of CF on the crushing strength and percent friability differ significantly ($p<0.05$).

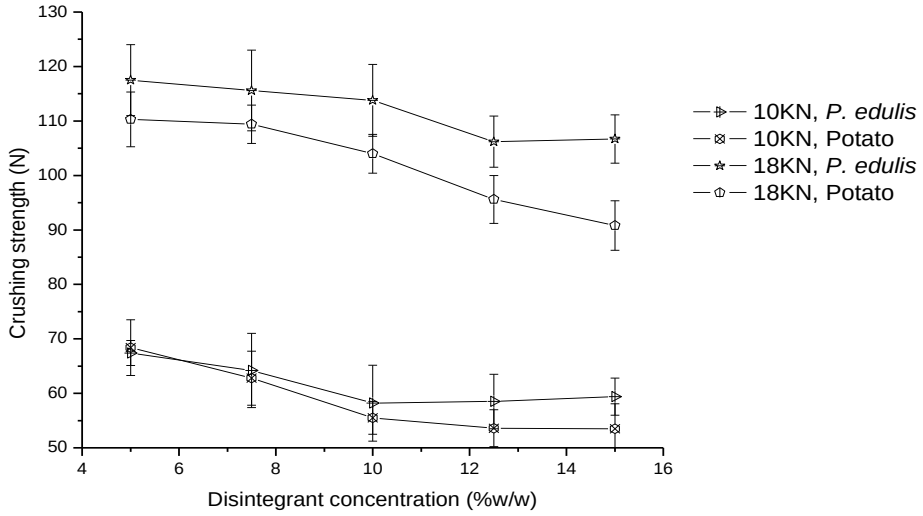

Figure 3.12: Effect of concentration of starches employed as disintegrants on the crushing strength of paracetamol tablets compressed at 10 and 18 KN.

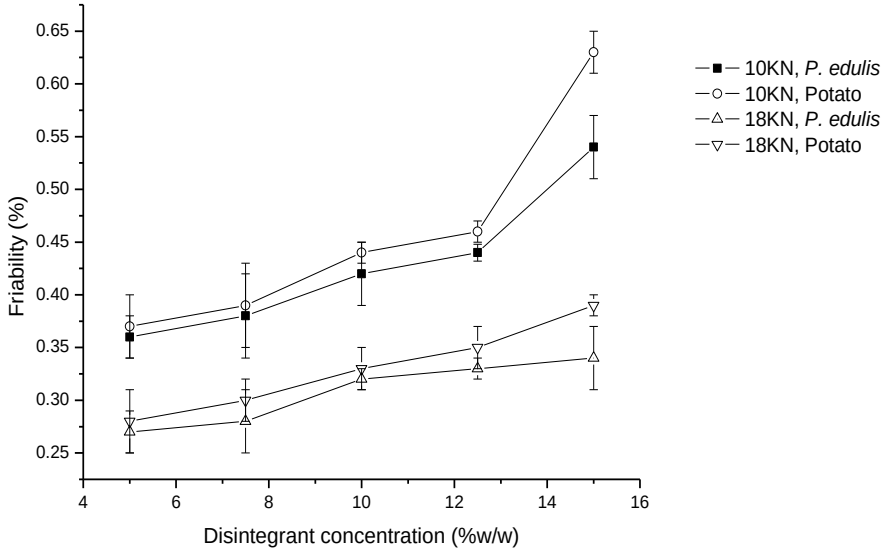

Figure 3.13: The relationship between disintegrant concentration and friability of paracetamol tablets compressed at 10 and 18 KN.

3.6.3. Disintegration time

The disintegration time of tablets formulated from *P. edulis* and potato starch at different concentrations of disintegrants is depicted in Figure 3.14. As can be seen from the figure, tablets formulated with *P. edulis* starch disintegrated faster than those formulated with potato starch (concentration 5-10%), but slightly longer disintegration time was observed thereafter for tablets with *P. edulis* starch. The rapid disintegration of the tablets with *P. edulis* starch (at low concentration) can be explained by its higher swelling, moisture sorption and hydration capacities (Figure 3.7, Figure 3.8 and Table 3.1, respectively) (Isah *et al.*, 2009; Rajeevkumar *et al.*, 2010). And the oblong shape (Figure 3.2) of *P. edulis* starch granules- providing large surface area of the starch to come in contact with the matrix of the tablet, into which water enters by capillary action (wicking action), thereby creating internal pressure which subsequently breaks up the tablet into fine particles (Musa *et al.*, 2011).

However, an increase in disintegration time with an increase in *P. edulis* starch concentration was observed for its concentration above 10%; this may be due to the higher content of protein and lipid in the starch (Table 3.1). Surface lipids and proteins affect the diffusion of water into starch granules thereby altering starch properties by reducing penetration of water and swelling of starches (Okpanachi *et al.*, 2012).

As seen in Figure 3.14, the increase in CF increases the disintegration time of paracetamol tablets formulated with *P. edulis* and potato starches as disintegrants. This increase in CF, decreases the porosity of tablets by forming more solid bridges, and hence increases in tablet strength, by enhancing the formation of a continuous interparticulate space, thereby increasing the disintegration times of the tablets (Gebre-Mariam *et al.*, 1996). This results in impeding of water penetration into tablets mass, consequently reducing the swelling of disintegrants and the development of the active mechanism of disintegration (Bi *et al.*, 1999). The disintegration time of tablets compressed at higher CF are longer than those compressed at lower CF for all the disintegrant concentrations studied. All formulations generally passed the official disintegration test for uncoated tablets, i.e., <15 min (USP 30/NF 25, 2007).

It was observed that the disintegration time decreased with increase in concentration of *P. edulis* starch up to its critical level. *P. edulis* starch was more effective in lowering the disintegration times of the paracetamol tablets especially at lower concentrations. This indicates that Ethiopian potato (*P. edulis*) starch has favorably comparable disintegrant property with potato starch.

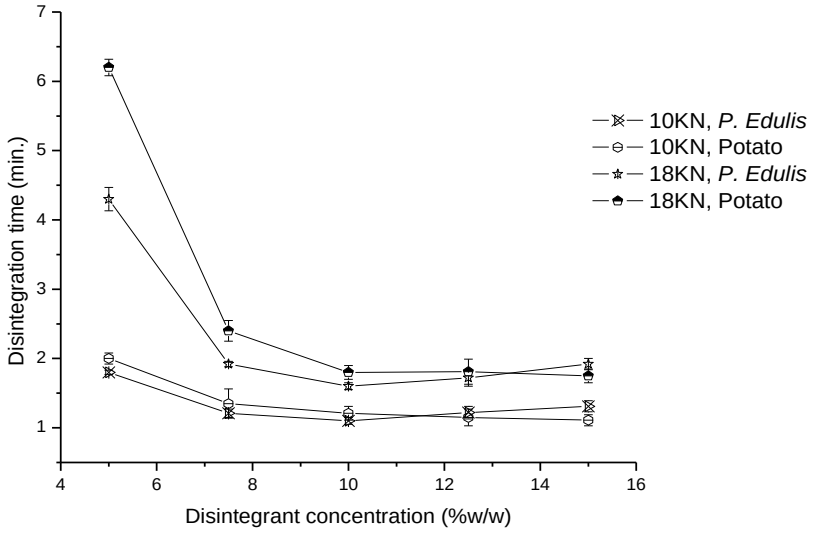

Figure 3.14: The effect of the concentration of *P. edulis* and potato starches as disintegrants on the DT of paracetamol tablets compressed at 10 and 18 KN.

3.6.4. Drug dissolution

The dissolution profiles of paracetamol tablets of low (5% (w/w)) and high (15% (w/w)) disintegrant concentrations compressed at 10 and 18 KN are shown in Figure 3.15. The figure shows that paracetamol tablets prepared with *P. edulis* and potato starch as disintegrants at the CFs studied, released more than 80% of the drug within 30 min, complying with USP 30/NF 25 (2007) specification.

Tablets having higher disintegrant concentrations and compressed at lower CF yielded a higher dissolution profile as compared with those having lower disintegrant concentration and compressed at higher CFs. However, the difference in their dissolution profiles are not statistically significant ($p>0.05$). At each disintegrant concentration, however, dissolution decreased with an increase in CF (Figure 3.15). Since CF and disintegrant concentration influenced the DT of the tablets as well as the dissolution of paracetamol tablets formulated using *P. edulis* and potato starch as disintegrants. The effects of CF and disintegrant concentration on the DT was reflected on the dissolution profiles of the tablets (Marais *et al.*, 2003).

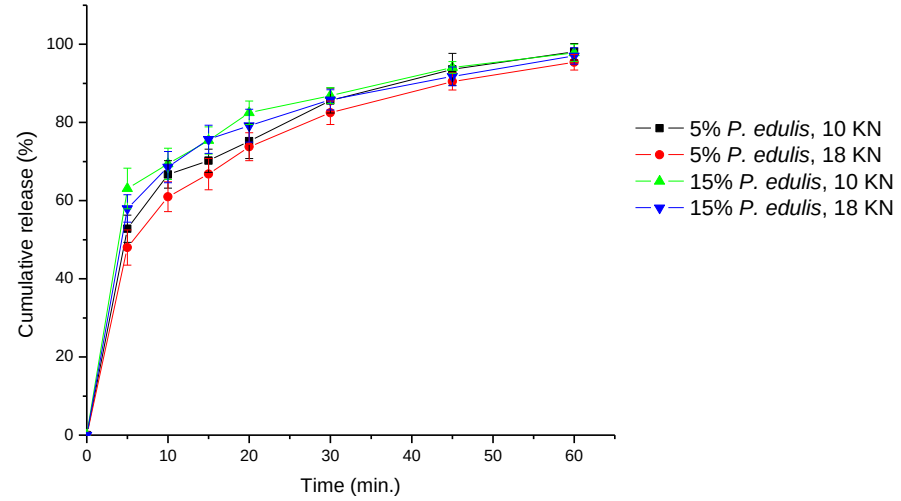

(A)

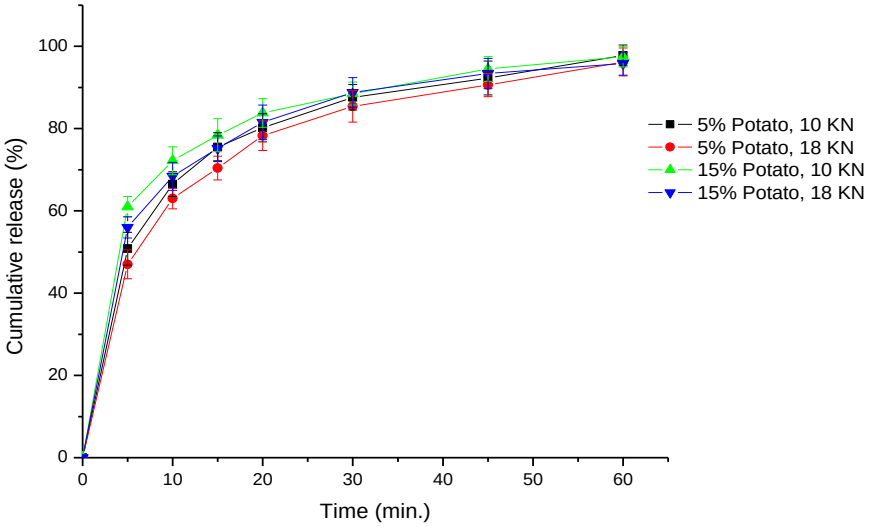

(B)

Figure 3.15: Dissolution profile of paracetamol tablet containing low (5% (w/w)) and high (15% (w/w)) disintegrant (A and B, *P. edulis* and Potato starch, respectively) concentration compressed at 10 and 18 KN.

3.7. Optimization study

Rapid disintegration is an essential attribute of conventional tablets and capsules especially those intended for rapid release of the active ingredient (Bolhuis and Chowhan, 1996). The needs for materials with enhanced disintegration ability as well as imparting high mechanical strength are among the reasons for optimizing the different factors involved in the manufacture of tablet formulation.

Preliminary experiments were carried out to determine the range of disintegrant and CF for the compression of paracetamol tablet using *P. edulis* starch as a disintegrant. And the effects of these

variables on the characteristics of paracetamol tablets were further studied and optimized using response surface methodology (RSM). To calculate quadratic regression model coefficients, each design variable must be studied at least at three distinct levels (Freiberg and Zhu, 2004), and consequently a CCD was used in the optimization study as it considers five distinct levels. The key characteristics selected as response variables for the optimization purpose were hardness, friability and disintegration time of the tablets.

From the preliminary experiments, disintegrant concentration of 5 to 15% (w/w), and CF of 10 to18 KN were considered. For CCD of two factors, a full 2^2 factorial design was combined with five replicates of the centre point and 2×2 axial points (Table 3.8). Experiments were carried out in random order to minimize the effects of uncontrolled variables that might introduce bias into the measurements. The 13 formulations of paracetamol tablets obtained by Design Expert 8.0.7.1 software as per CCD are shown in Table 3.8.

Table 3.8: Formulations of paracetamol tablet as given by the CCD.

Formulation code	Point type	Factors	
		CF (KN)	Disintegrant conc. (%w/w)
F1	Factorial	10 (-1)	5 (-1)
F2	Factorial	18 (+1)	15 (+1)
F3	Factorial	18 (+1)	5(-1)
F4	Factorial	10 (-1)	15 (+1)
F5	Axial	19.7 (+α)	10 (0)
F6	Axial	8.34 (-α)	10 (0)
F7	Axial	14 (0)	17. 1 (+α)
F8	Axial	14 (0)	2.93 (-α)
F9	Center	14 (0)	10 (0)
F10	Center	14 (0)	10 (0)
F11	Center	14 (0)	10 (0)
F12	Center	14 (0)	10 (0)
F13	Center	14 (0)	10 (0)

3.7.1. Granule characteristics

Pre-compression parameters are the key factors in tablet production as these could affect the packing arrangements, tablet integrity, uniformity and weight variation (Masareddy *et al*., 2012). The physical properties of the granules (bulk density, tapped density, compressibility index, Hausner ratio, and angle of repose) of all the 13 formulations were determined and are presented in Table 3.9.

The bulk density of the formulations ranged from 0.40 g/ml to 0.43 g/ml and the tapped density ranged from 0.44 g/ml to 0.48 g/ml. The granules had excellent to good flow properties for all formulations with the angle of repose values ranging from 30.65^{o} to 32.83^{o} according to the fixed funnel method. The values of compressibility index ranged between 6.52% and 13.04%, while the Hausner ratios were between 1.07 and 1.13; and flow rate of 4.20 g/sec. to 4.70 g/sec., indicating excellent flow properties.

Table 3.9: Granule characteristics of paracetamol formulations given by CCD (Mean ± SD, n = 3).

Formulation Code	Bulk density (g/ml)	Tapped density (g/ml)	Compressibility Index (CI %)	Hausner ratio (HR)	Flow rate (g/sec.)	Angle of Repose (^{o})
F1	0.42±0.02	0.45±0.00	6.67±0.04	1.07±0.12	4.70±0.12	32.83±0.05
F2	0.43±0.00	0.48±0.02	10.42±0.01	1.12±0.01	4.60±0.07	31.54±0.15
F3	0.43±0.01	0.46±0.03	6.52±0.00	1.07±0.02	4.54±0.06	32.08±0.02
F4	0.40±0.02	0.45±0.00	13.04±0.00	1.13±0.12	4.55±0.04	31.40±0.02
F5	0.41±0.01	0.46±0.03	10.87±0.06	1.12±0.00	4.61±0.15	32.83±0.03
F6	0.42±0.3	0.46±0.01	8.70±0.08	1.09±0.20	4.57±0.05	31.95±0.01
F7	0.42±0.00	0.45±0.00	6.67±0.03	1.07±0.00	4.67±0.03	32.55±0.08
F8	0.43±0.02	0.47±0.00	8.51±0.01	1.09±0.01	4.60±0.02	31.91±0.05
F9	0.40±0.00	0.45±0.02	11.11±0.00	1.12±0.03	4.20±0.03	32.41±0.10
F10	0.41±0.01	0.45±0.01	8.89±0.00	1. 10±0.02	4.61±0.00	30.65±0.02
F11	0.43±0.02	0.47±0.02	8.51±0.05	1.10±0.01	4.65±0.03	32.55±0.12
F12	0.41±0.02	0.45±0.00	8.89±0.04	1.09±0.05	4.41±0.02	31.68±0.02
F13	0.41±0.00	0.44±0.03	6.82±0.02	1.07±0.04	4.63±0.04	31.54±0.19

Table 3.10: Summary of experimental values of hardness, friability and DT of the 13 formulations.

	Responses		
Formulation Code	Hardness (N)	Friability (%)	DT (min)
F1	68	0.4	1.44
F2	98	0.44	1.9
F3	120	0.28	3
F4	60	0.55	1.63
F5	114	0.31	1.3
F6	53	0.6	0.84
F7	70	0.48	1.69
F8	100	0.25	21
F9	93	0.34	0.94
F10	94	0.36	0.96
F11	92	0.33	0.87
F12	90	0.34	0.94
F13	92	0.32	0.84

3.7.2. Response model selection

Polynomial models including linear, interaction and quadratic terms were generated for all the response variables using Design Expert software. Response models for the responses were selected based on the fit summary statistics. It displays statistics such as lack of fit (LOF) p-values and R-squared (R^2) values for comparing models for each response. The best fitting mathematical model was selected based on the comparisons of several statistical parameters including the coefficient of variation (CV), the multiple correlation coefficient (R^2), adjusted multiple correlation coefficient (adjusted R^2) and the predicted residual sum of square (PRESS) provided by Design Expert software (Huang *et al.*, 2005; Meka *et al.*, 2012).

A model is considered for further use if the model term's p-value is less than 0.05 and the LOF p-value is greater than 0.05. The program selects and suggests use of the highest order polynomial where the additional terms are significant, the model is not aliased and *Adj* R^2 and *Pred* R^2 are in a

reasonable agreement. PRESS indicates how well the model fits the data, and for the chosen model it should be small relative to the other models under consideration (Mujtaba *et al*., 2014). The fit of the model can be evaluated through R^2-value. For the model to best fit to the experimental data, the R^2 value should be close to 1. The smaller the value of R^2, the lesser will be the fit of the model to the experimental data (Wu *et al*., 2010).

From the model term's *p-value* and the *LOF p-values* presented in Table 3.11, the quadratic model is suggested for hardness (p = 0.0046, p = 0.2727), friability (p = 0.0018, p = 0.1407) and disintegration time (p = 0.0001, p = 0.0772). The goodness of fit of the model was evaluated by determination R^2 of >90% for all the responses; which indicates a high degree of correlation between the experimental and predicted responses. The '*Pred* R^2' value is in good agreement with the '*Adj* R^2' value, resulting in reliable models. The model selected has smaller PRESS value relative to the other models under consideration. Cubic model is not suggested since it is aliased by the software. To make the ANOVA valid, the fit summary output was analyzed by performing inverse transformation for disintegration time. Table 3.11 shows the fit summary output of the responses.

Table 3.11: Fit summary statistics for hardness, friability and disintegration time.

Response	Source	R^2	Adjusted R^2	Predicted R^2	p-value	LOF p-value	PRESS	Remark
Hardness	Linear	0.9509	0.9410	0.9126	< 0.0001	0.0038	363.91	
	2FI	0.9611	0.9482	0.9214	0.1575	0.0048	316.85	
	Quadratic	0.9916	0.9856	0.9507	0.0046	0.2727	60.48	Suggested
	Cubic	0.9960	0.9905	0.8614	0.1543	0.2843	135.10	Aliased
Friability	Linear	0.7672	0.7206	0.5776	0.0007	0.0016	0.051	
	2FI	0.7673	0.6898	0.4157	0.9338	0.0013	0.063	
	Quadratic	0.9617	0.9343	0.7644	0.0018	0.1407	0.010	Suggested
	Cubic	0.9925	0.9820	0.9353	0.0169	0.1968	0.021	Aliased
DT	Linear	0.1484	-0.0219	-0.5501	0.4479	0.0008	2.53	
	2FI	0.1603	-0.1195	-1.1158	0.7289	0.0007	3.18	
	Quadratic	0.9385	0.8946	0.6216	0.0001	0.0772	0.47	Suggested
	Cubic	0.9746	0.9391	0.0364	0.1095	0.2790	0.44	Aliased

3.7.3. Model adequacy checking

The ANOVA is the most important tool for the evaluation of significance and goodness of fit of the regressional model and significance of individual model coefficients (Noordin *et al*., 2004). Hence, in this study, ANOVA was applied to test the significance of the selected model and model coefficients for the responses. The regression and model terms are considered to be significant when a p-value is less than 0.05 (Sahoo *et al*., 2011). As shown in Table 3.12, the quadratic model is statistically significant for all three responses ($p< 0.05$), which is desirable as it indicates that the terms (factors) in the model have significant effect on the response.

Lack of fit test is a special diagnostic test for adequacy of a model that compares the pure error and describes the variation of data around the fitted model (Nasirizadeha *et al.*, 2012). For a model to be successfully used for prediction, the lack of fit (LOF) should be insignificant (Sahoo *et al*., 2011). The LOF p-values of hardness, friability and disintegration time (0.2727, 0.1407 and 0.0772, respectively) were greater than 0.05, which further strengthen the reliability of the models.

The ANOVA table (Table 3.12) also revealed that the main effects of both factors; CF ($p < 0.0001$ or $p = 0.0163$) and disintegrant level ($p < 0.0001$ or 0.0328), were significant for the responses of the quadratic model. For the quadratic model of hardness, for instance, the main effects of both parameters, the interaction effect (X_1X_2) ($p = 0.0220$), and the quadratic effects, X_1^2 ($p =0.0041$) and X_2^2 ($p =0.0122$) were significant model terms.

Table 3.12: Summary of ANOVA results of response surface ***quadratic model*** for hardness, friability and disintegration time.

Responses	Source	Sum of squares	Df	Mean Square	F value	p value	Remark
Hardness (N)	Model	4734.03	5	946.81	165.82	< 0.0001	Significant
	CF (X_1)	3883.76	1	3883.76	680.19	< 0.0001	Significant
	DC (X_2)	655.70	1	655.70	114.84	< 0.0001	Significant
	X_1X_2	49.00	1	49.00	8.58	0.0220	Significant
	X_1^2	99.79	1	99.79	17.48	0.0041	Significant
	X_2^2	64.18	1	64.18	11.24	0.0122	Significant
	Residual	39.97	7	5.71			
	Lack of fit	31.17	3	10.39	4.72	0.2727	*Insignificant*
	Pure error	8.80	4	2.20			
Friability (%)	Model	0.13	5	0.025	35.14	< 0.0001	Significant
	CF (X_1)	0.051	1	0.051	70.62	< 0.0001	Significant
	DC (X_2)	0.050	1	0.050	69.55	< 0.0001	Significant
	X_1^2	0.025	1	0.025	34.96	0.0006	Significant
	Residual	5.07×10^{-3}	7	7.25×10^{-4}			
	Lack of fit	4.197×10^{-3}	3	1.40×10^{-3}	6.41	0.1407	*Insignificant*
	Pure error	8.800×10^{-4}	4	2.20×10^{-4}			
DT (min.)	Model	1.485		0.30	21.38	0.0004	Significant
	CF (X_1)	0.14	1	0.14	9.87	0.0163	Significant
	DC (X_2)	0.097	1	0.097	7.04	0.0328	Significant
	X_2^2	1.22	1	1.22	88.06	< 0.0001	Significant
	Residual	0.097	7	0.014			
	Lack of fit	0.080	3	0.027	6.41	0.0772	*Insignificant*
	Pure error	0.017	4	4.2×10^{-3}			

CF – compression force, DC – disintegrant concentration, DT – disintegration time

The adequacy of the models was also confirmed with residual plot tests of regression models. Hence, residuals plots: the normal probability plot of residuals and the plot of internally studentized residuals versus predicted values were considered as additional tests of model adequacy checking tools (Kusic *et al*., 2010).

The normal probability plot is a graphical technique for assessing whether or not a data set is approximately normally distributed. The residual is the difference between the observed and the predicted value (or the fitted value) from the regression. If the points on the plot fall fairly close to the straight line then the data are normally distributed (Savic *et al*., 2014).

The normal probability plot of residuals and the plot of residuals versus predicted values of the responses for hardness, friability and disintegration time are shown from Figures 3.16-3.21. The results in Figure 3.16, 3.18 and 3.20 indicate that the residuals can be considered to fall on a straight line implying that the errors follow a normal distribution. The data in the graph follow the line representing a normal distribution and support the assumptions of the empirical models. Furthermore, the residuals appear to be randomly scattered about zero and all other points were found to fall in the range of +3 to −3. These results again indicate that the model satisfies the assumptions of the analysis of variance.

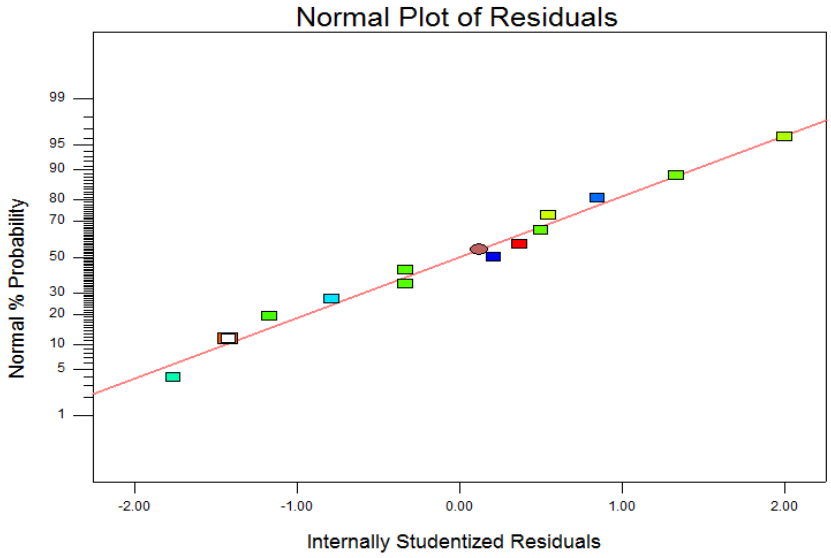

Figure 3.16: Normal probability plot of residuals for hardness data.

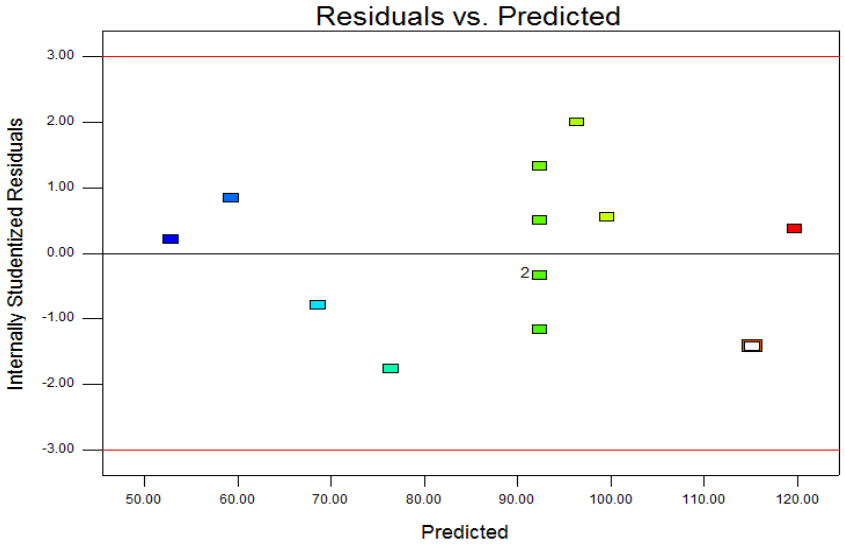

Figure 3.17: Plots of the residuals against predicted response for hardness.

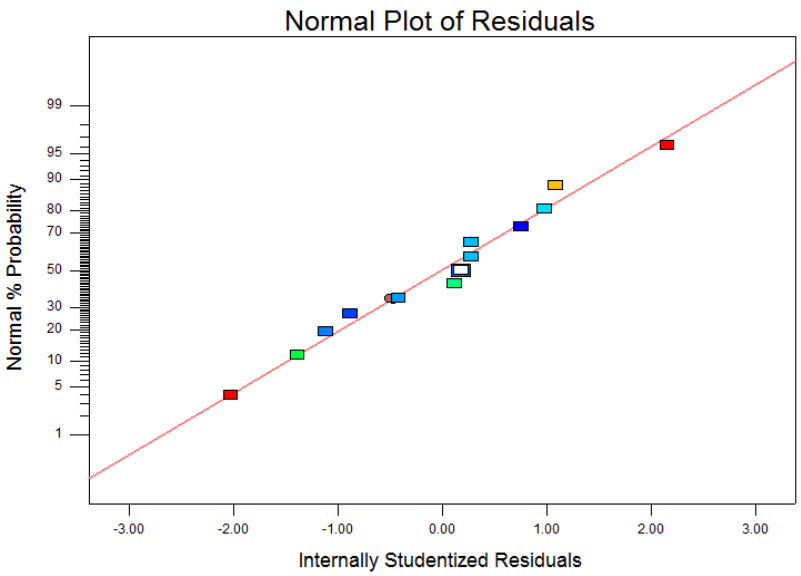

Figure 3.18: Normal probability plot of residuals for friability

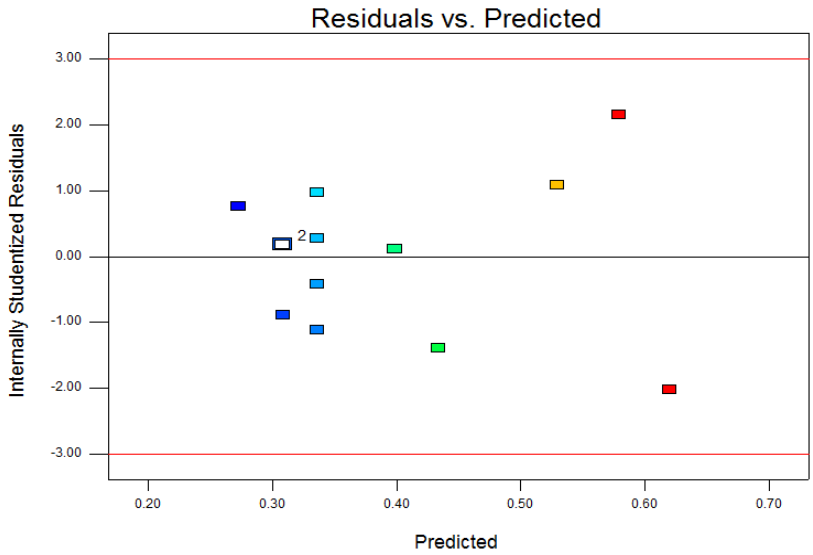

Figure 3.19: Plots of the residuals against predicted response for friability

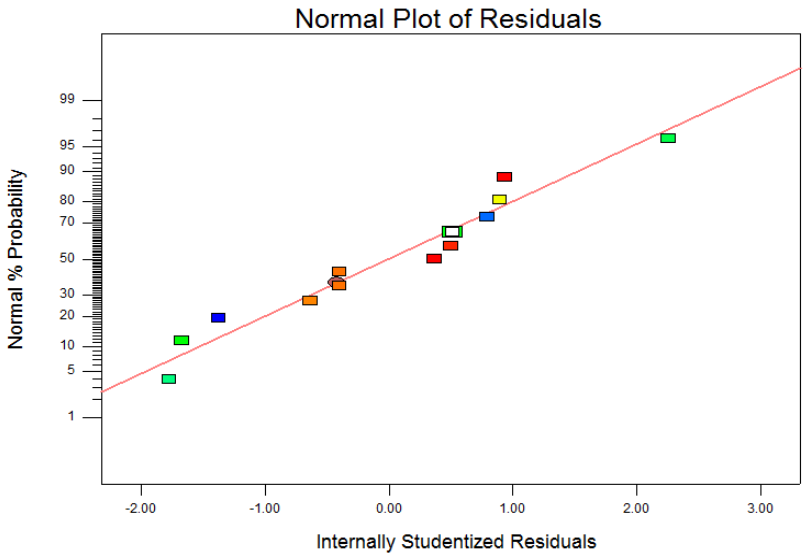

Figure 3.20: Normal probability plot of residuals for DT

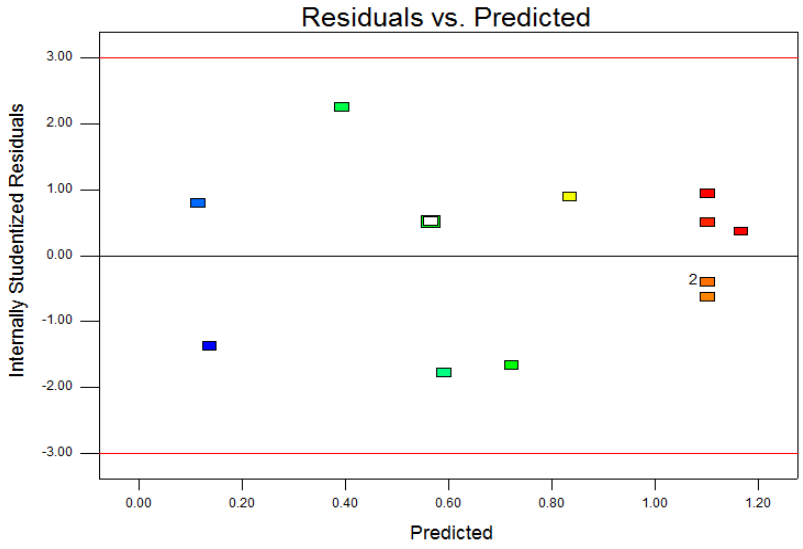

Figure 3.21: Plots of the residuals against predicted response for DT

It can be concluded from these analyses that the proposed models are adequate for the observed set of data and there is no reason to infer any violation of the independence or constant variance assumption (Bari *et al*., 2010; Savic *et al*., 2014).

Therefore, in order to determine the levels of factors which yield optimum mechanical strength and disintegration efficiency of the formulation, mathematical relationships between the dependent and independent variables (Eq. 3.1, Eq. 3.2 and Eq. 3.3) were developed:

$$\text{Hardness} = +92.20+22.03X_1-9.05X_2-3.50X_1X_2-3.79X_1^2-3.04X_2 \quad \text{Eq. (3.1)}$$

$$\text{Friability} = +0.34 - 0.080X_1 + 0.079X_2 + 0.060X_1^2 \quad \text{.....Eq. (3.2)}$$

$$\text{Disintegration Time} = -1.10 + 0.13X_1 - 0.11X_2 + 0.42X_2^2 \quad \text{.....Eq. (3.3)}$$

Where X_1 is level of CF and X_2 is disintegrant concentration.

From equations 3.1, 3.2 and 3.3, it can be observed that CF (X_1) has a positive effect on hardness and disintegration time and negative effect on friability of the formulations; which implies increasing CF increases hardness and disintegration time, but decreases friability of the tablets. On the other hand, increasing disintegrant concentration (X_2) decreases hardness and disintegration time, but increases the friability of the tablets. The negative coefficient for interaction term (X_1X_2) in eq. 3.1 suggests negative interaction between disintegrant concentration and CF on the response, hardness.

Positive sign before a factor in polynomial equations indicates that the response increases with the factor. On the other hand, a negative sign means the response and factors have reciprocal relation (Nutan *et al.*, 2005). The CF was more determinant factor on hardness as it had higher coefficient (+22.03) than the disintegrant level (−9.05). But both factors were almost equally important on the friability and DT of the tablets.

3.7.4. Contour plot and surface response analysis

The 2D contour and 3D response surface plots are graphical representations of the fitted regression models. These plots, presented on the basis of the model equations, display the interaction between the independent variables and assist in determining the optimum values of the variables within the ranges considered (Sampaio *et al.*, 2006; Kshirsagar *et al.*, 2012).

The contour and surface response plots for the interaction between the level of CF and disintegrant concentration and their interactive effects on the three responses are shown in Figure 3.22 to 3.24.

The contour and response surface plots shown in Figure 3.22 A and B, respectively, indicate the combined effect of level of CF and disintegrant concentration on the hardness of the formulations. The curved lines on the contour plot indicate that there is interaction effect of the two parameters on the hardness of the formulations. The plots indicate that the CF has a more pronounced effect on the hardness of the formulation. The curved contours and response surfaces, and the ANOVA results in Table 3.12 ($p = 0.0220$) indicate that the interaction effect of the two variables is significant.

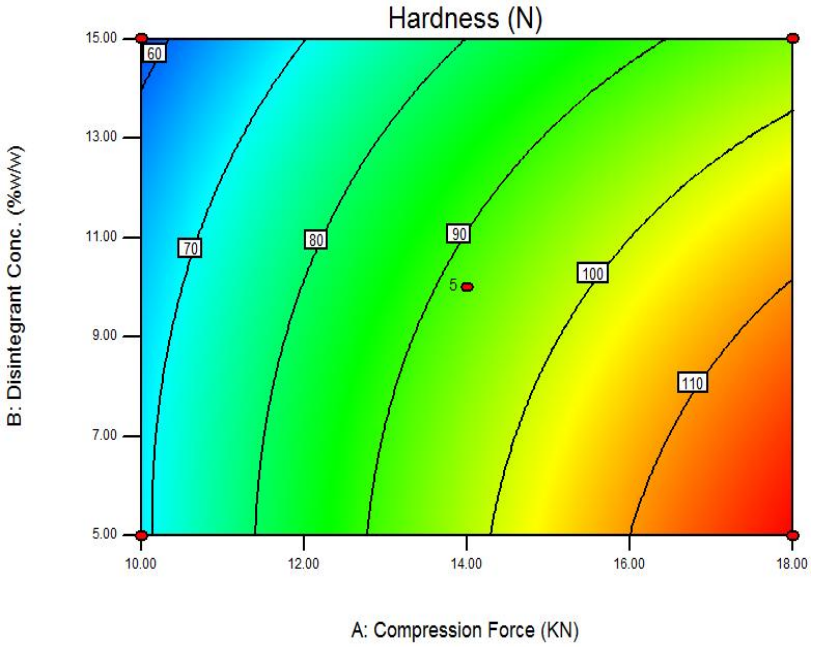

(A)

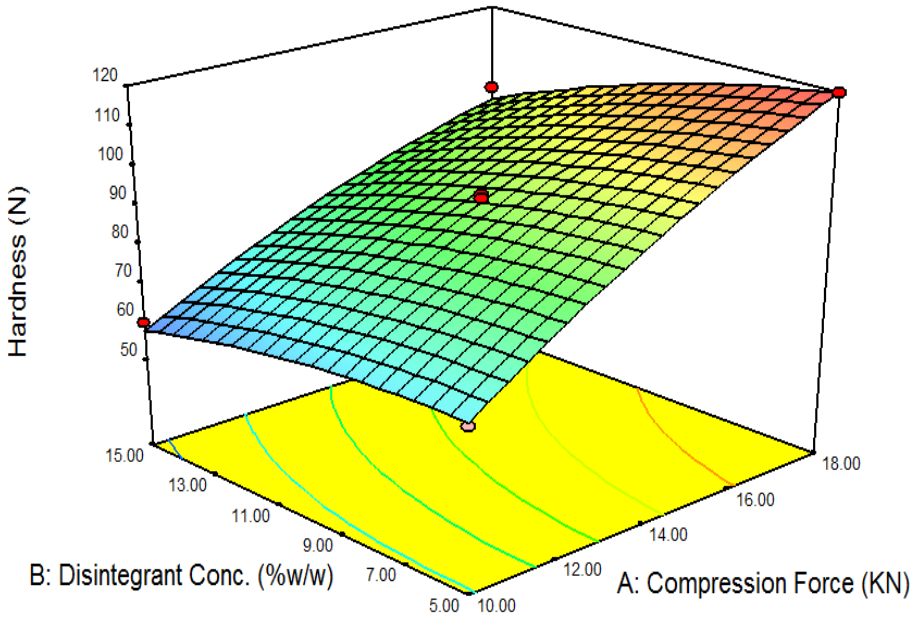

(B)

Figure 3.22: Contour plots (A) and Surface response (B) of hardness of paracetamol tablets in relation to CF and disintegrant concentration.

The 2D and 3D plots shown in Figure 3.23 A and B, respectively, indicate the combined effect of level of CF and disintegrant concentration on the friability of formulations. The plots indicate that the CF and disintegrant concentration were more or less equally important in friability ($p < 0.0001$).

The 2D and 3D, and the ANOVA results in Table 3.12 (p =0.8580) indicate that the interaction effect of the two variables was not significant.

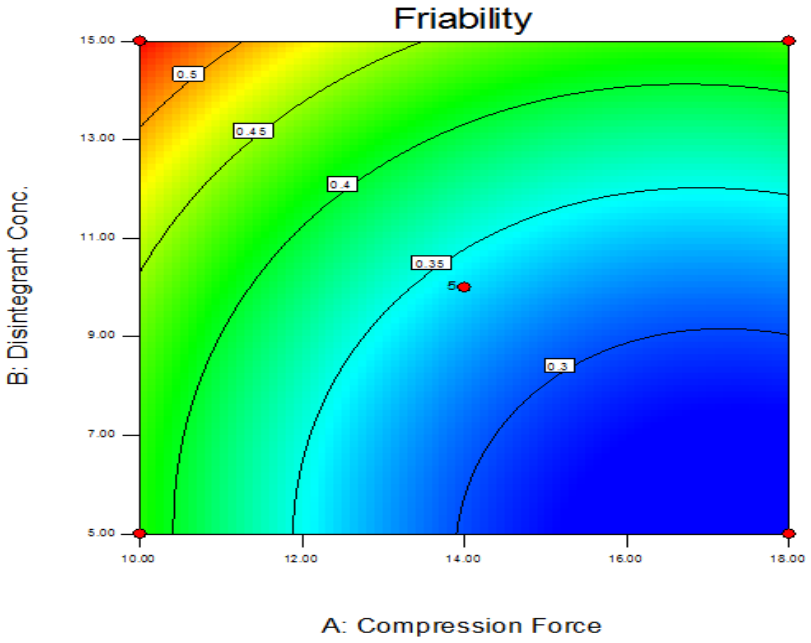

(A)

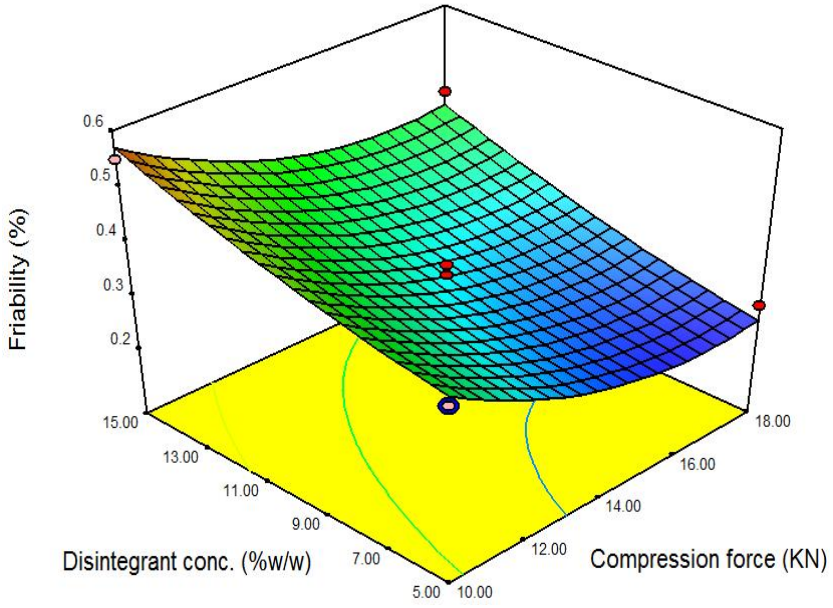

(B)

Figure 3.23: Contour (A) and surface response (B) plots of the effects of CF and disintegrant concentration on friability of paracetamol formulations.

The 2D and 3D plots shown in Figure 3.24 A and B, respectively, indicate the effects of amount of CF and disintegrant level on the DT of the formulations. Both parameters have a significant effect on the DT (p=0.0163, p=0.0328, respectively) (Table 3.12). According to this figure, the most suitable conditions for fast disintegration within the investigated ranges were found to be at lower CF and at the intermediate disintegrant level.

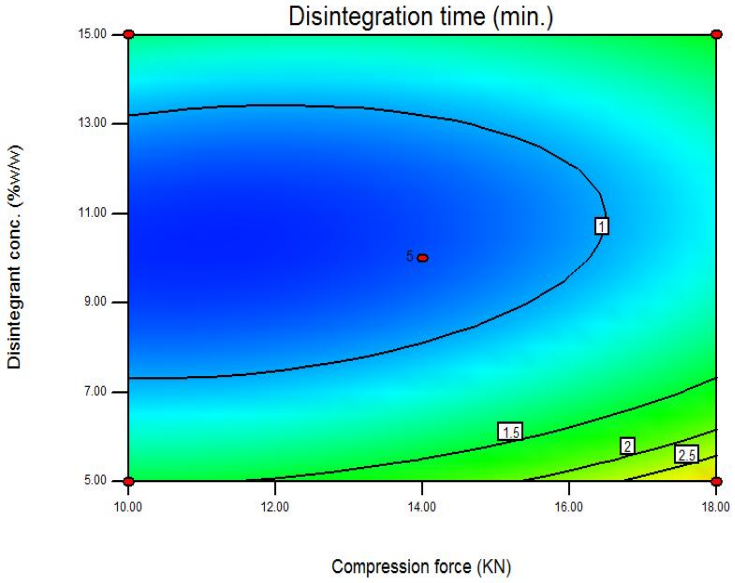

(A)

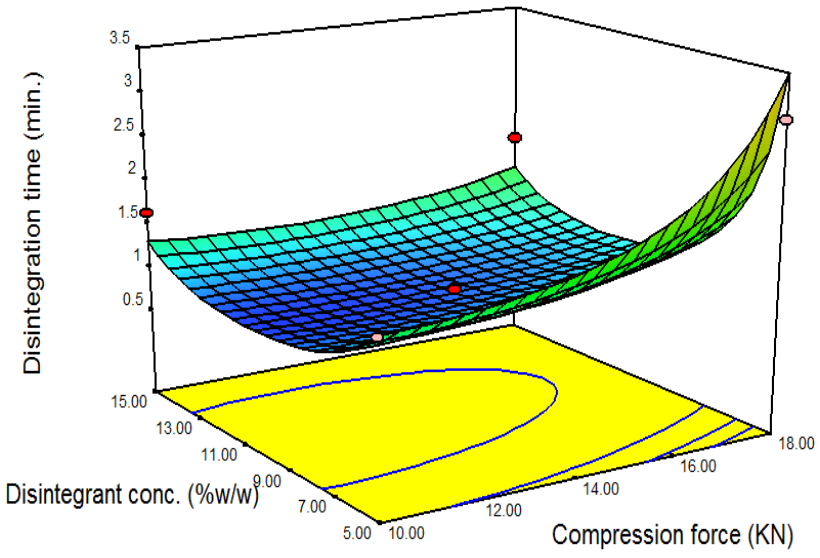

(B)

Figure 3.24: Contour (A) and Surface response (B) plots of DT of paracetamol tablets in relation to CF and disintegrant concentration.

The plots indicate that both factors play very important roles in influencing the response, DT. However, as the curvilinear contours of Figure 3.24 and the ANOVA results in Table 3.12 (p = 0.2819) indicate, the interactive effect of the two variables was not significant.

3.7.5. Simultaneous optimization of hardness, friability and disintegration time

One useful approach to optimization of multiple responses is to utilize the simultaneous optimization technique (Derringer and Suich, 1980). The technique tries to compromise among various responses and searches for a combination of factor levels that jointly optimize a set of responses by satisfying the requirements for each response in the set.

The key aim of this work is therefore, to simultaneously obtain rapid disintegration of the tablets while maintaining reasonable hardness and minimum friability on the formulation. Hence, both numerical by the desirability approach and graphical overlay plot optimization techniques (Meka *et al.*, 2012) of Design-Expert software (Version 8.0.7.1, Stat- Ease Inc, Minneapolis, MN) were utilized. Table 3.13 shows constraints of factor and responses set to obtain optimum formulation of paracetamol tablet using *P. edulis* starch as a disintegrant.

Table 3.13: Constraints of factors and responses for optimization of paracetamol formulations

Factor Constraints				
	Low	*High*		
Factor				
Comp. Force (KN)	10	18		
Disint Conc (%w/w)	5	15		
Response constraints	*Goal*	*Lower limit*	*Upper limit*	*Importance*
Response				
Hardness (N)	Target= 100	70	110	4
Friability (%)	Range	0	0.5	4
Disint. time (min.)	Range	0.01	5	5

3.7.5.1. Numeric optimization

Numerical optimization is used in order to find the specific point that maximizes the global desirability function. The desirability function approach is one of the most widely used methods for optimization of multiple responses (Kim and Lin, 2000). To find the global desirability function, the software performs thousands of calculations and finally arrives at the maximum desirability

condition. It ranges from 0 to 1, with value closer to one indicating a higher satisfaction of response goal(s) (Yang and El-Haik, 2008).

In this study, the values of desirability functions for all responses were obtained to be 1 (Figure 3.26). The predicted optimum values and the corresponding levels of parameters according to the set goals were obtained as presented in Figure 3.25. A dot indicates the best solution found by the Design Expert solver.

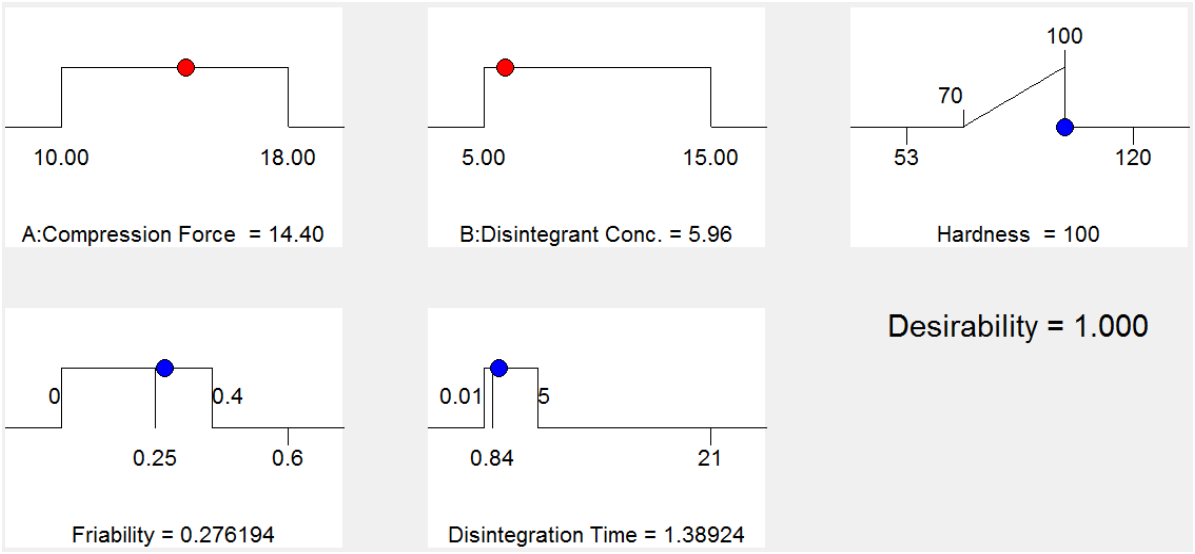

Figure 3.25: Numerical optimization results of predicted optimum values and the corresponding levels of parameters.

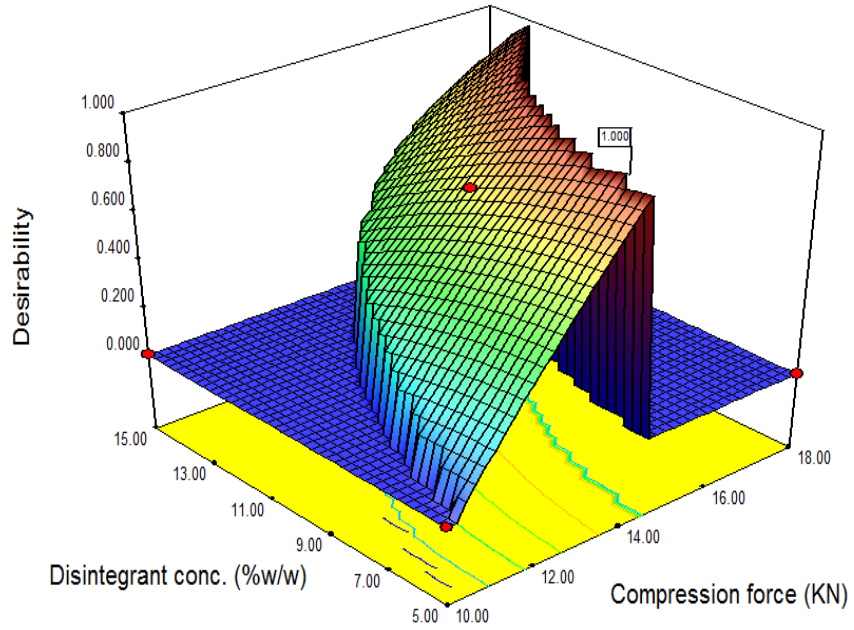

Figure 3.26: 3D plot of the overall desirability function.

3.7.5.2. Graphical optimization

Graphical optimization allows for visual selection of the optimum conditions of the parameters according to the set criteria. It utilizes the same criteria already set in numerical optimization and provides results in terms of overlay plots. The region is highlighted wherein all the responses are acceptable. Within this area, an optimum is located, trading off different responses (Singh *et al.*, 2008).

Figure 3.27 shows the overlay plot in which the yellow area represents the area satisfying the imposed criteria. The point identified by the flag was chosen in the graph as representative of the optimized area corresponding to CF of 14.40 KN and disintegrant level of 5.96%. Under these conditions the model predicts hardness of 100 N, disintegration time of 1.39 min. and friability of 0.28%.

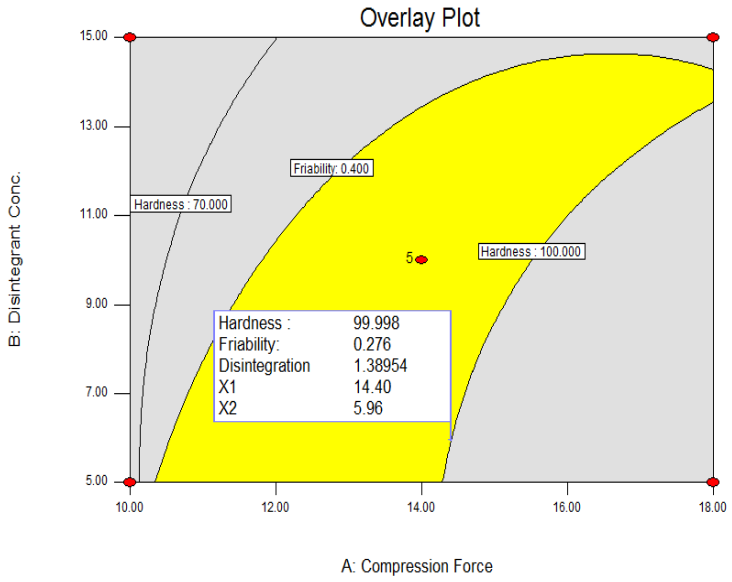

Figure 3.27: Optimum region identified by overlaying plots of the responses (hardness, friability and disintegration time) as functions *P. edulis* disintegrant concentration and CF.

3.7.5.3. Validation of the optimum formulation

To experimentally confirm the validity of obtained optimal point, confirmation experiments were carried out in triplicate at the optimal combinations of the factors (X1=14.40 KN, X2=5.96% w/w).

The optimized formulation was evaluated for its granule and tablet properties and the results are presented in Tables 3.15 and 3.16, respectively. The angle of repose, Hausner ratio and Carr's index

values were 31.26 ± 0.24°, 1.10 ± 0.01 and 10.59 ± 2.20%, respectively, indicating that the granules of the optimized formulation have excellent flow property.

Table 3.14: Granule properties of three batches of optimum formulation of paracetamol tablets (mean ± SD, n=3).

Batches	Flow rate (g/sec.)	BD (g/ml)	TD (g/ml)	Carr's Index (CI %)	Hausner ratio (HR)	Angle of Repose (°)
B_1	3.75	0.41	0.44	8.82	1.07	31.04
B_2	3. 70	0.40	0.46	13.04	1.15	31.51
B_3	3. 80	0.41	0.45	9.90	1.10	31.22
Mean ± SD	3.75 ± 0.1	0.41 ± 0.01	0.45 ± 0.01	10.59 ± 2.20	1.10 ± 0.01	31.26 ± 0.24

SD*- standard deviation; BD- bulk density; TD- tapped density; B_1, B_2, B_3 are batch 1, 2 and 3, respectively

The tablet properties of the three batches of the optimum formulation of paracetamol tablets are shown in Table 3.15. As seen from the table, the values of percentage errors had fallen within about 5% (except for friability) confirming that the experimental values of the optimized formulations agree well with the predicted values (Mohajeri *et al*., 2010). However, the friability of the optimum formulation was slightly higher than the predicted value. Nevertheless, it could be concluded that there is a high correlation between the predicted tablet properties and optimum values. The slight variation in hardness, friability and disintegration among the batches could be attributed to variations in processing variables.

Table 3.15: Properties of the three batches of paracetamol tablets of the optimum formulation and their predicted values, experimental results and the percentage errors.

Batches	Weight (g)	Thickness (mm)	Hardness (N)	Friability (%)	DT (min.)
B1	0.304 (0.005)	3.43 (0.01)	104.5 (4.50)	0.317 (0.05)	1.40 (0.31)
B2	0.302 (0.002)	3.50 (0.03)	98.3 (5.01)	0.288 (0.02)	1.28 (0.12)
B3	0.308 (0.003)	3.44 (0.02)	102.7 (7.10)	0.296 (0.07)	1.34 (0.20)
Mean (SD)	0.305 (0.003)	3.46 (0.04)	101.8 (3.19)	0.300 (0.015)	1.34 (0.06)
PV*	-	-	100	0.28	1.39
% Error	-	-	1.83	6.7	3.74

PV– predicted value, B1, B2, B3 – batches of optimum formulation; and SD- standard deviation.

The dissolution profiles of the paracetamol tablets of optimum formulation prepared with 5.96% *P. edulis* starch disintegrant concentration and compressed at 14.40 KN is shown in Figure 3.28. All the formulations released more than 80% of the drug within 30 min. Rapid release of the drug was observed as the tablets disintegrated rapidly, although in some cases, disintegration does not necessarily guarantee good dissolution profile. Thus, the dissolution profile of paracetamol tablets prepared with optimum concentration of *P. edulis* starch as disintegrant complies with its monograms.

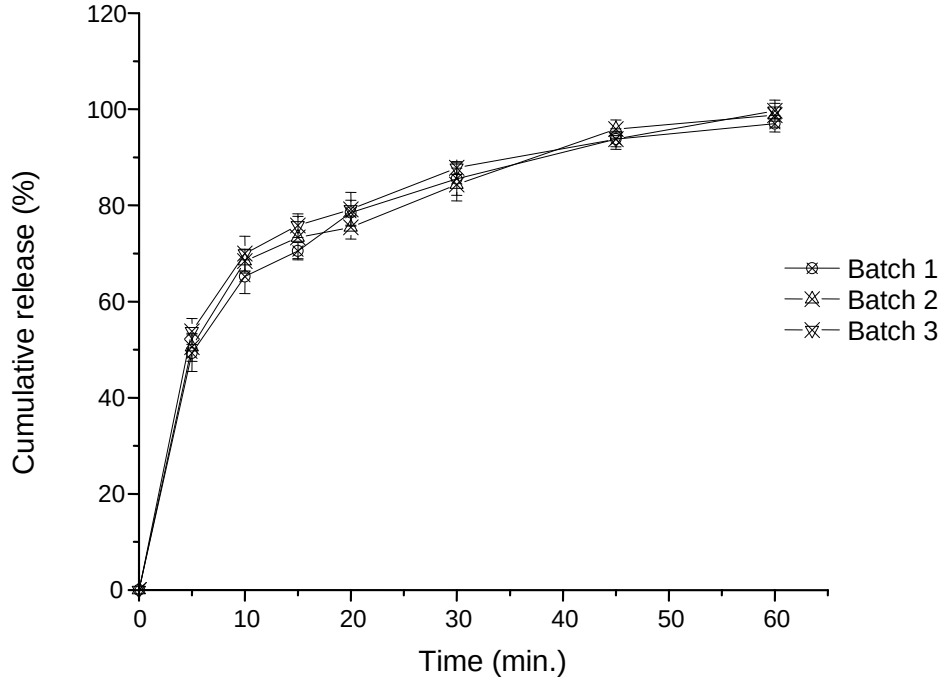

Figure 3.28: Dissolution profiles of paracetamol tablets of the optimum formulation (5.96% disintegrant concentration and 14.40 KN CF).

4. CONCLUSIONS

From the foregoing, the following can be concluded about *Plectranthus edulis* (Vatke) (Ethiopian potato), and its starch as a pharmaceutical excipient in tablet formulations.

Plectranthus edulis (Vatke) (Ethiopian potato) is one of the indigenous plants of Ethiopia and has been cultivated for its edible tubers in an array of agro-economical zones. The tuber yield of the plant is extremely higher than Irish potato when adequate irrigation and plant nutrients are provided.

As tubers are among the most abundant sources of starch, *P. edulis* can be a potential source of starch for pharmaceutical and other industrial applications. From the foregoing study, starch is the major component of *P. edulis* tubers, and has been observed to have favorable physicochemical characteristics to be used as a pharmaceutical excipient. In its native form, the starch has been observed to have a comparable disintegrant property to potato starch in paracetamol tablet formulations. Thus, the results of this study suggest further investigation of study of the pasting characteristics of the starch, correlation between chemical composition and physicochemical properties of the starch, various modifications of the starch and its applications in pharmaceutical and other industries.

The *P. edulis* plant has advantages of wide availability of information regarding its planting/agronomy and age of tuber collection, and wide adaptability to various regions so that large scale farming of the plant can be established at any part of the country. The plant needs small amount of rainfall, and it is highly pest and disease resistant. However, its production is declining due to various factors like pressure from the newly introduced species of root crops, recurrent droughts, land scarcity in the farming family, and long maturation period coupled with its short shelf life.

Commercially, the tubers of *P. edulis* and cost of planting are very cheap. The plant has the potential of being used as an important source of starch for various applications in pharmaceutical, food, paper and textile industry.

5. SUGGESTIONS FOR FURTHER WORK

The results of this study suggest further investigation on the following directions:

- Study of the pasting characteristics of *P. edulis* starch;
- Correlation between DSC thermograms and viscoamlograph characteristics of *P. edulis* starch; and
- Relationship between crystallinity (amylopectin), amylose content and DSC parameters (such as DSC thermograms and enthalpy of gelatinization) of *P. edulis* starch.

6. REFERENCES

Adane M, Gamal MA, Gebre-Mariam T (2006). Evaluation and optimization of godare starch as a binder and disintegrant in tablet formulation. *Ethiop Pharm J* 24:106-115.

Adebayo SA, Brown-Myrie E, Itiola OA (2008). Comparative disintegrant activities of breadfruit starch and official corn starch. *J Pow Tec* 181: 98-103.

Adikwu MU (1998). Moleculer weight and Amylose/Amylopectin ratio of starch from *Gladiolus actinomorphantus. Nig J Nat Prod Med* 2: 54-56.

Ahmed A, Ali SA, Hassan F, Ali SS, Haque N (2001). Evaluation of acetaminophen tablets by control test. *Pak J Pharm Sci* 14: 47-55.

Airaksinen ST (2005). Role of excipients in moisture sorption and physical stability of solid pharmaceutical formulations. pp 1-51 (http://ethesis.helsinki.fi/) (Accessed on 10/12/ 2013).

AOAC (2000). Official Methods of Analysis, 17th ed. Association of Official Analysis Chemists (AOAC), Washington, DC, USA.

Asfaw Z, Woldu Z (1997). Crop association of homegardens in Welayta and Gurage in Southern Ethiopia. *SINET: Ethiop J Sci* 20: 73–90.

Atichokudomchai N, Varavinit S (2003). Charecterization and utilization of acid modified cross-linked tapioca starch in pharmaceutical tablets. *Carbohydr Polym* 53: 263-270.

Bari N, Alam Z, Muyibi SA, Jamal P, Al-Mamun A (2010). Statistical optimization of process parameters for the production of citric acid from oil palm empty fruit bunches. *Afr J Biotechnol* 9: 554-563.

Barmpalexis P, Kanaze FI, Kachrimanis K, Georgarakis E (2010). Artificial neural networks in the optimization of a nimodipine controlled release tablet formulation. *Eur J Pharm Biopharm* 74: 316–323.

Bashar HQ (2010). Quantitative determination of paracetamol in pharmaceutical formulations by FTIR spectroscopy. *Eng Tech J* 28: 20-28.

Bello-Pérez, LA, Contreras-Ramos SM, Jìmenez-Aparicio A, Paredes-López O (2000). Acetylation and characterization of banana (*Musa paradisiaca*) starch. *Acta Cient Venez* 51: 143-149.

Bhowmik D, Chiranjib B, Yadav J, Chandira RM, Kumar KPS (2010). Emerging trends of

disintegrants used in the formulation of solid dosage form. *Der Pharmacia letter* 2: 495-504.

Bi Y, Yonezawa Y, Sunada H (1999). Rapidly disintegrating tablets prepared by the wet compression method: Mechanism and optimization. *J Pharm Sci* 88: 1004–1010.

Bolhuis GK, Chowhan ZT (1996). Materials for direct compression, pharmaceutical powder compaction technology. In: Alderborn G, Nystrom C, (ed.) Pharmaceutical powder compaction technology. Marcel Dekker, USA; pp. 419–499.

BP (2009). British Pharmacopoeia: The Pharmaceutical Press, Her Majesty's Stationery Office, London, vol. I−VI.

Builders PF, Anwunobi PA, Mbah CC, Adikwu MU (2013). New direct compression excipient from Tigernut starch: physicochemical and functional properties. *AAPS Pharm Sci Tech*, 14: 818-827.

Buléon A, Colonna P, Planchot V, Ball S (1998). Starch granules: structure and biosynthesis. *Int J Biol Macromol* 23: 85-112.

Buléon A, Gallant DJ, Bouchet B, Mouille C, D'Hulst C, Kossmann J, Ball S (1997). Starches from A to C'. *Chlamydomonas veinhardtii* as a model microbial system to investigate the biosynthesis of the plant amylopectin crystal. *Plan Physiol* 115: 949-957.

Callens C, Pringels E, Remon JP (2003). Influence of multiple nasal administrations of bioadhesive powders on the insulin bioavailability. *Int J Pharm* 25: 15–22.

Celebi N, Yildiz N, Demir AS, Calimli A (2008). Optimization of benzoin synthesis in supercritical carbon dioxide by response surface methodology (RSM). *J Supercrit Fluid* 47: 227–232.

Charles A, Chang Y, Ko W, Sriroth K, Huang T (2004): Some physical and chemical properties of starch isolates of cassava genotypes. *Starch/Starke* 56: 413–418.

Chaudhary KPR, Rao DS, Sujatha RS (1992). Formulation and Evaluation of Dispersible tablets of poorly soluble drugs. *Indian J Pharm Sci*: 31-32

Cheetham NWH, Tao L (1998). Variation in crystalline type with amylose content in maize starch granules: an x-ray power diffraction study. *Carbohydr polym* 36: 277-284.

Chen Z (2003). Physicochemical properties of sweet potato starches and their application in noodle products. PhD thesis dissertation, Wageningen University, The Netherlands ISBN: 90-5808-887-1.

Chiotelli, and Meste (2002): Effect of small and large wheat starch granules on thermo-mechanical behavior of starch. *Cereal Chem*. 79: 286-293.

Chowdary KPR, Enturi V (2011): Preparation, characterization and evaluation of starch citrate-a new modified starch as a disintegrant in tablet formulations. *IJPRD* 12: 9–17.

Cristina Freire A, Fertig CC, Podczeck F, Veiga F, Sousa J, (2009). 'Starch-based coatings for colon-specific drug delivery. Part I and II: The influence of heat treatment on the physico-chemical properties of high amylose maize starches'. *Eur J Pharm Biopharm* 72: 574-586.

Dayner K, Johnson P, Zeeman, S, Smith AM (2001). The control of amylose synthesis. *J plant physiol* 158: 479-487.

Debjit B, Chiranjib B, Yadav J, Chandira RM, Sampath KP (2010). Emerging trends of disintegrants used in formulation of solid dosage form. *Der Pharmacia Lettre*: 2: 495-504.

Derringer G, Suich R (1980). Simultaneous Optimization of Several Response Variables *J Qual Technol* 12(4): 214-219.

Enauyatifard R, Azadbakht M, Fadakar Y (2012). Assessment of *Ferula gummosa* gum as a binding agent in tablet formulations. Drug Research. *Acta Pol Pharm* 69: 291-8.

ENBSAP (2005). Ethiopian National Biodiversity Strategy and Action Plan. Institute of Biodiversity Conservation, Addis Ababa, Ethiopia.

Fontes GC, Priscilla V, Alexandre F, Rossic M, Helena M, Rocha-Leao M (2012). Optimization of penicillin G microencapsulation with OSA starch by factorial design. *Chem Eng Trans* 27: 85-90.

Freiberg S, Zhu X (2004). Polymer microspheres for controlled drug release. *Int J Pharm* 282: 1-18.

Gadalla MAF, Abd El-Hameed MH, Ismail AA (1989). A comparative evaluation of some starches as disintegrants for double compressed tablets. *Drug Dev Ind Pharm* 15: 427-446.

Gebre-Mariam T, Schmidt PC (1998). Some physicochemical properties of dioscorea starch from Ethiopia. *Starch/Stärke* 50: 241-246.

Gebre-Mariam T, Armstrong NA (1995). A Comparative study the use of enset and potato

starches in tablet formulations. *Drug Dev Ind Pharm* 21: 1211-1221.

Gebre–Mariam T, Schmidt PC (1996a). Isolation and physicochemical properties of Enset starch. *Starch/Starke* 48: 208-214.

Gebre-Mariam T, Schmidt PC (1996b). Characterization of enset starch and its use as a binder and disintegrant for tablets. *Pharmazie* 51: 303-311.

Gebre-Mariam T, Winnemöller M, Schmidt PC (1996). An evaluation of the disintegration efficacy of a sodium starch glycolate prepared from enset starch in compressed tablets, *Eur J Phar. Biopharm* 43: 124 - 132.

Gissinger D, Stamm A (1980). A comparative evaluation of the properties of some tablet disintegrants. *Drug Dev Ind Pharm* 6: *5*-11.

Hamed E, Sakr A (2001). Application of multiple response optimization technique to extended release formulations design. *J Control Release* 73: 329–338

Hancock BC, Shamblin SL (1998). Water vapour sorption by pharmaceutical sugar. *Pharm Sci Technol Today* 8: 345–351.

Hashim DBM, Moorthy SN, Mitchell JR, Hill SE, Linfoot KJ, Blanshard JMV (1992). The effect of low levels of antioxidants on the swelling and solubility of cassava starch. *Starch/Stärke* 44: 471-475.

Hedberg I, Kelbessa E, Edwards S, Demissew S, Persson E (2006). Gentianaceae to Cyclocheilaceae. Flora of Ethiopia and Eritrea. National Herbarium Vol 5: 595.

Hizukuri S (1985). Relationship between the distribution of the chain length of amylopectin and crystalline structure of starch granules. *Carbohydr Res* 141: 295-306.

Hoag SW, Dave VS, Moolchandani V (2008). Compression and Compaction. In: Augsberger, L.L., Hoag, S.W. (eds) Pharmaceutical Dosage Forms: Tablets 3rd edn., Informa Healthcare Inc, New York, Vol. 1, pp. 555-619.

Hofvander P (2004). Production of amylopectin and high-amylose starch in separate potato genotypes. Doctoral thesis Swedish University of Agricultural Sciences, Acta Universitatis agriculturae Sueciae Agraria, Uppsala, Sweden. Available at: http://pub.epsilon.slu.se/688/. Accessed on 20/5/2013.

Hoover R (2001). Composition, molecular structure, and physicochemical properties of tuber and root starches: a review. *Carbohydr Polym* 45: 253-267.

Huang YB, Tsai YH, Lee SH, Chang JS, Wu PC (2005). Optimization of pH-independent release of nicardipine hydrochloride extended-release matrix tablets using response surface methodology. *Int J Pharm* 289: 87–95.

Isah AB, Abdulsamad A, Gwarzo MS, Abbah HM (2009). Evaluation of the disintegrant properties of microcrystalline starch obtained from cassava in metronidazole tablet formulations. *Nig J Pharm Sci* 8: 26–35.

Jayakody L, Hoover R, Liu Q, Donner E (2007). Studies on tuber starches. II. Molecular structure, composition and physicochemical properties of yam (*Dioscorea spp*.) starches grown in Sri Lanka. *Carbohydr Polym* 69: 148-163.

Jubril I, Muazu J, Mohammed GT (2012). Effects of phosphate modified and pregelatinized sweet potato starches on disintegrant property of paracetamol tablet formulations. *J App Pharm Sci* 02: 32-36.

Karim AA, Norziah MH, Seow CC (2000). Methods for the study of starch retrogradation. *Food Chem* 71: 9-36.

Kemas UC, Nep EI, Agbowuro AA, Ochekpe NA (2012). Effect of chemical modification on the proximate composition of *Plectranthus esculentus* starch and characterization using FTIR spectroscopy. *WJPR*. 5: 1234-1249.

Kim KJ, Lin DKJ (2000). "Simultaneous optimization of mechanical properties of steel by maximizing exponential desirability functions" *J R Stat Soc* 49: 311-326.

Koksel H, Masatcioglu T, Kahraman K, Ozturk S, Basman A (2008). Improving effect of lyophilization on functional properties of resistant starch preparations formed by acid hydrolysis and heat treatment. *J Cereal Sci* 47: 275-282.

Kshirsagar SJ, Gupta AS, Kachare S, Bhalekar MR (2012). Design and development of sustain release matrix tablets of an antipsychotic drug quetiapine fumarate and optimization by a 3-level full factorial statistical design. *JAPS* 2: 267-277.

Kusic H, Jovic M, Kos N, Koprivanac N, Marin V (2010). The comparison of photo-oxidation processes for the minimization of organic load of colored waste water applying the response surface methodology. *J Hazard Mater* 183: 189 - 202.

Le Corre D, Bras J, Dufresne A (2010). 'Starch Nanoparticles'. *Biomacromolecules* 11: 1139–1153.

Lindeboom N, Chang P, Tyler R (2004). Analytical, biochemical and physicochemical

aspects of starch granule size, with emphasis on small granule starches. *Starch/Stärke*; 56: 89-99.

Loss PJ, Hood LF, Graham HD (1981): Isolation and characterization of starch from breadfruit. *Cereal Chem* 58: 282-286.

Louis MN, Peter AW (2011). Comparative study of physicochemical properties of breadfruit (*Artocarpus altilis*) and white yam starches. *Carbohydr Polym* 85: 294-302.

Lu TJ, Lin CL, Chen JC, Chang YH (2008). Characteristics of taro (*Colocasia esculenta*) starches planted in different seasons and their relations to molecular structure of starch. *J Agr Food Chem* 56: 2208-2215.

Lundstedt T, Seifert E, Abramo L, Thelin B, Nystrom A, Pettersen J, Bergman R (1998). Experimental design and optimization. *Chemometr Intell Lab Syst* 42: 3-40.

Madu SJ, Muazu J, Mohammed GT (2011). The role of acid treated sweet potato starch (microcrystalline starch) on disintegrant property of paracetamol tablet formulation. *Int J Pharm Res Innov* 4: 32-39.

Mandal U, Gowda V, Ghosh A, Selvan S, Solomon S, Pal TK (2007). Formulation and optimization of sustained release matrix tablet of metformin HCl 500mg using response surface methodology. *Yakugaku Zasshi*; 127:1281-1290.

Marais AF, Song M, deVilliers MM (2003). Effect of compression force, humidity and disintegrant concentration on the disintegration and dissolution of directly compressed furosemide tablets using croscarmellose sodium as disintegrant. *Trop J Pharm Res* 2: 125-135.

Masareddy RS, Kendalkar PV, Belekar AM (2012). Eeffect of polymers as matrix system in formulation of sustained release theophylline matrix tablet. *Int J Pharm Pharm Sci* 4: 409-414.

Meka VS, Nali SR, Songa AS, Battu JR, Kolapalli VRM (2012). Statistical optimization of a novel excipient (CMEC) based gastro retentive floating tablets of propranolol HCl and its in vivo buoyancy characterization in healthy human volunteers. *J Pharm Sci* 20:1-12.

Mekbib Y, Weibull J, Balcha G (2007). Phenotypic variation and local customary use of Ethiopian potato (*P. edulis* (Vatke) Agnew). Master Theses, Swedish Biodiversity Centre, Uppsala. Available at:

http://www.cbm.slu.se/eng/mastersprog/thesis2007/.pdf. Accessed 10/05/2013.

Miyamoto Y, Ryu A, Sugawara S, Miyajima M, Matsui M, Takayama K, Nagai T (1998). Optimization of the granulation process for designing tablets. *Chem Pharm Bull* 46: 1432-1437.

Mohajeri L, Aziz H, Isa M, Zahed M (2010). A statistical experiment design approach for optimizing biodegradation of weathered crude oil in coastal sediments. *Bioresource Technol* 101: 893-900.

Mohammed K, Endale A, Gebre-Mariam T (2007). Isolation, acetylation and physicochemical characterization of kottee harree (*dioscorea bulbifera*) starch, MSc Thesis, School of Pharmacy, Addis Ababa University.

Moorthy SN (2002). Physicochemical and functional properties of tropical tuber starches: a review. *Starch/Stärke* 54: 559–592.

Morrison WR, Azudin MN (1987). Variation in the amylose and lipid contents and some physical properties of rice starches. *J Cereal Sci* 5: 35-37.

Muazu J, Girbo A, Usman A, Mohammed TG (2012a). Preliminary studies on Hausa potato starch II: The binding properties. *J Pharm Sci Tech* 4: 965–971.

Muazu J, Musa H, Isah AB, Bhatia PG (2012b). Comparative tableting properties of three local potato starches III: The disintegrant properties. *Am J Pharm Tech Res* 2: 2249-3387.

Muazu J, Musa H, Isah AB, Bhatia PG, Tom GM (2011). Extraction and characterization of Kaffir Potato Starch: A potential source of pharmaceutical raw material. *J Nat Prod Plant Resour* 1: 41-49.

Mujtaba A, Ali M, Kohli K (2014). Statistical optimization and characterization of pH-independent extended-release drug delivery of cefpodoxime proxetil using Box–Behnken design. *Chem Eng Res Des* 92: 156–165.

Mulugeta T, Willemien, Lommen JM, Struik PC (2007). Indigenous multiplication and production practices for the tuber crop *P. edulis* in Chencha and Wolaita, Southern Ethiopia. *Exp Agr* 43: 381–400.

Mulugeta TA (2008). Studies on agronomy and crop physiology of *P. edulis* (Vatke) Agnew. PhD thesis, Wageningen University, Wageningen, The Netherlands. Available at*: http://edepot.wur.nl/121998*. Accessed on 12/11/2012.

Musa H, Ochu SN, Bhatia PG, Mshelbwala K (2011). Evaluation of barley *hordeum vulgare* starch as tablet disintegrant. *Int J Pharm Pharm Sci* 3: 75-79.

Mustapha MA, Igwilo CI, Silva BO (2010). Performance equivalence study of sodium starch glycolate, modified maize starch and maize starch as disintegrants in paracetamol tablet formulation. *Med J Islamic World Acad Sci* 18: 61-67.

Nang'ayo F, Omanya G, Bokanga M, Odera M, Muchiri N, Ali Z, Werehire P (eds.) (2005). A strategy for industrialization of cassava in Africa: Proceedings of a small group meeting, 14–18 November 2005, Ibadan, Nigeria. Nairobi, Kenya: African Agricultural Technology Foundation.

Nasirizadeha N, Dehghanizadeh H, Yazdanshenas ME, Moghadam MR, Karimi A (2012). Optimization of wool dyeing with rutin as natural dye by central composite design method. *Ind Crop Prod* 40: 361–366.

Nelles EM, Dewar J, Bason ML, Taylor JRN (2000). Maize starch biphasic pasting curves. *J Cereal Sci* 31: 287-294.

Nigussie T, Endale A, Gebre-Mariam T (2006). Isolation, characterization and evaluation of binding and disintegrant effects of anchote starch in paracetamol tablet formulation, MSc Thesis, School of Pharmacy, Addis Ababa University.

Noordin M, Venkatesh V, Sharif S, Elting S, Abdullah A (2004). Application of response surface methodology in describing the performance of coated carbide tools when turning AISI 1045 steel. *J Mater Process Technol* 45: 46-58.

Nutan MTH, Soliman MS, Taha EI, Khan MA (2005). Optimization and characterization of controlled release multi-particulate beads coated with starch acetate. *I J Pharm* 294: 89–101.

Nuwamanya E, Baguma Y, Emmambux N, Taylor J, Patrick R (2010). Physicochemical and functional characteristics of cassava starch in Ugandan varieties and their progenies. *J Plant Breed Crop Sci* 2: 001-011.

Odeku OA, Picker-Freyer KM (2009). Evaluation of the material and tablet formation properties of modified forms of dioscorea starches. *Drug Dev Ind Pharm* 35: 1389-1406.

Odeku OA, Schimdt W, Picker-Freyer KM (2008). Material and tablet properties of pregelatinized (thermally modified) *dioscorea* starches. *Eur J Pharm Biopharm* 70: 357-371.

Ofoefule SI, Osuji AC, Okorie O (2004). Effects of physical and chemical modifications on the

disintegrant and dissolution properties of tacca involucrate starch. *Bio Res* 2: 97-102.

Ohwoavworhua FO, Adelakun TA, Kunle OO (2007). A Comparative evaluation of the flow and compaction characteristics of a-cellulose obtained from waste paper. *Trop J Pharm Res* 6: 645-651.

Okpanachi GO, Musa H, Isah AB (2012). Physicochemical characterization of microcrystalline starch derived from *digitaria iburua (poaceae). Nig J Pharm Sci* 11: 66–76.

Olayemi OJ, Oyi AR, Allagh TS (2008). Comparative evaluation of maize, rice and wheat starch powders as pharmaceutical excipients. *Nig J Pharm Sci* 7: 131-138.

Omojola MO, Akinkunmi YO , Olufunsho KO, Egharevba HO, Martins EO (2010). Isolation and physico-chemical characterization of cola starch. *AJFAND* 10: 2884-2900

Ozdemir E, Duranoglu D, Bekerb U, Avci AO (2011). Process optimization for Cr (VI) adsorption onto activated carbons by experimental design. *Chem Eng J* 172: 207–218.

Paulos G, Endale A, Bultosa G, Gebre-Mariam T (2009). Isolation and physicochemical characterization of cassava starches obtained from different regions of Ethiopia. *Ethiop Pharm J* 27: 42-54.

Peroni FHG, Rocha TS, Franco CML (2006). Some structural and physicochemical characteristics of tuber and root starches. *Int J Food Sci Technol* 12: 505–513.

Philip FB, Agbo MB, Adelakun T, Larry CO, Anthony AA (2010). Novel multifunctional pharmaceutical excipients derived from microcrystalline cellulose-starch microparticulate composites prepared by compatibilized reactive polymer blending, *Int J Pharm* 388: 159-167.

Puwastien P, Siong TE, Kantasubrata J, Craven G, Feliciano RR, Judprasong K (2011). Asian manual of food analysis. Regional centre of Asian network of food data system. Institute of nutrition, Mahidol University, Thailand.1st ed. pp 11-13.

Rajeevkumar P, Rajeev R, Anilkumar N (2010). Studies on *Curcuma angustifolia* starch as a pharmaceutical excipient. *Int J Pharm Tech Res*, 2: 2457–2460.

Ratnayakea WS, Hoovera R, Warkentinb T (2002). Pea Starch: Composition, Structure and Properties: a review, *Starch/Stärke* 54: 217–234.

Rice LJ, Brits GJ, Potgieter CJ, Staden JV (2011). Plectranthus: A plant for the future? *S Afr J Bot* 77: 947–959.

Richardson S, Gorton L (2003). Characterisation of the substituent distribution in starch and

cellulose derivatives: review. *Anal Chim Acta* 497: 1427-1465.

Robertson MI (1999). 'Regulatory issues with excipients'. *Int J Pharm* 187: 273-276.

Roosta M, Ghaedi M, Daneshfar A, Darafarin S, Sahraei R, Purkait MK (2014). Simultaneous ultrasound-assisted removal of sunset yellow and erythrosine by ZnS:Ni nanoparticles loaded on activated carbon: Optimization by central composite design. *Ultrason Sonochem* 21: 1441–1450.

Sahoo BK, Mishra AK, Pal TK (2011). Optimization and validation of modulated release formulation of ranitidine HCl by response surface methodology. *IJPSDR* 3: 13-18.

Salwa M, Hanan MA, Nessrien MN (2010). Physicochemical properties of starch extracted from different sources and their application in pudding and white sauce. *WJDFS* 5: 173-182.

Sampaio F, Faveri D, Mantovani H, Passos F, Perego P, Converti A (2006). Use of response surface methodology for optimization of xylitol production by the new yeast strain. *J Food Eng* 76: 376 - 386.

Sarangapani S, Rajappan M (2012). Pharmacognostical and pharmaceutical characterisation of delonix regia - a novel matrix forming natural poymer. *Int J Pharm* 2: 564-573.

Savic IM, Savic IM, Stojiljkovic ST, Gajic DG (2014). Modeling and optimization of energy-efficient procedures for removing lead (II) and zinc (II) ions from aqueous solutions using the central composite design. *Energy*. 30: 1-7.

Schoch TJ (1994). Swelling power and solubility of granule starches. In: Whistler R.L. (Ed.), Methods in carbohydrate chemistry Volume IV starch, Academic press, London: 106-108.

Schüssele A, Bauer-Brandl A (2003). Note on the measurement of flowability according to the European Pharmacopoeia. *Int J Pharm* 257: 301-304.

Sekkal M, Dincq V, Legrand P, Huvenne JP (1995). Investigation of the glycosidic linkages in several oligosaccharides using FT-IR and FT Raman spectroscopies. *J Molec Struc* 349: 349-352.

Sharma R, Saxena DD, Dwivedi AK, Misra A (2001). Inhalable microparticles containing drug combinations to target alveolar macrophages for treatment of pulmonary tuberculosis. *Pharm Res* 18: 1405-1410.

Sheffield C (1986). Plant Genetic Resources Centre/Ethiopia ten years of (1976-1986)

collection, conservation and utilization, Addis Ababa, Ethiopia.

Singh B, Dahiya M, Saharan V, Ahuja N (2005). Optimizing drug delivery systems using systematic “design of experiments.” Part II: retrospect and prospects. *Crit Rev Ther Drug Carrier Syst* 22: 215–293.

Singh B, Kumar R, Ahuja N (2004). Optimizing drug delivery systems using systematic "Design of Experiments." Part I: Fundamental aspects. *Crit Rev Ther Drug Carrier Syst* 22: 27–105.

Singh KP, Gupta S, Singh AK, Sinha S (2011). Optimizing adsorption of crystal violet dye from water by magnetic nanocomposite using response surface modeling approach. *J Hazard Mater* 186: 1462–1473.

Singh N, Kaur L, Sandhu KS, Kaur J, Nishinari K (2006). Relationships between physicochemical, morphological, thermal, rheological properties of rice starches. *Food Hydrocolloid* 20: 532-542.

Singh N, Singh J, Kaur L, Sodhi NS, Gill BS (2003). Morphological, thermal and rheological properties of starches from different botanical sources. *Food Chem* 81: 219–231.

Singh S, Bandopadhyay R, Kapil R, Ahuja N (2008). Systematic optimization of drug delivery systems: an insight. *Pharm Rev* 7: 146-186.

Sinka IC, Schneider LCR, Cocks ACF (2004). Measurement of the flow properties of powders with special reference to die fill. *Int J Pharm* 280: 27-38.

Sitohy MZ, Labib SM, El-Saadany SS, Ramadan MF (2000). Optimizing the conditions for starch dry phosphorylation with sodium mono- and dihydrogen orthophosphate under heat and vacuum *Starch/Staerke* 52: 95-100.

Staniforth JN (1996). *In*: Aulton M.E. (Ed). Pharmaceutics –The Science of Dosage Form Design. Churchill Livingston. Pp 600–615.

Stevenson DG, Jane J, Inglett GE (2006). Physicochemical properties of pin oak (*quercus palustris muenchh*). A corn starch. *Starch/Stärke* 58: 553-560.

Swaminathan V, Kildsig DO (2001). An examination of the moisture sorption characteristics of commercial magnesium stearate. *AAPS Pharm Sci Tech* 2:1-28.

Talegaonkar S, Khan AY, Khar RK, Ahmad FJ, Khan ZI (2007). Development and characterization of paracetamol complexes with hydroxypropyl-β-cyclodextrin. *Iran J Pharm Res* 6: 95-99.

Techapun C, Charoenrat T, Watanabe M, Sasaki K, Poosaran N (2002). Optimization of thermostable and alkaline-tolerant cellulose-free xylanase production from agricultural waste by thermotolerant Streptomyces sp. Ab106, using the central composite experimental design. *Biochem Eng J* 12: 99–105.

Tester RF, Karkalas J, Qi X (2004). Starch-composition, fine structure and architecture. *J Cereal Sci* 39: 151–165.

The United States Pharmacopoeia 30th ed. National Formulary 25 ed. (USP30-NF25) (2007). The United states Pharmacopeial Convention, Inc., Rockville, Maryland.

Thomas DJ, Atwell WA (1999). Starches: Practical guides for the food industry. Eagan Press, St Paul, Minnesota, USA.

Vasanthan T, Bergthaller W, Driedger D, Yeung J, Sporns P (1999). Starch from Alberta Potatoes: Wet isolation and some physicochemical properties. *Food Res Int* 32: 335-365.

Wang TL, Bogracheva TY, Hedley CL (1998). Starch: as simple as A, B, C? A review. *J Exp Bot* 49: 481–502.

Wells J (2002). Pharmaceutical preformulation: the physicochemical properties of drug substances. In: Aulton, M. E. (ed.), Pharmaceutics: The science of dosage form design, 2nd ed., Harcourt, Churchill living stone, London, pp. 113 - 151.

Wu H, Feng TC, Chung TW (2010). Studies of VOCs removed from packed-bed absorber by experimental design methodology and analysis of variance. *Chem Eng J* 157: 1–17.

Yang K, El-Haik B (2008). Design for Six Sigma: a Roadmap for Product Development. 2nd ed. McGraw-Hill Co. Inc., New York. pp 611 - 642.

Yeshitila M, Weibull J (2007). Phenotypic variation and local customary use of Ethiopian potato (*P. edulis* (Vatke) Agnew). Master Theses, Swedish Biodiversity Centre, Uppsala.http://www.cbm.slu.se/eng/mastersprog/thesis. Accessed 10/05/2013.

Yüksel N, Karata A, Baykara T (2003). Comparative evaluation of granules made with different binders by a fluidized bed method. *Drug Dev Ind Pharm* 29: 387-395.

Zeng J, Li G, Gao H, Ru Z (2011). Comparison of A and B starch granules from three wheat varieties. *Molecules* 16: 10570-10591.

Zobel HF, Young SN, Rocca LA (1988). Starch gelatinization: an x-ray diffraction study.

Cereal Chem 65: 443-446.

Zuluaga M, Baena Y, Mora C, D'León LP (2007). Physicochemical characterization and application of yam *(dioscorea cayenensis-rotundata)* starch as a pharmaceutical excipient. *Starch/Stärke* 59: 307-317.